9-27-2017 2:00 PM

Generic Numerical Tornado Model for Common Interpretation of Existing Experimental Simulators

Anant Gairola
The University of Western Ontario

Supervisor
Bitsuamlak, Girma
The University of Western Ontario

Graduate Program in Civil and Environmental Engineering
A thesis submitted in partial fulfillment of the requirements for the degree in Master of Engineering Science

Abstract

There are difficulties in making a common interpretation of results of similar experiments done in different experimental tornado simulation facilities. This is primarily because of the differences in vortex generation mechanisms utilized as well as geometric differences in these facilities. Therefore, in an attempt to facilitate a universal interpretation of results, a generic numerical tornado model, representing the three major existing experimental tornado simulators, is developed in this study. The three experimental simulators in consideration are VorTECH at Texas Tech University, Tornado Simulator at Iowa State University and WindEEE Dome at Western University as representatives of "Ward" type, "top-down" type and "3-D wind chamber" type facilities, respectively.

First, the three experimental facilities and their corresponding flow-fields are replicated using CFD simulations and then the differences and similarities in their flow-fields are identified. It is demonstrated that it is possible to link different experimental facilites through a generic numerical model by characterizing a tornado-like vortex using parameters strictly obtained from the flow-field, as opposed to the common practice of using geometric dimensions of the experimental facilities to extract these parameters. This part of the study requires an extensive parametrization to characterize these vortices, hence computationally effective and reasonably accurate Reynolds Stress Model (RSM) is used. Further, the potential application of this generic numerical model to bluff-body aerodynamics and wind load evaluation is demonstrated by using a more accurate Large Eddy Simulation technique. While the results show some minor but explainable discrepancy with experimentally obtained data, the proposed generic numerical model displays a promise towards its application for preliminary tornadic aerodynamic data generation.

Keywords

Tornado-like vortices, numerical tornado simulation, flow-field charaterization, experimental tornado simulators, generic numerical model, bluff-body aerodynamics, wind load evaluation.

Co-Authorship Statement

Chapter two will be submitted for publication under the co-authorship of Gairola, A. and Bitsuamlak, G.T.

Chapter three will be submitted for publication under the co-authorship of Gairola, A. and Bitsuamlak, G.T.

Acknowledgments

I want to begin by expressing my utmost gratitude to Dr. Girma Bitsuamlak for his excellent supervision and feedback during the last two years. He gave me the time, resources and freedom to grow as a researcher. This work would not have been possible without his pricless guidance.

I would also like to extend my heartfelt gratitude to my research colleagues (Zoheb, Ahmed, Tibebu, Meseret, Anwar, Matiyas, Abiy, Bariello, Kim, Chris and Tsniuel) who have been extremely helpful and friendly.

A big thank you to the technical staff working back stage to facilitate my research. This includes Dr. Ge Baolai and Dr. Tyson Whitehead from SHARCNET and Mr. Gerald Dafoe and Mr. Andrew Mathers at WindEEE for all their help and patience in dealing with my queries.

My officemates (Rahul, Emilio, Arif, Sarah and Aaron) have been so amazing and have kept me such great company that I almost never realized that our small office with oddly green colored walls has no windows. Cheers to all the fun times and great memories we shared in and outside the office. It has also been a pleasure knowing the other research students (particularly in wind and structural engineering groups) who have been very friendly to me. I would also like to thank my other friends here in London and back in New York who have always believed in me.

I am also grateful to Dr. Partha Sarkar from Iowa State University for giving me a chance to work in his wind tunnel as an under-graduate intern back in the summer of 2014. I picked up a career in wind engineering largely because of my experience working with him.

Special thanks Matiyas ("*ambesaw*") and Tibebu ("*aleka*") for their valuable input throughout. I would also like to thank Dr. Zoheb Nasir for his expert feedback and comments on my work.

I would also like to thank my examiners, Dr. Horia Hangan, Dr. Han-Ping Hong and Dr. Eric Savory, for taking the time out of their busy schedules and helping me improve my thesis with their valuable feedback during my defence examination.

At last but not the least, I would like to thank my family, especially my parents (Ajay and Shipra) and my sister (Ritika), for all their love and support.

Table of Contents

List of Tables

List of Figures

List of Nomenclature

a	Aspect ratio
C_p	Pressure coefficient
h_u	Height of updraft hole, m
h_0	Inflow height, m
P	Static pressure, Pa
P_0	Reference static pressure, Pa
P	Far field static pressure, Pa
Q	Volumetric flow rate per unit axial length, m^2/s
Q'	Volumetric flow rate, m^3/s
Re_r	Radial Reynolds Number
r_u	Radius of updraft hole, m
r_0	Radius of updraft, m
r_c	Core radius, m
S	Swirl ratio
v_r	Radial velocity, m/s
v_t	Tangential velocity, m/s
v_z	Axial velocity, m/s
z	Height above the ground, m
Γ	Circulation, m^2/s

Γ_∞	Maximum circulation, m^2/s
ρ	Fluid (air) density, kg/m^3
θ	Vane angle, degrees
Ω	Rotation rate, rad/s
LES	Large Eddy Simulation
NS	Naiver-Stokes
RANS	Reynolds-Averaged Naiver-Stokes
ISU	Iowa State University
TTU	Texas Tech University
WU	Western University
WindEEE	Wind Engineering Energy and Environment

Chapter 1

1 Introduction

Analyzing the effects of extreme weather phenomena, like tornadoes, on structures (bluff bodies) has received an increased attention in the past few decades. This is largely because greater socio-economic losses would occur in the event of such a catastrophic weather phenomenon now, more than ever before, due to recently increased urbanization and economic development. Wind Hazard Reduction Coalition statistics reveal that, on an average, about 800-1000 tornadoes annually strike US alone, causing 80 deaths, 1500 injuries and $850 million in damage. In 2011, according to National Oceanic and Atmospheric Administration (NOAA), tornadoes killed 553 people and amassed $10 billion dollars in damage in the United States. NOAA also reported at least 5 tornadoes in US in 2015 to have caused over a billion dollars in damage each, with a preliminary tornado count for the year to be around 1200. While US is ranked first in terms of annual tornado occurrences, Canada is ranked second. However, unlike US, tornadoes in Canada were not well documented before 1980s, the reason for a relatively weak database of past tornadic events. Newark (1984), using newspaper clips, photographs and damage survey reports, developed a database for tornadoes in Canada from 1950 to 1979. It was reported that there had been over 700 confirmed tornadoes near Ontario region since the 1950s, making it a tornado prone region in Canada. A qualitative assessment of the database for tornado hazard carried out by Newark (1984) revealed that, on an average, there is an F3 tornado every five years in southern Ontario. Etkin (1999) reported that occurrence of tornadoes in southern Ontario is higher than any other part of the province and there could be major economic losses due to high intensity tornadoes because of concentration of population and industries in this area. Banik et al. (2008) assessed the tornado hazard for spatially distributed systems in southern Ontario and reported that while tornado hazard for a point structure might be low, it is significantly higher for a group of structures. A quantitative assessment of outbreak (occurrence of multiple tornadoes in a brief period in a region) hazard for an idealized southern Ontario city showed that for a region of interest greater than 100 km sq. the hazard assessment was less by an order of magnitude when an outbreak event is ignored (Banik et al. (2012)). Hall and Ashley (2008) reported that if the

Plainfield, Chicago (1990) tornado had struck in the year 2000 instead, 8629 more people and 3058 more houses would have been affected (compared to the 1990 scenario), implying a 50% hike in the property damage value, due to increased concentration of population. It is inferred from the above discussion that while tornadoes might be considered rare, but due to extreme consequences, especially for well populated and industrialized regions, the associated risk (or vulnerability) is considerably high. This calls for an urgent need to study tornadoes and understand their interaction with the built environment to develop a more tornado resilient society.

The current study is aimed at investigating tornado-like flow field and its interaction with bluff bodies using numerical and experimental methods. First, a generic numerical tornado model is developed that represents the three-major existing experimental tornado simulators. The generic numerical tornado model is then used to study the interaction of tornado-like vortices with building model and the numerical results are compared (and validated) with experimentally obtained data from WindEEE and then with previously conducted study (Yang et al. (2011)) .

1.1 Background

Tornado awareness and preparedness began in the early 1950s, prompting researchers around the world to learn more about this relatively rare, yet extreme weather phenomenon. Based on the available resources and technology, the trend in studying tornadoes has been evolving and can be broadly classified into 4 eras, as following:

1950s-1960s

At the advent of this period, very little was known about tornado wind field and its interaction with terrestrial structures, therefore, several attempts were made to study real tornadoes by gathering field data. However, due to poor storm predictions, limited technological resources and violent nature of tornadoes, it was rather very difficult to record any such field measurements. As a result, researchers often resorted to inferior quality motion pictures and photogrammetric techniques to estimate tornado wind speeds and qualitatively assess the damage patterns to gain insight into tornado wind field. A breakthrough in tornado research was achieved in 1957, when a full tornado life cycle was

captured, allowing researchers, for the first time, to examine the evolution of a tornado vortex. The 1957 tornadoes of Dallas, Texas and Fargo, North Dakota were extensively studied by Hoecker (1960) and Fujita (1960), respectively, using mostly photogrammetric tools. Hoecker (1960) compared the estimated wind field of the Dallas tornado with existing wind field models for tornado-like vortices (Dinwiddie (1952) and Hoecker (1957)) and confirmed the existence of a radial convergent layer in the lower part and the exhibition of Rankine type behaviour by analyzing the radial and vertical profiles of radial and tangential velocities. However, the study was limited to only one tornado and was therefore not entirely conclusive. It was suspected that other tornadoes can have some degree of differences in their behavior. Benjamin (1962) proposed a theory for vortex breakdown phenomenon (commonly observed in tornadoes) while studying vortices formed at the leading edge of a delta wing and demonstrated that the phenomenon is not a manifestation of instability and instead, is a transition between two dynamically conjugate states of an axisymmetric flow, analogous to hydraulic jump. Bossel (1969) illustrated that the phenomenon of vortex breakdown is neither due to hydrodynamic instability nor is it analogous to hydraulic jump, but instead it is a common feature of the solution of equations of motion under those conditions. An adverse pressure gradient develops along the central axis of the core as the pressure deficit near the ground increases (while the pressure deficit in upper part of the vortex core is not as high), leading to secondary flow within the core (known as vortex breakdown). Yin and Chang (1969) made one of the earliest attempts of understanding tornadoes by studying mechanically driven vortices, produced in laboratory with the help of a rotating screen to impart swirl and an exhaust fan to drive the flow. They reported a “reversed S” shaped vertical profile of radial velocity (convergent layer) and identified the outer flow region as potential vortex. However, due to limitations in instrumentation technology during that era, they could not make flow measurements near the core region (because of interference error). Lilly (1969), using a hydrostatic core model, proposed a thermodynamic speed limit of 65m/s in tornadoes by cyclostrophically relating the wind speeds to pressure deficit in the core. A fallacy in this theory would later be explained by a group of researchers from MIT and NCAR in 1986 (Fiedler and Rutono (1986)).

1970s-1980s

This era began with the introduction of Fujita scale (F-scale) by Fujita (1971), which is a forensic scale to categorize tornadoes based on their intensities. Damage indicators investigated during post storm surveys are linked to a wind speed and the tornado is classified into one of the six levels of the F scale (F0-F5, F0 being the weakest and F5 being the strongest tornado). The first remarkable attempt of experimentally studying tornadoes was made by Neil B. Ward in 1972 at the National Severe Storm Laboratory, Oklahoma, where he built, what we now call as the "Ward Type" tornado simulator. Ward (1972) studied tornado-like vortices under the assumption that real tornadoes are low aspect ratio (less than unity) phenomena and proposed that the radial momentum flux, possessed by the outer convergent layer, was one of the key parameters in sustaining these vortices. Davies-Jones (1973) reinterpreted Ward's results and suggested that increasing radial momentum flux is counter balanced by increasing outward pressure thrust (due to counter acting centrifugal forces) and, therefore, the volume flow rate (and not radial momentum flux) is a crucial factor in the formation of tornado-like vortices. Jischke and Parang (1973) proposed that viscous torque exerted on the vortex by the boundary layer region causes transition from a single to double vortex configuration. Harlow and Stein (1974) conducted a numerical investigation of the flow structure of tornado-like vortices and reported several previously experimentally obtained results like the dependence of flow structure on swirl ratio (inflow angles) and formation of multiple vortices at higher swirl ratios. Church et al. (1977) built a tornado simulator at Purdue University by improvising the original design by Ward. The wandering of vortex reported in the previous versions of such tornado simulators was mitigated in this design, primarily by the introduction of anti-turbulence screen at the inlet that removed unwanted inflow turbulence. They conducted some preliminary studies, mostly qualitatively in nature, to verify the previously reported observations like the occurrence of vortex break down, followed by the formation of multiple vortices, along with reporting the radial and axial profiles of the velocity components. Rotunno (1978) conducted a numerical study to explore the evolution of tornado like-vortices with change in swirl ratio and, complying with previous studies, reported the observation of vortex breakdown at moderate swirl ratios, followed by a drowned vortex jump leading to multiple vortices at higher swirl

ratios. Baker and Church (1979) conducted experiments to predict core radii and peak velocities for modelled vortices of various swirl ratios. Church et al. (1979) concluded that at sufficiently high Reynold's number, vortex flow structure is nearly independent of Reynold's number and is only a function of swirl ratio. They also highlighted that the flow structure is weakly dependent of aspect ratio and therefore swirl ratio is the governing parameter. Fiedler and Rutono (1986) put forward a theory for maximum wind speeds associated with tornadoes and suggested that the fallacy in theory of maximum wind speed proposed by Lilly (1969) was the assumption of a hydrostatic core. A tornado core can sustain a greater pressure deficit because of the central downdraft (that begins after vortex breakdown) and thus leads to wind speed higher than what a hydrostatic core model would predict. Lugt (1989) studied the vortex breakdown phenomenon and the associated instabilities, the various critical conditions for single and multicell structures and differences in the conditions for helically intertwined vortices and multiple vortices.

During this period, a significant contribution was made by researchers towards understanding the flow structure of tornado-like vortices, mostly using experimental and analytical methods. However, the interaction of tornadoes with bluff bodies, the effect of ground roughness and translation on tornado flow field were still to be explored. Wen (1975) was one of the rare (if not the only) studies during this period where the effect of dynamic tornadic winds on a structure (tall building) were investigated analytically. The limitation of experimental tornado simulators at that time was that they did not facilitate translation and were relatively small so a building model of a reasonable size could not be used to study the interaction with bluff bodies.

1990s-2005

This was a period of growing computational resources and therefore, given the limitations of experimental facilities at that time, researchers turned their focus towards using numerical techniques to study tornado-like vortices and their interaction with ground surface. During this period, almost all major studies were either numerical or analytical or both. Lewellen and Lewellen (1995) used LES to simulate tornado's interaction with ground and the effect of translation. They showed that the maximum mean tangential velocity occurs within 50 metres from the ground and that translation increases turbulence

(effectively increasing peak velocities) and induces a tilt that makes the flow asymmetric. Nolan and Farrell (1999) used numerical simulations to study tornado dynamics and suggested that vortex Re ($Re_v = \frac{\Omega L^2}{\nu}$; ratio of far field circulation to eddy viscosity) could be more effective than swirl ratio to characterize tornado structure. However, researchers (particularly experimentalists) continue to use swirl ratio, which is easily measurable in an experimental set up as opposed to vortex Re (since eddy viscosity is not an easily measurable quantity and is a byproduct of turbulence modelling). Lewellen and Lewellen (1998) used LES to study "corner flow" dynamics by using appropriate boundary conditions and suggested the concept of coherent turbulence structures that could potentially cause greater damage. Selvam and Millet (2003) used Large Eddy Simulation (LES) (utilizing finite difference scheme to solve the governing equations as opposed to present day practice of using finite volume formulation) to model tornadic loads on a cubic building model and concluded that wind loads on a building due to a translating tornado were higher than those caused by quasi-steady wind. They also observed that the localized suction pressure spots on the building were higher and occurred in multiple locations. Lee and Samaras (2004) analyzed the results of HITPU deployed in the path of Manchester, South Dakota tornado (2003). Nolan (2004) proposed a scaling technique for axisymmetric flows with the introduction of additional parameters and emphasized the role of vortex Reynolds number in controlling the flow structure. They concluded that a cyclostrophic momentum balance yielded reasonable estimates of maximum tangential velocity and core radius. Lewellen and Lewellen (2006) extended their previous work on tornado ground interaction and proposed "near ground intensification" using LES.

2006-present

This period saw the rise of experimental simulation of tornado-like vortices and their interaction with scaled building models with the construction of the first large scale translating tornado simulator at Iowa State University. With advancements in instrumentation technology, an increased use of Particle Image Velocimetry (PIV) method was commonly observed in experimental studies conducted during this period. Haan et al. (2006) discusses the design, construction and performance of this tornado simulator at Iowa State University. Kuai et al. (2008) used steady CFD simulations to inspect the effect of

various geometric parameters and surface roughness on tornadic wind field. Hangan and Kim (2008) first attempted to link swirl ratio to EF scale but the investigation was limited to only one case study. They also reported $r_{c\,max}$ to increase and z_{max} to decrease with increasing swirl ratio. Sengupta et al. (2008) used LES to study transient loading on buildings due to tornadoes and downbursts and found that the peak loads exceed the ASCE 7-05 provisions for ABL wind load by 1.5 times for F2 scale tornadoes. Mishra et al. (2008) analyzed the flow field and pressure profiles produced in TTU-VSII and obtained a length scale of 1: 3500 (for TTU-VSII produced vortices) by using cyclostrophic momentum balance. They proposed the construction of a larger simulator called VorTECH at TTU since the length of TTU-VSII was found to be an order of magnitude smaller than typical wind engineering length scales. Mishra et al. (2008) analyzed the forces and pressure coefficients on a cubic building model placed in TTU-VSII in various locations with respect to the vortex centre and demonstrated the inadequateness of scaling up straight line wind Cp for evaluating tornadic loads. They also emphasized on the need to construct a larger testing facility (VorTECH) to host building models of reasonable sized. Xu and Hangan (2009) analytically modelled inviscid tornado-like vortex using a free narrow jet solution combined with a modified Rankine vortex and the analytically obtained velocity components showed good agreement with experimental and numerical results. They also highlighted that experimental inputs could improve the robustness of their analytical model. Tamura (2009) discusses the influence of inflow conditions and swirl ratio on tornado-like vortices but was unable to confirm the appearance of multiple vortices at higher swirl ratio (expanded core only) in the experimental tornado simulator in Japan. Sabareesh et al. (2009) compared the surface pressure distribution on a cubic building under ABL and tornadic wind loading and found significant differences in statistical values of Cp. Haan et al. (2010) tested low-rise buildings under tornadic loading and reported peak loads up to 50% higher than ABL wind load provisions in ASCE-7-05. Hashemi et al. (2010) conducted PIV measurements to analyze the flow field of laboratory produced tornado-like vortices at a wide range of swirl ratios. They demonstrated the occurrence of maximum tangential and radial velocities close to the ground surface and reported an increase in shear stresses with an increase in swirl ratio due to the turbulent nature of the vortex at higher swirl ratios. Thampi et al. (2011) studied the impact of tornadoes on a

typical low-rise gable roof structure and progressively modeled the damage using finite element analysis. They reported a significant reduction in wind loads due to tornadoes once the roof was blown off for such structures. Yang et al. (2011) conducted PIV and force measurements on a high-rise building model and discussed the structure of highly turbulent wake around the building, along with variations in forces and moments with respect to building position. Zhang and Sarkar (2012) conducted experiments in a 1:3 scaled model version of the tornado simulator at ISU and quantified the extent of underestimation of tangential velocity and core radius due to wandering effects. Natarajan and Hangan (2012) used LES to study translational and roughness effects, reported reduction in max mean tangential velocity at lower swirl ratio and increase at higher swirl ratio. While Sabareesh et al. (2013) investigated the effect of openings in a building on peak roof loads under tornado-like wind, Sabareesh et al. (2013) studied the effect of ground roughness on internal pressure characteristics of a building subjected to tornado-like wind field. Case et al. (2014) experimentally studied the effect of low rise building geometry on tornado induced loads and found the peak loads to vary with eave height, pitch, aspect ratio etc. They highlighted the importance of adequate design of roof to wall connections for tornado resistant (up to EF3) design of low rise building. Refan et al. (2014) used a model of WindEEE as a proof of concept for WindEEE dome and developed a unique scaling technique to link laboratory produced vortices to real tornadoes. Refan (2014) conducted extensive PIV measurements to analyze tornado flow field in model WindEEE (1:11 scale replica of WindEEE Dome). Hangan (2014) discusses the design of the Wind Engineering Engery and Environment (WindEEE) Dome that was built at Western University and is a hexagonal shaped 3-D wind chamber capable of producing both synoptic and non-synoptic wind fields. Refan and Hangan (2016) showed the independence of flow structure and radial Reynolds number (above a threshold value) and its dependence of swirl ratio, for vortices produced in model WindEEE. Hanagn et al. (2016) discussed the application of the Wind Engineering Energy and Environment (WindEEE) Dome towards simulation of a large variety of wind systems (synoptic and non-synoptic).

More recently, Refan et al. (2017) demonstrated the independence of pressure distribution on a building model and radial Reynold's number. Karami et al. (2017) proposed Proper Orthogonal Decomposition (POD) method to extract the coherent structures in fluctuating

pressure field, enabling the reconstruction of large scale fluctuating pressure field. Nasir and Bitsuamlak (2016) used CFD (numerical methods) to study the effects of topographical changes on tornadic wind field and developed FSUR (fractional speed up ratio) for tornadoes analogous to straight-line ABL wind. Nasir and Bitsuamlak (2016) also computationally evaluated the effects of tornadic loads on a tall building. Nasir (2017) investigated the effect of tornado-like wind on typical flat roof mid-rise building and high-rise building and discussed the resulting surface pressure distribution and forces with respect to building location and orientation. Nasir (2017) also showed that for a building with opening(s), the external surface pressure distribution is sensitive to opening configuration, internal pressure, building location (for stationary vortex), building orientation and tornado translation. Kopp and Wu (2017) proposed the use of quasi-steady models to develop a framework to assess wind loads due to tornadoes while examining the differences in tornado and atmospheric boundary layer flow structures. They discussed the similarities and differences in wind loads predicted using quasi-steady theory and demonstrated the promise QS displayed for such purpose. Vickery et al. (2017) highlighted the problem in directly comparing external surface pressure coefficients due to tornadoes and ABL wind due to differences in normalizing velocity and due to local atmospheric pressure change experienced during tornadoes. They also compared their tornado load model, which accounts for debris and varying internal pressure, with damage observed during the Joplin tornado.

1.2 Motivation and objective

It is a common practice in experimental studies to use the geometric dimensions and configuration of physical elements (like guide vane angle, ceiling height, etc.) of the experimental simulators to characterize the generated vortices. However, the inherent differences in geometric dimensions and vortex generation mechanism of the existing experimental tornado simulators makes vortex characterization very specific to an individual facility and hinders direct comparison and validation of results.

In this research, it is envisioned to develop a simple, generic numerical model that would fit the flow structure of a tornado-like vortex and account for the geometric and mechanical differences in different experimental facilities while replicating the original flow field as

accurately as possible. To achieve this, the parameters used to characterize a tornado-like vortex (inflow depth, radius of updraft, etc.) are strictly extracted from the numerically produced flow-field inside the tornado simulators (as opposed to using physical dimensions of the simulators) during the development of the generic numerical tornado model. The developed generic numerical tornado model can then be used to directly compare results from different experimental simulators and facilitate a universal/common interpretation. The utility of this numerical model for bluff-body aerodynamics applications and wind-load evaluation is further demonstrated.

1.3 Thesis layout

This thesis is written in the integrated article format. Chapter 1 presents a brief introduction to tornado research. Chapter 2 is focused on developing a generic numerical tornado model. Chapter 3 discusses the application of this generic numerical tornado model to bluff-body aerodynamics and wind load evaluation. Chapter 4 presents the conclusions made from this study and lays out the scope of future research.

References

[1] Baker G.L., and Church C.R. "Measurements of core radii and peak velocities in modeled atmospheric vortices." *Journal of the Atmospheric Sciences* 36.12 (1979): 2413-2424.

[2] Banik S. S., Hong H. P., and Kopp G.A. "Assessment of tornado hazard for spatially distributed systems in southern Ontario." *Journal of Wind Engineering and Industrial Aerodynamics* 96.8 (2008): 1376-1389.

[3] Banik S. S., Hong H. P., and Kopp G.A. "Assessment of the wind hazard due to tornado outbreaks in southern Ontario." *Journal of Wind Engineering and Industrial Aerodynamics* 107 (2012): 28-35.

[4] Benjamin T.B. "Theory of the vortex breakdown phenomenon." *Journal of Fluid Mechanics* 14.4 (1962): 593-629.

[5] Bossel H. H. "Vortex breakdown flow field." *The Physics of Fluids* 12.3 (1969): 498-508.

[6] Case J, Sarkar P, and Sritharan S. "Effect of low-rise building geometry on tornado-induced loads." *Journal of Wind Engineering and Industrial Aerodynamics* 133 (2014): 124-134.

[7] Church C. R., Snow J. T, and Agee E.M. "Tornado vortex simulation at Purdue University." *Bulletin of the American Meteorological Society* 58.9 (1977): 900-908.

[8] Church C. R., Snow J. T, and Agee E.M. "Characteristics of tornado-like vortices as a function of swirl ratio: A laboratory investigation." *Journal of the Atmospheric Sciences* 36.9 (1979): 1755-1776.

[9] Davies-Jones R.P. "The dependence of core radius on swirl ratio in a tornado simulator." *Journal of the Atmospheric Sciences* 30.7 (1973): 1427-1430.

[10] Dinwiddie F.B., “Waterspout-Tornado Structure and Behavior at Nags Head, N.C., August 12, 1952,” *Monthly Weather Review*, Vol. 87, No. 7, July 1959, pp. 239-250.

[11] Etkin D. A. "Extreme events and natural disasters in an era of increasing environmental change." *Report of Workshop on Emerging Environmental Issues in Ontario. Environmental Monograph*. Vol. 15. 1999.

[12] Fiedler B.H., and Rotunno R. "A theory for the maximum windspeeds in tornado-like vortices." *Journal of the Atmospheric Sciences* 43.21 (1986): 2328-2340.

[13] Fujita T.T. “A detailed analysis of the Fargo tornadoes of June 20, 1957.” Vol. 30. *US Government Printing Office*, 1960.

[14] Fujita T.T. "Proposed characterization of tornadoes and hurricanes by area and intensity." (1971).

[15] Haan Jr, F L., Sarkar P.P, and Gallus W.A. "Design, construction and performance of a large tornado simulator for wind engineering applications." *Engineering Structures* 30.4 (2008): 1146-1159.

[16] Haan Jr, F. L., Balaramudu V.K, and Sarkar P. P. "Tornado-induced wind loads on a low-rise building." *Journal of Structural Engineering*136.1 (2009): 106-116.

[17] Hall S.G., and Ashley W.S. "Effects of urban sprawl on the vulnerability to a significant tornado impact in northeastern Illinois." *Natural Hazards Review* 9.4 (2008): 209-219.

[18] Hangan H., and Kim J. D. "Swirl ratio effects on tornado vortices in relation to the Fujita scale." *Wind and Structures* 11.4 (2008): 291-302.

[19] Harlow F.H., and Stein L.R. "Structural analysis of tornado-like vortices." *Journal of the Atmospheric Sciences* 31.8 (1974): 2081-2098.

[20] Hangan H., “The Wind Engineering Energy and Environment (WindEEE) Dome at Western University, Canada”, *Wind Engineers, JAWE*, Vol. 39, No.4 (2014)

[21] Hangan H., Refan M., Jubayer C., Parvu G., ""Big Data from Big Experiments. The WindEEE Dome", Springer Verlag, 2016.

[22] Hashemi T.P., Gurka R., and Hangan H. "Experimental investigation of tornado-like vortex dynamics with swirl ratio: the mean and turbulent flow fields." *Journal of Wind Engineering and Industrial Aerodynamics* 98.12 (2010): 936-944.

[23] Hoecker Jr, W.H., "The Dimensional and Rotational Characteristics of the Tornadoes and Their Cloud System," pp. 53- 113 of "The Tornadoes at Dallas, Tex., April 2, 1957," Research Paper No. 41, *U.S. Weather Bureau*, Washington, D.C., 180 pp. (in press).

[24] Hoecker Jr, W. H. "Wind speed and air flow patterns in the Dallas tornado of April 2, 1957." *Monthly Weather Review* 88.5 (1960): 167-180.

[25] Jischke M. C., and Parang M. "Properties of simulated tornado-like vortices." *Journal of the Atmospheric Sciences* 31.2 (1974): 506-512.

[26] Karami M., Romanic D., Maryam R., and Hangan H. "Modelling of tornado-like vortices." *100 Islands Fluid Mechanics Meeting, Ontario, Canada*. 2017.

[27] Kopp G.A and Wu C.H. "A framework for the aerodynamics of low-rise buildings in tornadoes: Can boundary layer wind tunnels give us everything we need?" *13th Americas Conference on Wind Engineering, Florida, USA*. 2017.

[28] Kuai Le, et al. "CFD simulations of the flow field of a laboratory-simulated tornado for parameter sensitivity studies and comparison with field measurements." *Wind and Structures* 11.2 (2008): 75-96.

[29] Lee J.J., Samaras T., and Young C. R. "Pressure measurements at the ground in an F-4 tornado." *Preprints, 22nd Conf. on Severe Local Storms, Hyannis, MA, Amer. Meteor. Soc., CD-ROM*. Vol. 15. 2004.

[30] Lewellen W. S., Lewellen D. C., and Sykes R. I. "Large-eddy simulation of a tornado's interaction with the surface." *Journal of the Atmospheric Sciences*54.5 (1997): 581-605.

[31] Lewellen D. C., Lewellen W. S., and Xia J. "The influence of a local swirl ratio on tornado intensification near the surface." *Journal of the Atmospheric Sciences* 57.4 (2000): 527-544.

[32] Lewellen D. C., and Lewellen W. S. "Near-surface intensification of tornado vortices." *Journal of the Atmospheric Sciences* 64.7 (2007): 2176-2194.

[33] Lilly K. "Tornado dynamics." (1969). *National Center for Atmospheric Research Manuscript* 69-117.

[34] Lugt H. J. "Vortex breakdown in atmospheric columnar vortices." *Bulletin of the American Meteorological Society* 70.12 (1989): 1526-1537.

[35] Matsui M, and Tamura Y. "Influence of swirl ratio and incident flow conditions on generation of tornado-like vortex." *Proc. 5th European-African Conferences on Wind Engineering, Florence, Italy*. 2009.

[36] Mishra A., R., Darryl L.J, and. Letchford C.W. "Physical simulation of a single-celled tornado-like vortex, part A: flow field characterization." *Journal of Wind Engineering and Industrial Aerodynamics* 96.8 (2008): 1243-1257.

[37] Mishra A. R., James D. L., and Letchford C. W. "Physical simulation of a single-celled tornado-like vortex, Part B: Wind loading on a cubical model." *Journal of Wind Engineering and Industrial Aerodynamics* 96.8 (2008): 1258-1273.

[38] Nasir Z., and Bitsuamlak G.T. "NDM-558: Computational modeling of Tornadic Load on a Tall Building." *CSCE Annual Conference, London Convention Center, London, Ontario, Camada* 2016.

[39] Nasir Z., and Bitsuamlak G.T. "NDM-557: Computational Modeling of Hill Effects on Tornado-like Vortex." *CSCE Annual Conference, London Convention Center, London, Ontario, Camada* 2016.

[40] Nasir Z., “Numerical modeling of tornado-like vortex and its interaction with bluff-bodies." *PhD Thesis. Western University, Canada* (2017).

[41] Natarajan D., and Hangan H. "Large eddy simulations of translation and surface roughness effects on tornado-like vortices." *Journal of Wind Engineering and Industrial Aerodynamics* 104 (2012): 577-584.

[42] Newark M. J. "Canadian tornadoes, 1950–1979." *Atmosphere-Ocean*22.3 (1984): 343-353.

[43] Nolan D.S., and Farrell B.F. "The structure and dynamics of tornado-like vortices." *Journal of the Atmospheric Sciences* 56.16 (1999): 2908-2936.

[44] Nolan D. S. "A new scaling for tornado-like vortices." *Journal of the atmospheric sciences* 62.7 (2005): 2639-2645

[45] Rajasekharan S.G., Matsui M., and Tamura Y. "Characteristics of internal pressures and net local roof wind forces on a building exposed to a tornado-like vortex." *Journal of Wind Engineering and Industrial Aerodynamics* 112 (2013): 52-57.

[46] Refan M., Hangan H., and Wurman J. "Reproducing tornadoes in laboratory using proper scaling." *Journal of Wind Engineering and Industrial Aerodynamics* 135 (2014): 136-148.

[47] Refan M. "Physical simulation of tornado-like vortices." *PhD Thesis. Western University, Canada* (2014).

[48] Refan M., and Hangan H. "Characterization of tornado-like flow fields in a new model scale wind testing chamber." *Journal of Wind Engineering and Industrial Aerodynamics* 151 (2016): 107-121.

[49] Refan M and Hangan H. "Surface pressures dependency on Reynolds number and swirl ratio in tornado-like vortices." *13th Americas Conference on Wind Engineering, Florida, USA*. 2017.

[50] Rotunno R. "A study in tornado-like vortex dynamics." *Journal of the Atmospheric Sciences* 36.1 (1979): 140-155.

[51] Sabareesh G. R., et al. "Pressure acting on a cubic model in boundary-layer and tornado-like flow fields." *Proceedings of the 11th American Conference on Wind Engineering, Puerto Rico, USA*. 2009.

[52] Sabareesh G.R, Matsui M., and Tamura Y. "Ground roughness effects on internal pressure characteristics for buildings exposed to tornado-like flow." *Journal of Wind Engineering and Industrial Aerodynamics* 122 (2013): 113-117.

[53] Selvam R. P, and Millett P.C. "Computer modeling of tornado forces on a cubic building using large eddy simulation." *Journal of the Arkansas Academy of Science* 57.1 (2003): 140-146.

[54] Sengupta A., Haan Jr F.L., Sarkar P., and Balaramudu V. "Transient loads on buildings in microburst and tornado winds." *Journal of Wind Engineering and Industrial Aerodynamics* 96.10 (2008): 2173-2187.

[55] Thampi H., Dayal V., and Sarkar P. "Finite element analysis of interaction of tornados with a low-rise timber building." *Journal of Wind Engineering and Industrial Aerodynamics* 99.4 (2011): 369-377.

[56] Vickery J.P, Banik S, Twisdale Jr. L., and Long P. Tornado damage modelling: Understanding the role of local atmospheric change, wind directionality, and transient wind field intensity" *13th Americas Conference on Wind Engineering, Florida, USA*. 2017.

[57] Ward N. B. "The exploration of certain features of tornado dynamics using a laboratory model." *Journal of the Atmospheric Sciences* 29.6 (1972): 1194-1204

[58] Wen Y.K. "Dynamic tornadic wind loads on tall buildings." *ASCE Journal of the Structural Division* 101.1 (1975): 169-185.

[59] Xu Z. and Hangan H. "An Inviscid Solution for Modeling of Tornado-like Vortices." *ASME Journal of Mechanics*, DOI 101115/1.3063632, Vol. 76, 031011 (5pp), 2009.

[60] Yang Z., Sarkar S., and Hu H. "An experimental study of a high-rise building model in tornado-like winds." *Journal of Fluids and Structures* 27.4 (2011): 471-486

[61] Ying S. J., and Chang C. C. "Exploratory model study of tornado-like vortex dynamics." *Journal of the Atmospheric Sciences* 27.1 (1970): 3-14.

[62] Zhang W., and Sarkar P. "Near-ground tornado-like vortex structure resolved by particle image velocimetry (PIV)." *Experiments in Fluids* 52.2 (2012): 479-493.

Chapter 2

2 Generic numerical tornado model for common interpretation of existing experimental simulators

The current state of the art in studying tornado-like vortices at engineering scale (which is to be differentiated from meteorological scale, for example Orf et al. (2014), Orf et al. (2016)) dictates the use of mechanically driven vortices in experimental simulators. However, the differences in mechanisms utilized to produce these vortices coupled with the physical limitations of measuring various characterizing parameters of a tornado-like vortex (aspect ratio, swirl ratio etc.) in an experimental set up and geometric differences in various facilities, often lead to misinterpretation of results and makes these results very specific to the experimental set-up in consideration. The present study develops a generic numerical simulator that unifies the existing experimental simulators and facilitates a universal interpretation. For this purpose, VorTECH at Texas Tech University (TTU), Tornado Simulator at Iowa State University (ISU) and WindEEE Dome at Western University (WU), are chosen as representatives of "Ward" type, "top-down" type and "3D wind chamber" type simulators, respectively. In the first stage, each experimental simulator is numerically modelled without any simplification (or modification) and placed in a bigger computational domain to simulate its placement in a lab environment with closed-circuit flow. Then, the relevant boundary conditions and flow parameters are extracted for different configurations of each physical simulator to allow simplification of the original models during the second stage of the study. The simplification of the original models is primarily based on the geometric and kinematic parameters used to characterize these vortices, obtained from the numerical results of the first stage and the type of flow in the original models (bounded or unbounded). The parameters (geometric and kinematic) used to characterize a vortex (inflow depth, radius of updraft, swirl, etc) are strictly obtained from the flow-field as opposed to the commonly observed practice of directly using the geometric dimensions and configuration of physical elements (like guide vane angle, ceiling height, etc) of the experimental simulators. Although the flow structure of tornado-like vortices is seen to be independent of the radial Re_r (above $Re_r \sim 10^4$), which is consistent with previous studies (Church et al. (1979)), a calibration of the velocity

magnitude (Re_r or volume flow rate) is conducted, as and when required, to maintain similar magnitudes of velocities and pressures in the flow field apart from preserving the original flow structure. The analysis of the velocity and pressure profiles obtained from the original models leads to a generic simplified numerical tornado model, which can still be linked to the experimental simulators using a unique calibration scheme developed during this study. Thus, a numerical tornado model is obtained that could (i) aid in linking the interpretation of results between the various experimental simulators, and (ii) produce preliminary tornado design parameters numerically.

2.1 Tornado-like vortices

Experimentally and numerically produced vortices are most commonly characterized by three non-dimensional parameters, aspect ratio (geometric), swirl ratio (kinematic) and radial Reynolds number (dynamic), which are defined below.

Aspect ratio (a): $a = \frac{h_0}{r_0}$, here h_0 is the inflow depth and r_0 is the radius of updraft ($v_z \approx 0$ approximation should hold good at $r = r_0$). It is widely believed that tornadoes are low aspect ratio (less than or around unity) phenomena in nature (Ward (1972), Davies-Jones (1973), etc).

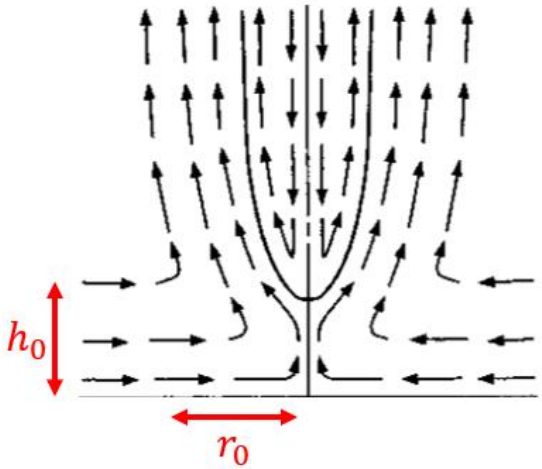

Figure 2-1 Tornado flow structure as shown depicted in Davies-Jones (1981)

Swirl ratio (S): $S = (\frac{v_t}{v_r.2a})_{r=r_0} = (\frac{r_0\Gamma_\infty}{2Qz})_{r=r_c}$

Here, v_t is tangential velocity, v_r is radial velocity, a is aspect ratio, r_0 is the radius of updraft, r_c is the core radius, Q is the volume flow rate per unit axial length and z is the axial location, Γ_∞ is the maximum circulation, which is further defined as following (integral below is evaluated along the circumference of the core).

$$\Gamma_\infty = \oint v_t \, dr$$

Swirl ratio is a function of position, i.e. $S(r, z)$. Thus, swirl ratio definition would yield different values at various locations in the wind field. Although, no clear guidelines were found in previous studies regarding the location of calculating swirl ratio, Refan (2014) demonstrated that the angle based definition applied at the radius of updraft yields values close to those obtained by applying the circulation based definition at the core radius. Therefore, care must be taken while calculating swirl ratio, to avoid any discrepancy in results. Due to uncertainties associated with core radius measurements (because of vortex wandering) needed for circulation based definition, the inflow angle based definition (applied at the radius of updraft) is used throughout the analysis in the present study.

Radial Reynolds Number (Re_r): $Re_r = \frac{Q}{2\nu}$, Q is the volume flow rate per unit axial length and ν is the kinematic viscosity. Church (1979) showed the independence of flow structure from radial Reynolds number (provided Re_r is above $\sim 10^4$).

It should be noted that the above parameters are not identifiable for real tornadoes and therefore linking simulated (experimentally and numerically) vortices to real tornadoes remains one of the biggest challenges. In this regard, Refan et al. (2014) proposed a unique scaling technique to link simulated vortices to real tornadoes using a common length scale (axial and radial), developed during a matching process. Therefore, a simulated vortex at a specific swirl ratio could replicate the aerodynamic effects of a real tornado (or a target tornado) at a certain length scale, provided the flow structure of the simulated vortex bears enough resemblance with the target tornado.

2.1.1 Tornado-like wind field description

Mathematically, a two-dimensional sink vortex (in r- θ plane) can be characterized as

$$(v_t + v_r)r = C \qquad \textbf{Equation 2-1}$$

Where v_t and v_r are the tangential and radial components of the velocity and C is a constant. The equation above can be further decomposed as following,

$$v_t r = c_1 \qquad \textbf{Equation 2-2}$$

$$v_r r = c_2 \qquad \textbf{Equation 2-3}$$

Here, c_1 and c_2 are constants. Equation 2-2 arises from conservation of angular momentum while Equation 2-3 arises from conservation of mass in the r- θ plane for 2-dimensional flow.

However, tornado-like wind field is 3-dimensional in nature with significant axial velocity (v_z). Due to the three dimensionality of a tornado-like wind field, the constraint imposed by Equation 2-3 is removed.

$$v_r r \neq c_2 \qquad \textbf{Equation 2-4}$$

The flow is now free to expand along the r-z plane as it approaches the core region and the loss of radial momentum is seen in the form of increasing axial flux. The flow field (depicted by streamlines), outside core region is spiral with significant radial velocity. However, there is a constant trade-off between axial and radial velocities as the flow approaches the core, resulting in loss of radial momentum. Tangential velocity, on the other hand, constantly increases towards core region, due to conservation of angular momentum (Equation 2-2). The core, also seen as the limit of radial convergence, is that region in tornado-like wind field where the converging force (possessed by radial momentum) is counter balanced by the centrifugal force (possessed by angular momentum). As a result of this balance, the flow wraps itself into a tight spin, rotating a column of air like a solid

body under its shear, thereby forming the core. The flow in the core region has negligible radial velocity and is dictated only by tangential velocity, so the streamlines inside the core are ideally expected to be concentric circles. This solid body rotation of core results in a linearly decreasing tangential velocity towards the centre, as shown below.

$$v_t = \omega r \qquad \textbf{Equation 2-5}$$

Similar behaviour of tangential velocity along the radial direction is also seen in the modified Rankine vortex model (shown in Equation 2-6) , which is one of the most commonly adopted model for describing the radial profile of tangential velocity in tornado-like wind field.

$$v_t(\mathrm{r}) = \frac{r\Gamma_\infty}{\pi(r^2 + r_c^2)} \qquad \textbf{Equation 2-6}$$

It should be noted that the above description of tornado wind field is idealized and the wind field of real (and experimental) tornadoes can have deviations from this description due to interaction with ground and translational effects. The description of flow field within the core fits better for a hydrostatic core model and thus tends to deviate at higher swirl ratio due to vortex breakdown. Further, even for low swirl ratios, the idealized description of the vortex may not fit exactly due to instabilities associated with low swirl vortex cores. A detailed explanation of these deviations is, however, beyond the scope of the present work. This description of tornado wind field, none the less, forms the basis of numerical modelling of tornadoes. It is expected that the ease of simplification process and the accuracy of the generic model proposed in this study would also depend (to some extent) on how closely the experimentally produced wind field matches the idealized mathematical description explained in this section.

2.1.2 Simplification strategy for numerical simulation of tornado-like vortices

The simplification of experimental tornado simulators into one numerical model is based on identifying the characterizing parameters for various configurations of each experimental facility and then utilizing them for a generic model. These parameters like radius of updraft, inflow depth, etc, are strictly obtained from the flow-field inside the experimental simulators (generated numerically), as opposed to directly using the physical dimensions of the experimental facilities to obtain the same. First the geometric parameters of the flow structure are identified, i.e. inflow depth (h_0) and radius of updraft (r_0). An important characteristic of the flow at the radius of updraft is that $v_z \approx 0$ approximation should hold good (negligible updraft). Then, the geometric parameters of the physical simulator are identified, i.e. height of location of updraft hole (or bell mouth of the exhaust region) (h_u), and the radius of the updraft of hole (or bell mouth) (r_u). It will be seen in the sections to follow that the effective radius of updraft hole may or may not be equal to the actual radius of the physical updraft hole in an experimental set-up. Thus, for each configuration, the flow geometric parameters (h_0 and r_0) and simulator geometric parameters (h_u and r_u) dictate the dimensions of the simplified computational domain, while the kinematic parameter (swirl ratio or ratio of v_t and v_r at inlet) governs the inflow boundary condition. This has been illustrated in Figure 2-2. The height of the convection region is kept 15 times h_u ("far enough") to allow the top of the cylindrical domain to be treated as "pressure outlet" boundary. In the initial phase of this study, different heights of the convection region were simulated (25 times h_u , 20 times h_u, etc). It was found that while in an experimental set-up, the height of convection region could affect the flow structre (due to the location of honeycomb section to decouple the fan vorticity), but in a simplified numerical model, this height of convection region was found to be independent of flow structure, at least upto 15 times h_u. Further reduction in the height of the convection region might be possible, but that would require an independent parametric study. For the present research, we will use 15 h_u, as the height of convection region). A crucial difference between bounded systems like VorTECH and unbounded systems like ISU Tornado Simulator and WindEEE is that the for bounded system $h_0 = h_u$ (inflow in bounded) while for unbounded systems $h_0 < h_u$. This has been illustrated in Figure 2-3.

At last, the inflow velocities v_t and v_r are identified (no v_z since $v_z \approx 0$ at r_0). The idea is to use "double concentric" cyclinders as shown in Figure 2-2 that would require only uniform tangential and radial velocities (the inflow velocity profiles at the radius of updraft were observed to be uniform, and will be shown in the following sections) as the inflow boundary condition, but could still replicate the laboratory produced flow field as accurately as possisble.

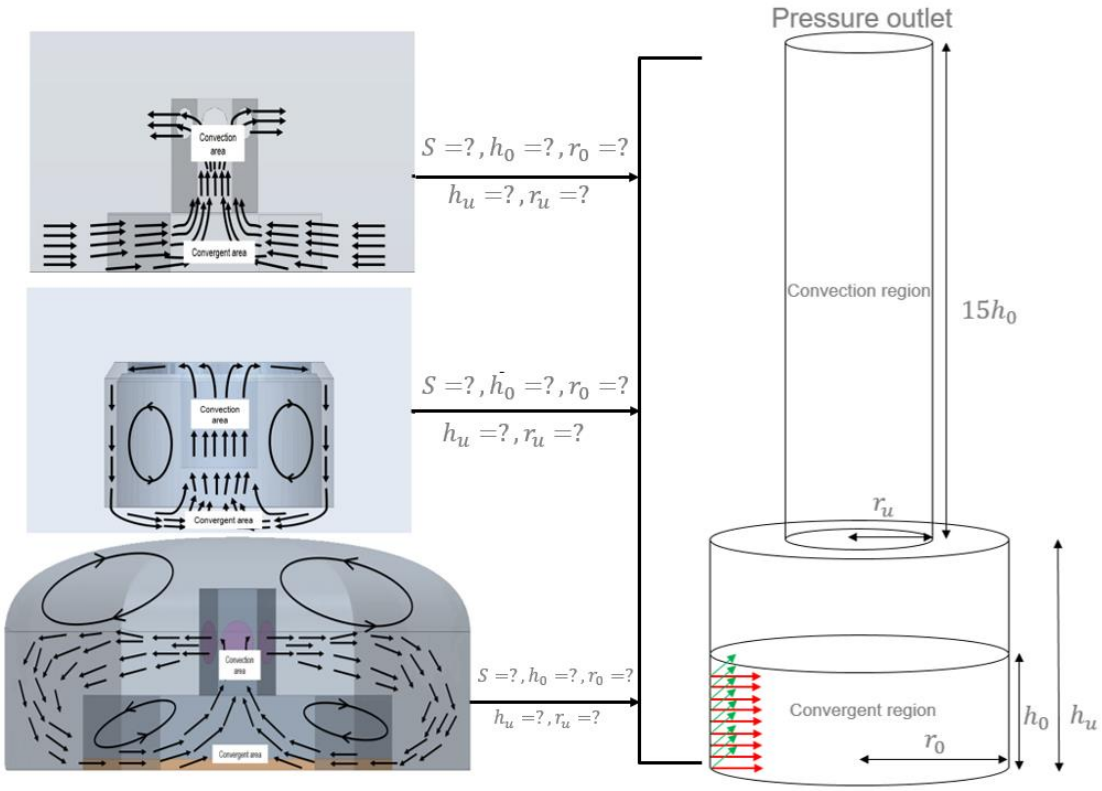

Figure 2-2 Simplification strategy.

During this study, the ground static pressure profile, radial profile of tangential velocity at various heights and qualitative appearance of the vortex flow structure are used to compare the flow-fields obtained from full CFD models (of each experimental facility) with those obtained from generic numemrical model. Further, for comparing ground static pressure profiles, all pressures are referenced to the ground static pressure at the radius of updraft (i.e. with conditions upstream of the flow), previously done by Nasir (2017) for numerical tornado simulation.

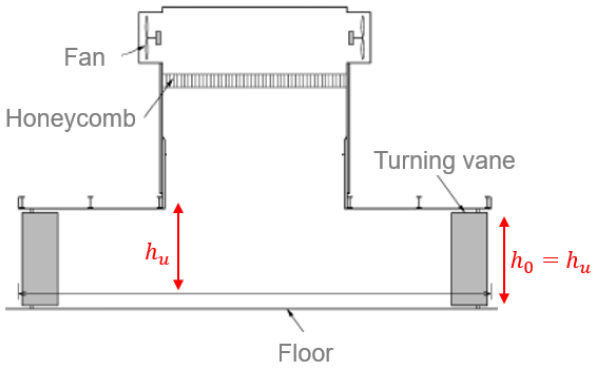

(a) VorTECH at Texas Tech University (bounded flow)

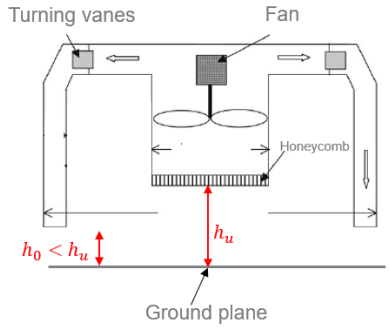

(b) Tornado Simulator at Iowa State University (unbouned flow)

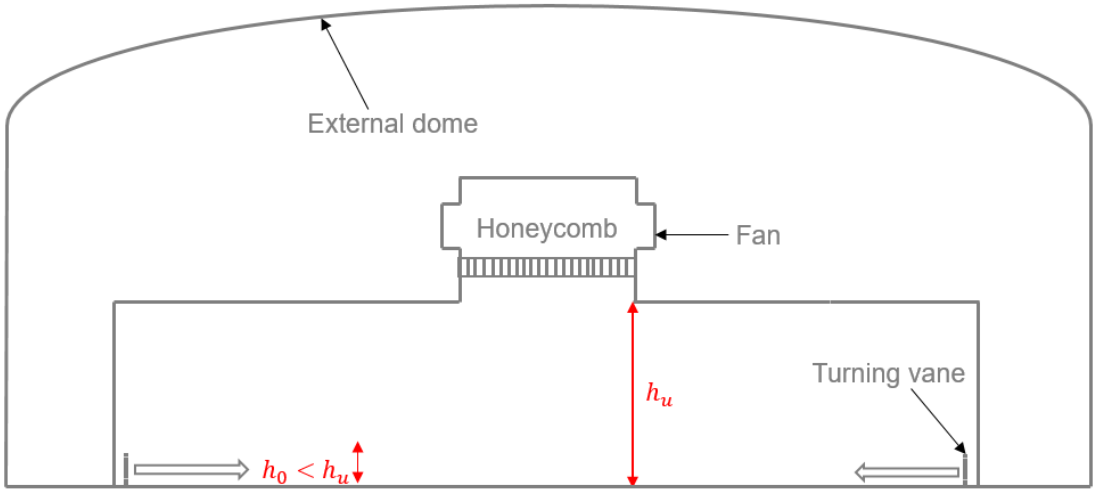

(c) WindEEE Dome at Western University (unbounded flow)

Figure 2-3 Illustration of difference between bounded and unbounded flow.

The idea behind this study is that while various experimental facilities might have their differences (geometric dimensions and vortex generation mechanism), they can still be unified with a generic numerical model, if the characterizing parameters are extracted from the flow field inside the experimental simulators, as opposed to using geometric dimensions of the facilities to obtain them. This has been illustrated in Figure 2-4.

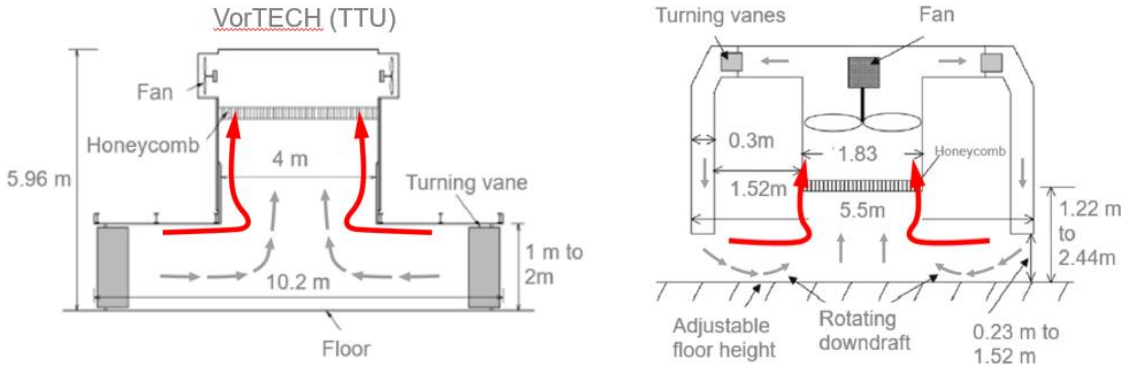

(a) VorTECH at TTU (b) Tornado Simulator at ISU

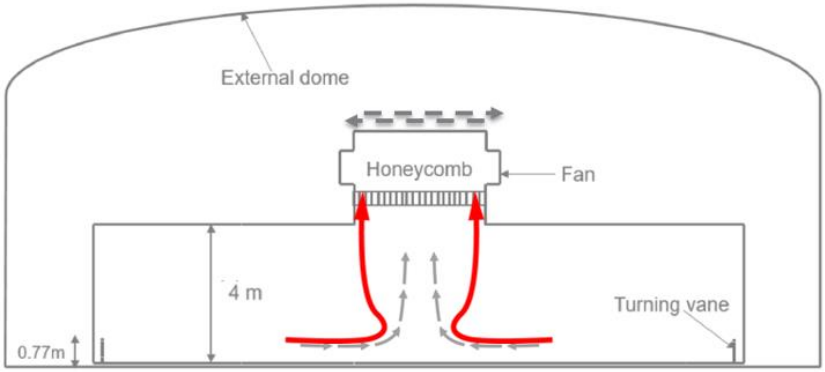

(c) WindEEE Dome at WU

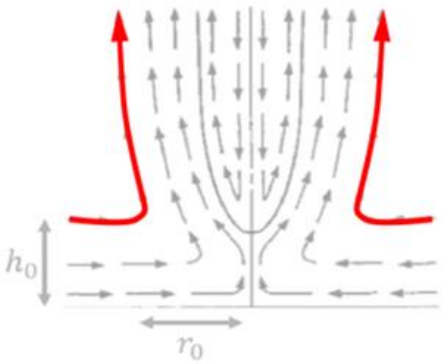

(d) Tornado-like vortex flow structure

Figure 2-4 Unification of experimental facilities.

The configurations for each facility considered in the present study have been summarized in Table 2-1. The details of configurations for TTU VorTECH and ISU Tornado Simulator were obtained from Mayer (2010) and Haan et al. (2008) respectively.

VorTECH (TTU)	Tornado Simulator (ISU)	WindEEE Dome (Western)
10- degree (vane angle) 20- degree (vane angle) 30- degree (vane angle) 40- degree (vane angle) 50- degree (vane angle) 60- degree (vane angle) 70- degree (vane angle)	Vane 1 Vane 2 Vane 3 Vane 4 Vane 5 Fan 1 Fan2 Fan3 Floor 1 Floor 2 Floor3	15-degree (vane angle)

Table 2-1 Summary of configurations considered.

It should be noted that due to unavailability of documentation of other configurations of WindEEE and time constrain posed during this study, only one WindEEE configuration was considered. It would be desirable to simulate more WindEEE configurations for future studies.

2.2 Experimental tornado simulators

A brief description of the three experimental tornado simulation facilities in consideration has been presented in this section.

2.2.1 VorTECH at Texas Tech University

VorTECH at Texas Tech University, inspired by the original design built by Ward (1972), is an octagonal shaped experimental tornado simulator that is driven by 8 exhaust fans, installed in a 4-m wide upper chamber. The lower chamber (10.2-m wide) consists of 64 guide vanes at the inlet that can be set to various angles to impart desired swirl to the flow. The schematic of this simulator, adapted from Zhou et al. (2016), is shown in Figure 2-5 This simulator can generate tornado like vortices with aspect ratios ranging from 0.5 to1, swirl ratios ranging from 0 to 2.2 and Re_r of the order of 10^5 (Zhou et al. (2016)). The aspect ratio is changed by altering the ceiling height of the lower chamber with the help of a sliding neck that connects the lower and upper chamber. To facilitate a varying aspect

ratio, guide vanes were built with a dual height design and can be dismantled into half height to lower the bottom chamber ceiling as explained in Mayer (2010). The present design allows two pre-set aspect ratios (0.5 and 1) and to provide any other aspect ratio, a new set of guide vanes with suitable height would have to be fabricated. The swirl ratio is controlled by guide vane angles and Re_r is controlled by the rpm of exhaust fans. A honeycomb section is located between the experimental volume and exhaust fan region to remove any unwanted vorticity and turbulence imparted by the rotation of fans. The flow is bounded (inflow is protected by a physical wall on top) so the simulator can only produce stationary vortices since the upper chamber is fixed to the lower chamber.

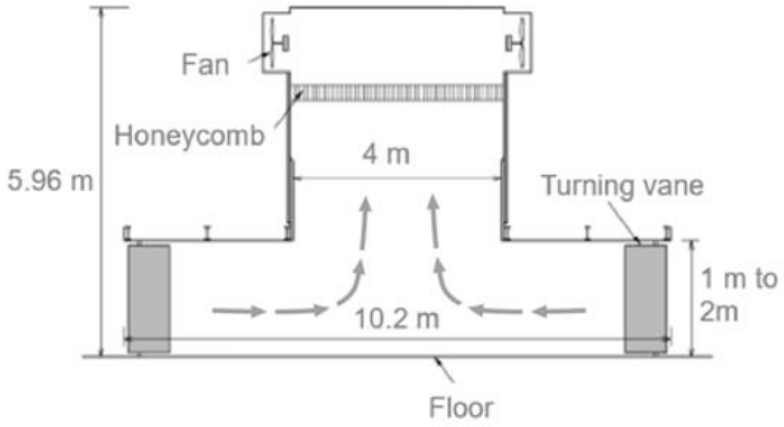

Figure 2-5 VorTECH at Texas Tech University schematic adapted from Zhou et al. (2016).

2.2.2 Tornado Simulator at Iowa State University

Tornado simulator at Iowa State University has a unique "top-down" design, which was adapted to facilitate translation. The simulator, consisting of a 0.3 m wide cylindrical annular duct suspended upside down from a crane, drives the flow with a 1.83 m wide exhaust fan and utilizes a forced rotating downdraft mechanism as explained in Haan et. al (2008). While, 37 guide vanes are located at the top of the duct to impart swirl to the flow, an adjustable height ground plane is used to change aspect ratio. Like other experimental facilities, a honeycomb section is located between the experimental volume and exhaust

fan region to remove any unwanted vorticity and turbulence imparted by the rotation of fans. A schematic of the design, adapted from Haan et. al (2008), is presented in Figure 2-6.

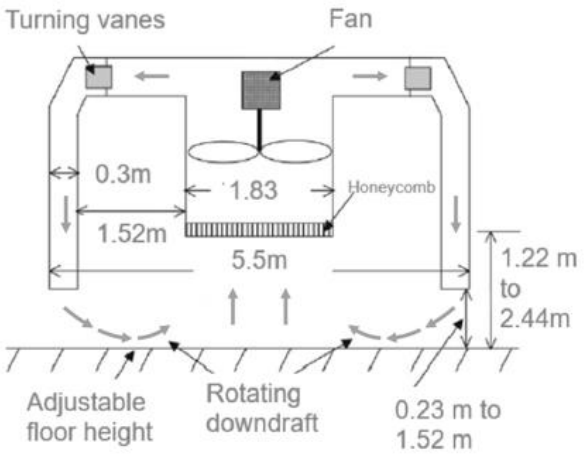

Figure 2-6 Tornado Simuator at Iowa State University schematic adapted from Haan et. al (2008).

2.2.3 WindEEE Dome at Western University

The Wind Engineering, Energy and Environment (WindEEE) dome (Hangan (2014)), located at Western University, is a closed circuit hexagonal 3D wind chamber that has 6 exhaust fans and 48 peripheral fans. Guide vanes are installed in front of the peripheral fans to impart an angle to the inflow to create a swirl, while sucking air out of the experimental volume with the help of 6 exhaust fans located in the upper plenum, thereby producing a tornado-like vortex. WindEEE can generate tornado-like vortices by two methods, guide vane method and horizontal shear method. In the first method, guide vanes are used to impart swirl by controlling the inflow angle. In the second method, the peripheral fans are operated at different speeds along each row and the swirl is controlled by varying the gradient of inflow speed along the peripheral fans. In this facility, the inflow is not bounded by physical walls which allows the upper plenum section to move, thereby facilitating translation.

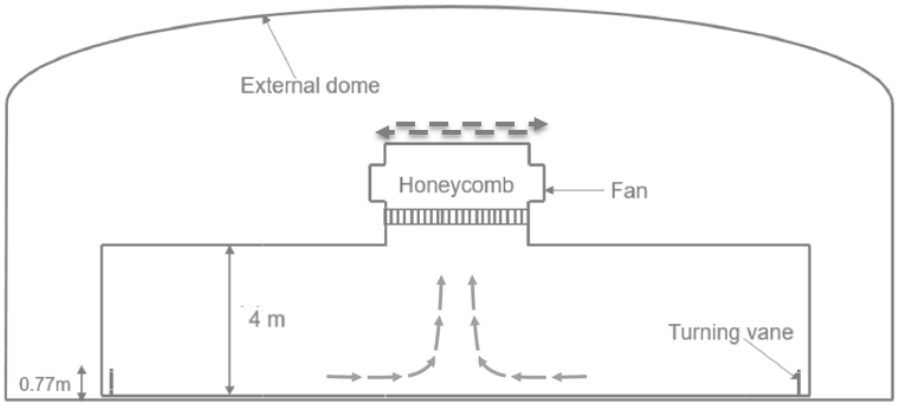

Figure 2-7 WindEEE Dome at Western University schematic.

2.3 Numerical simulation of tornado-like vortices

It is to be recalled that studying tornado-like vortices poses various challenges which arise not only from the complexity of the flow field, but also due to extensive parametrization needed to characterize these vortices. Due to the parametric nature of this study, a large number of cases (or configurations) had to be analyzed. As a result, computationally effective but reasonabily acucurat Rynolnds Stress Model (RSM) has been opted for the parametric flow structure studies. However, for tornadic wind load evaluation (Chapter 3), a more robust, Large Eddy Simulation technique has been utilized. In both cases a commercial software package STAR-CCM+ (version 10.06.010) was used to carry out the CFD simulations for this study. All simulations were run on SHARCNET (Shared Hierarchical Academic Research Computing), high performance parallel computing consortium at Western University. All CAD modelling was done in AutoCAD and the geometries prepared in AutoCAD were imported to STAR-CCM+ for CFD modelling.

2.3.1 RANS (steady) simulations

2.3.1.1 Turbulence model

The Reynolds Stress Model (RSM) is the most complete physical representation of the flow, at least in the RANS framework. It can capture complex strains and is more accurate model for swirling flows, as compared to the eddy viscosity models like $k-\varepsilon$ and $k-\omega$. RSM has also been extensively used by researchers in the past for numerical simulation of

tornadoes, for example Hangan and Kim (2008), Natarajan (2012) and Nasir (2017), etc. As a result, RSM is used for steady simulations in this study. While Large Eddy Simulations are more accurate than steady RANS, we chose steady RANS (RSM) due to time constrained posed by this parametric study with several configurations/cases. A brief description of RANS/RSM has been presented in this section.

Fluid flow is governed by a set of second order, non-linear, coupled, partial differential equations knowns as Navier-Stokes (NS) equations as shown below.

$$\rho\left(\frac{\partial \boldsymbol{u_i}}{\partial t}+\boldsymbol{u_i}\frac{\partial \boldsymbol{u_i}}{\partial x_i}+\boldsymbol{u_j}\frac{\partial \boldsymbol{u_i}}{\partial x_j}\right)=-\frac{\partial \boldsymbol{p}}{\partial x_i}+\frac{\partial}{\partial x_j}(2\mu \boldsymbol{s_{ij}})$$

Incompressibility assumption is invoked as following.

$$\frac{\partial \boldsymbol{u_i}}{\partial x_i}=0$$

This reduces the above equation to

$$\rho\left(\frac{\partial \boldsymbol{u_i}}{\partial t}+\boldsymbol{u_j}\frac{\partial \boldsymbol{u_i}}{\partial x_j}\right)=-\frac{\partial \boldsymbol{p}}{\partial x_i}+\frac{\partial}{\partial x_j}(2\mu \boldsymbol{s_{ij}})$$

The instantaneous quantities are subjected to Reynolds decomposition as shown below.

$$\boldsymbol{u}=U+u$$

Navier-Stokes (NS) equations are then averaged and written as Reynolds Averaged Navier Stokes (RANS) equations as shown below.

$$\rho\left(\frac{\partial U_i}{\partial t}+U_j\frac{\partial U_i}{\partial x_j}\right)=-\frac{\partial P}{\partial x_i}+\frac{\partial}{\partial x_j}(2\mu S_{\boldsymbol{ij}}-\overline{u_iu_j}\rho)$$

The RANS equations are analogous to NS equations if instantaneous quantities are replaced by mean quantities expect RANS equations have additional unknown terms, $\overline{u_iu_j}$, called Reynolds stresses. Various turbulence models under the RANS framework are deployed to tackle this additional unknown term (or the Reynolds stresses). While the eddy

viscosity models like $k-\varepsilon$ and $k-\omega$ use Boussinesq assumption to relate Reynolds stresses to mean velocity gradients, RSM solves six additional transport equations (one for each Reynolds stress) and therefore captures more physics. The transport equation for Reynolds stress can be obtained by multiplying the NS with fluctuations and then averaging as shown.

$$\overline{u_i NS\left(U_j+u_j\right)+u_j NS(U_i+u_i)}=0$$

$$\frac{D(\overline{u_i u_j})}{Dt}=-\frac{\partial}{\partial x_l}\left[-\overline{u_i u_j u_l}-\frac{p}{\rho}\left(\delta_{jl}u_i+\delta_{il}u_j\right)\right]+\nu\frac{\partial\overline{u_i u_j}}{\partial x_l}-(\overline{u_i u_l}\frac{\partial U_j}{\partial x_l}+\overline{u_j u_l}\frac{\partial U_i}{\partial x_l})+$$

$$\left(2\nu\overline{\frac{\partial u_i}{\partial x_l}\frac{\partial u_j}{\partial x_l}}\right)+\frac{p}{\rho}(\frac{\partial u_i}{\partial x_l}+\frac{\partial u_j}{\partial x_l})$$

On the right-hand side of this equation, the first, second, third, fourth and fifth terms are turbulent diffusion, molecular diffusion, production, dissipation and pressure-strain interaction terms, respectively. It should be noted that this equation gives rise to additional third order moment term ($\overline{u_i u_j u_l}$). The transport equation for third moment term gives rise to fourth moment term and so on and so forth. This essentially leads to turbulence closure problem. While solving the transport equations for subsequently higher order moments would capture more physics, it would also make the computation very expensive. Therefore, RSM works out a trade off by modelling the five terms in the transport equations of the first order moments with the help of semi empirical relations.

To demonstrate the difference in flow-fields predicted by various closure models for steady RANS, a basic comparison of results obtained from RSM, $k-\varepsilon$ and $k-\omega$ was conducted in a preliminary study. For this purpose, floor 3 configuration from Haan et al. (2008) was used for ISU tornado simulator model. The choice of tornado simulator and configuration were purely arbitrary and were used, in the beginning, only for a comparison of turbulence models. All three turbulence models were compared at the same grid resolution and the number of mesh cells used were about 1.75 M.

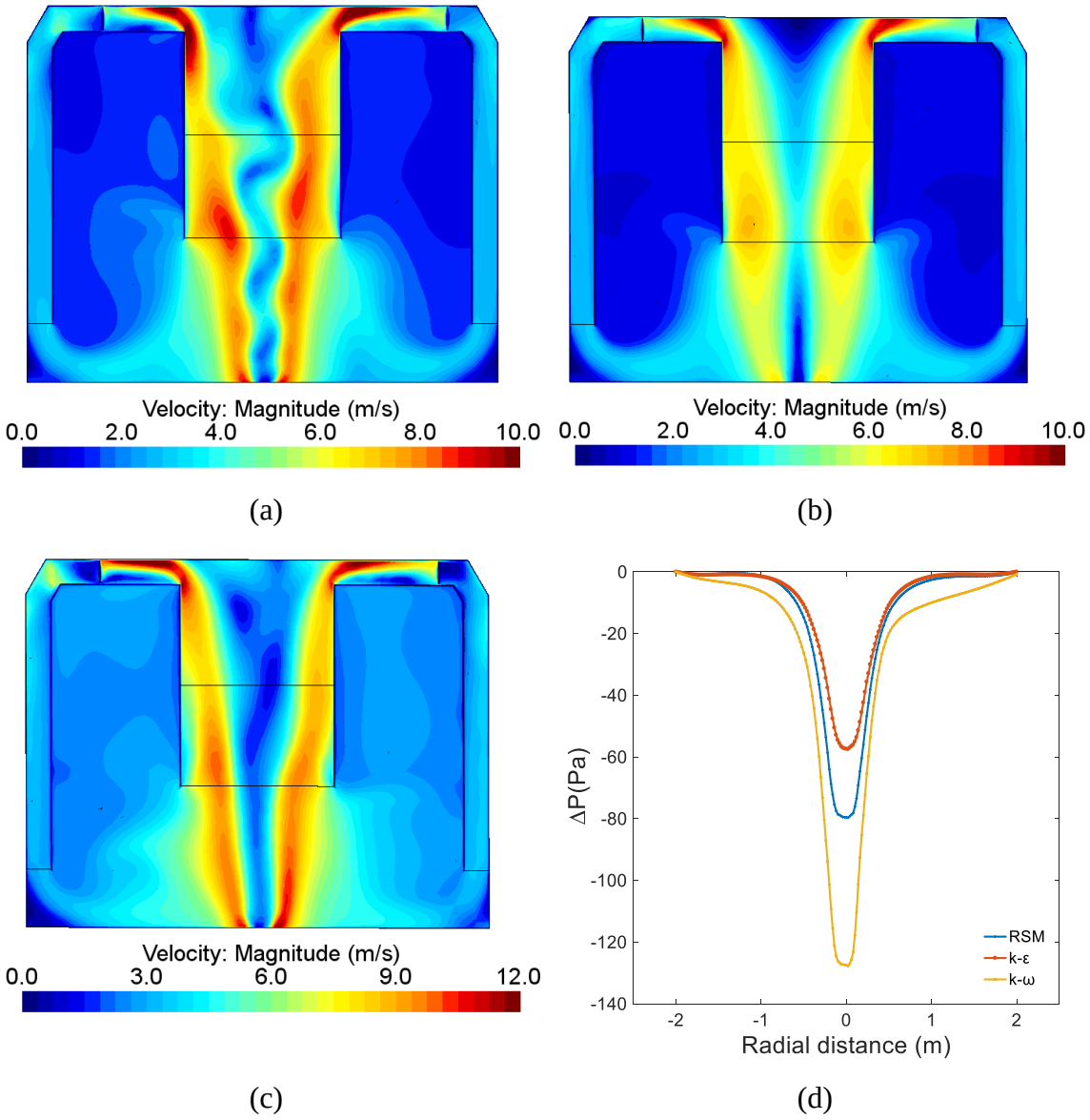

Figure 2-8 Flow fields from (a)RSM, (b) $k-\varepsilon$, (c) $k-\omega$ turbulence models.

Differences in flow structures and characteristic ground static pressure profiles can be instantly noticed from Figure 2-8.

2.3.1.2 Discretization

Although the Reynolds Stress Model (RSM) is more accurate for swirling flows, it is computationally expensive and less forgiving to poor grid resolution. As a result, mesh quality plays a key role in speedy and accurate convergence of the solution.

2.3.1.2.1 Grid strategy

To maintain a balance between good mesh quality and a fast converging solution, the entire computational domain was subdivided into various regions of fine and coarse mesh. In regions of interest (like near the core), regions of high gradients and areas with small dimensions (like guide vanes which are usually thin), the mesh was kept finer. Polyhedral meshes with two layered prism layers near the walls were used. Mesh for a typical configuration of each simulator has been shown in Figure 2-9.

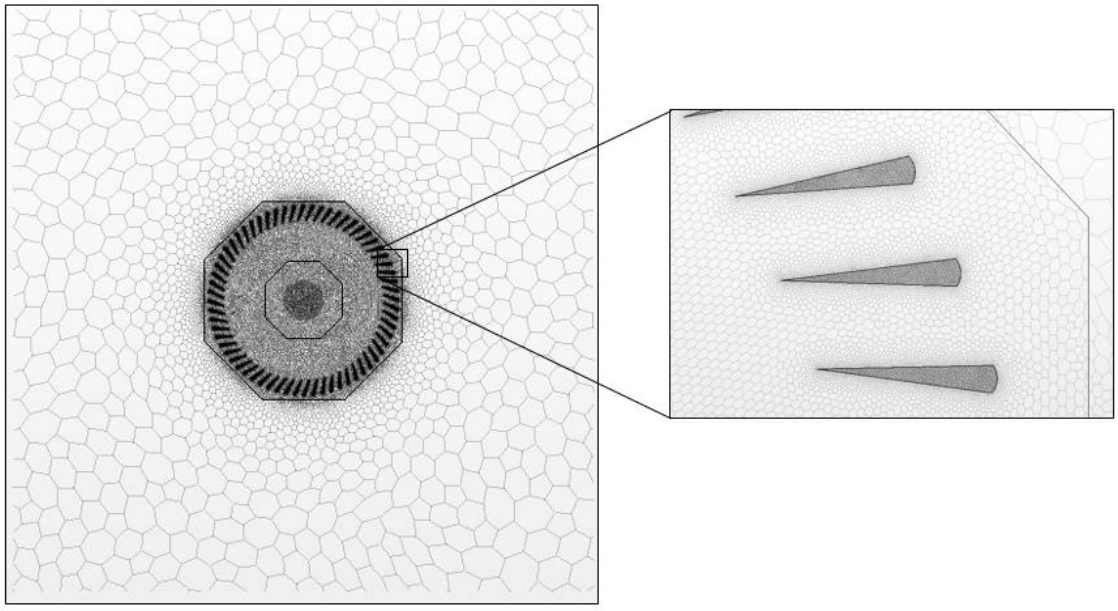

(a) VorTECH mesh

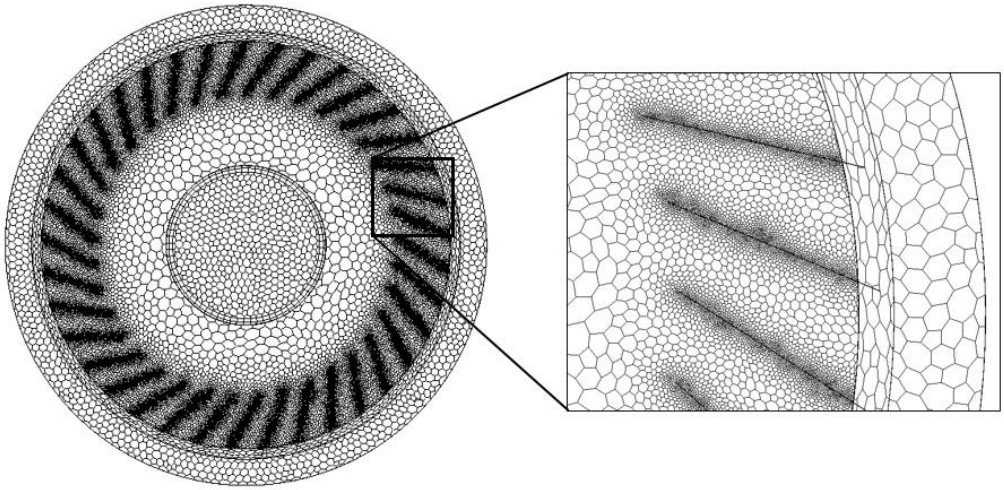

(b) ISU Tornado Simulator mesh

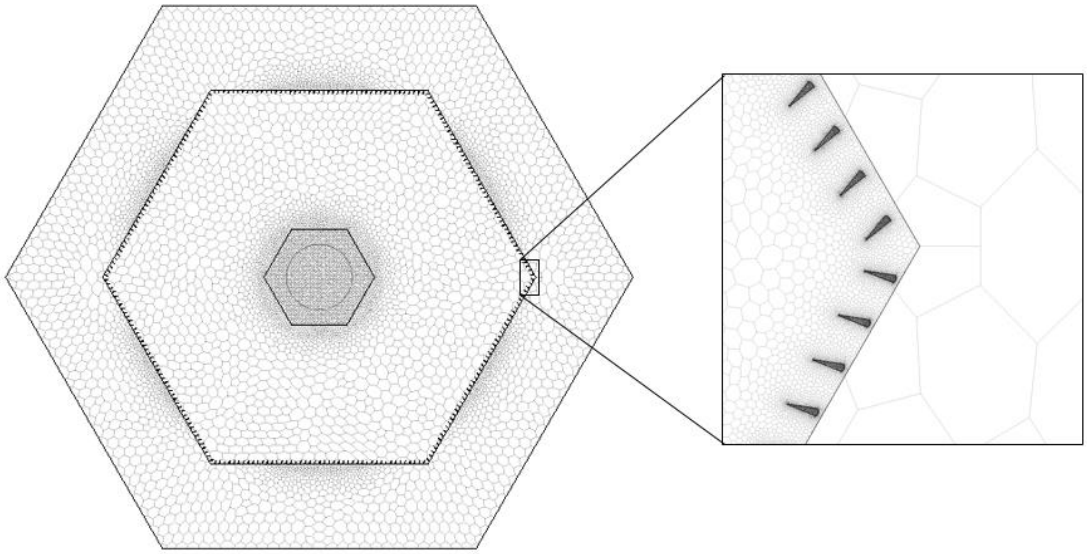

(c) WindEEE mesh

Figure 2-9 Meshing strategy.

2.3.1.2.2 Grid independence

A grid independence test was carried out for floor 3 configuration from Haan et al. (2008) by using three grid resolutions (G1, G2 and G3), the details of which can be found in Table 2-2. It can be seen from Figure 2-10 that the solution is independent of the grid resolution.

As a result, for this study, G2 grid resolution with about 1.75 million cells was used for ISU tornado simulator.

Grid resolution	G1	G2	G3
Cell count	1M	1.75M	2.6M

Table 2-2 Grid resolution.

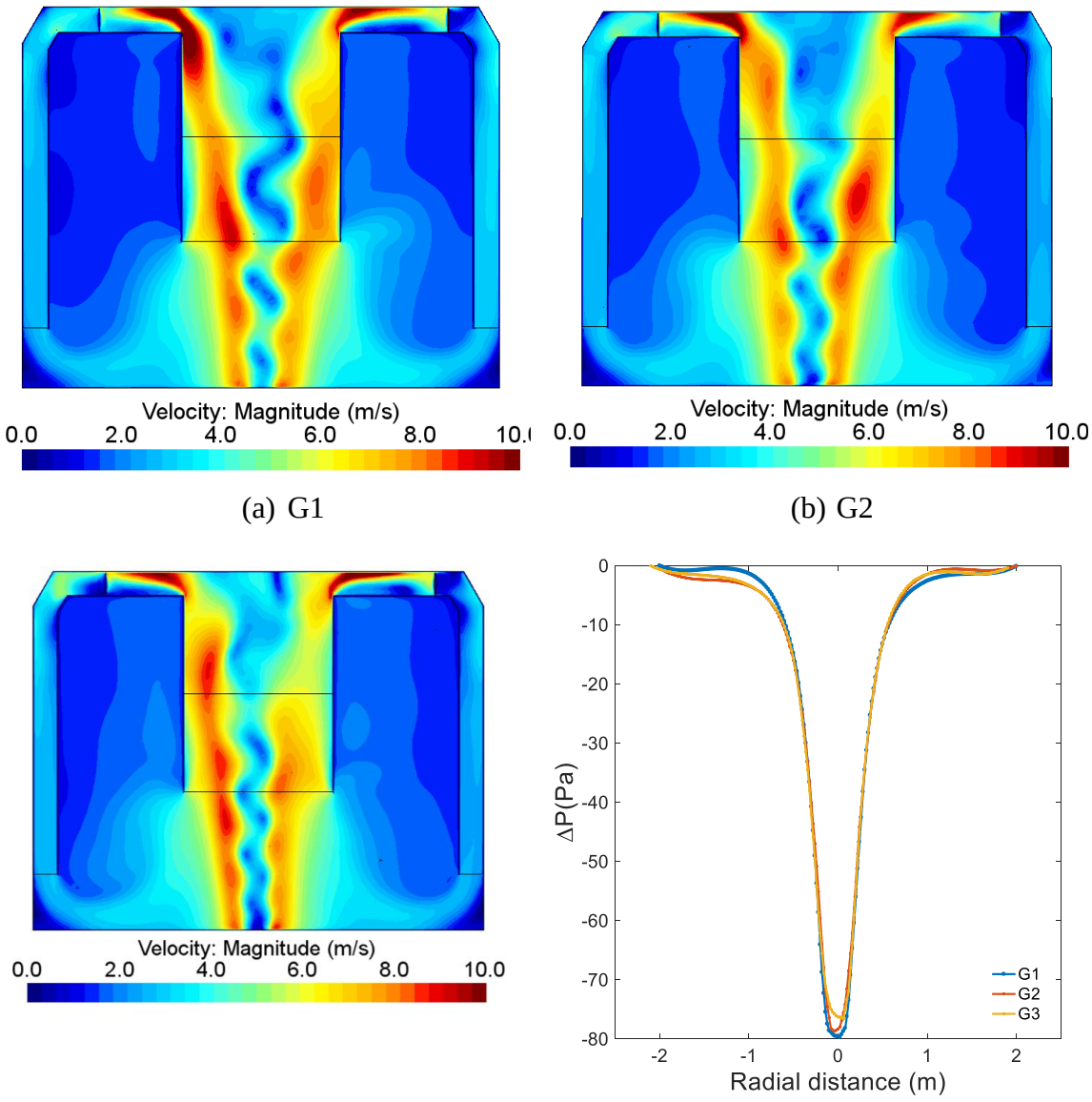

(a) G1 (b) G2

(c) G3 (d) Ground static pressure profile

Figure 2-10 Grid independence test.

Similarly, grid independence tests were carried out for VorTECH and WindEEE as well.

2.3.1.3 Boundary conditions and details of CFD modelling in STAR-CCM+

Mass flow rate was used to drive the flow, due to the unavailability of the fan performance curve, for modelling the full system of VortTECH, ISU Tornado Simulator and WindEEE. The fan was treated like an interface with a specified mass flow rate (obtained from Mayer (2009) and Haan et al. (2008)). The guide vanes were physically modelled to direct the flow. Typical geometric models for the three facilities with details of boundary conditions used are shown below. For the ISU model (as shown in Figure 2-11), the boundary condition marked "pressure outlet" was based on a preliminary study where whole simulator was placed in a bigger computational domain (to simulate external lab environment). It was found that the static pressure at the boundary marked "pressure outlet" below was zero.

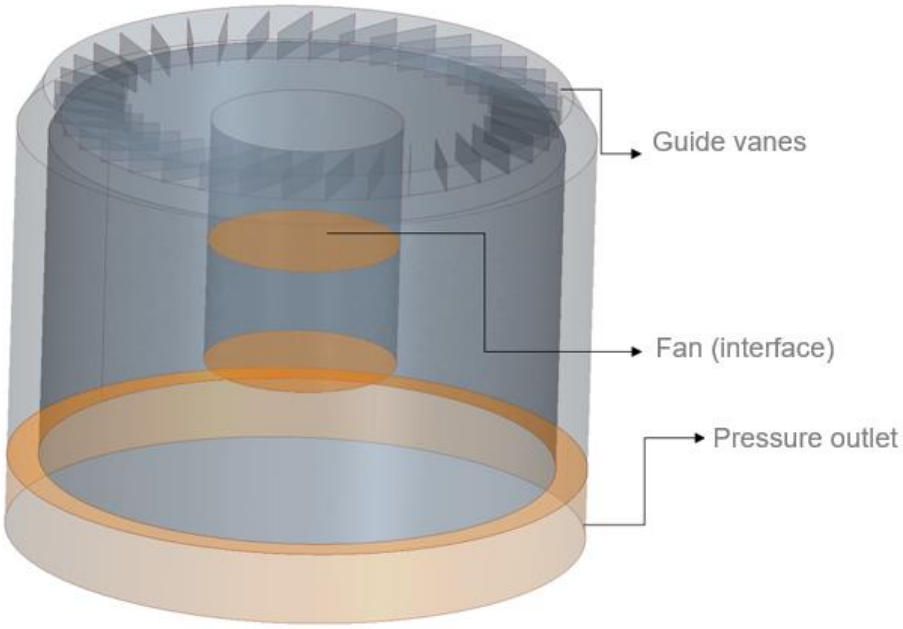

Figure 2-11 Tornado Simulator at Iowa State University CFD model.

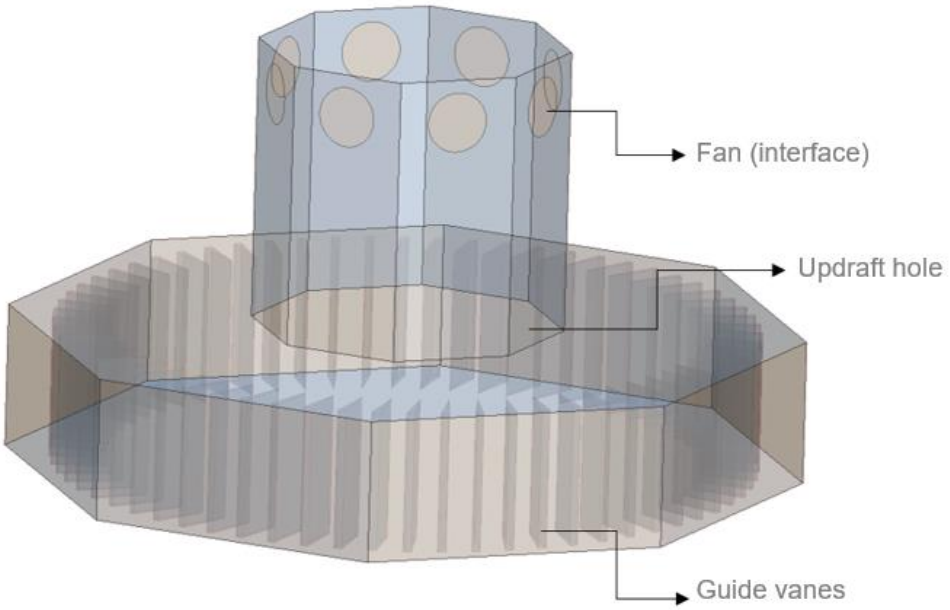

Figure 2-12 VorTECH at Texas Tech University CFD model.

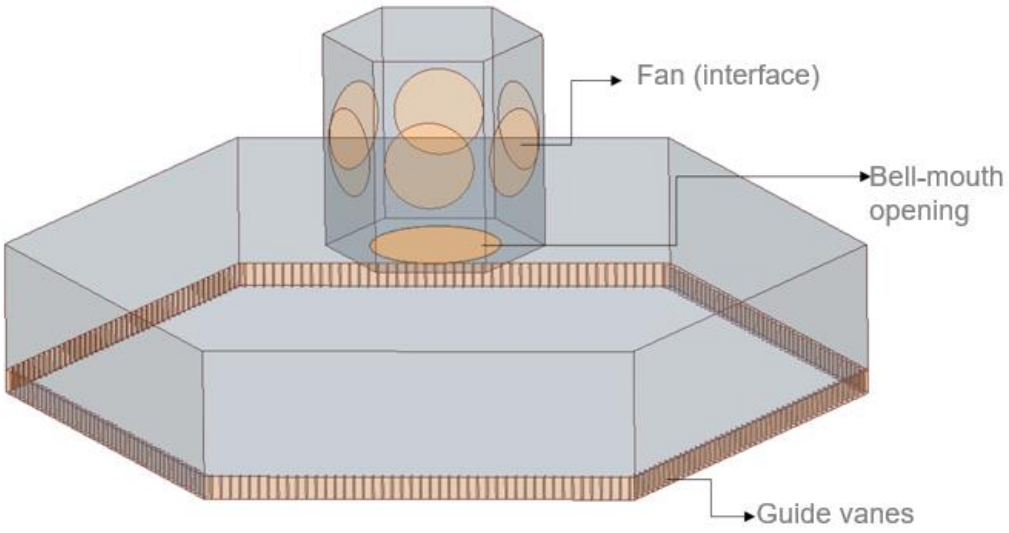

Figure 2-13 WindEEE Dome at Western University CFD model.

2.3.2 Vortex wandering

A series of steady RANS simulations showed some discrepancy in vortex core features (core radius, maximum tangential velocity, etc.) when compared to experimentally reported values. Core radii obtained from steady RANS simulations were consistently smaller than the experimentally reported values (by about 10%-20%) in most cases.

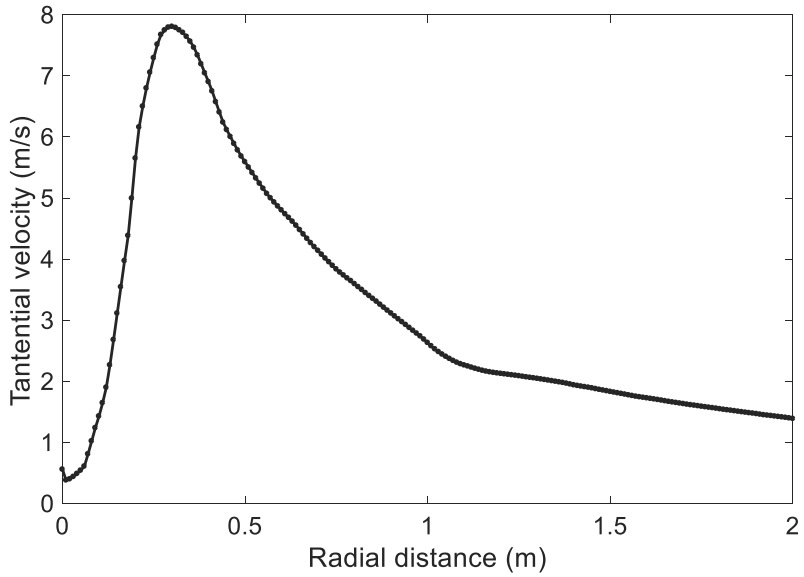

Figure 2-14 Numerically obtained radial profile of tangential velocity (ISU, floor3).

For example, Figure 2-14 shows the radial variation of tangential velocity obtained using ISU Tornado Simulator CFD model for floor 3 configuration. It can be be seen that the core radius obtained (numerically) is around 0.34m with a tangential velocity (at core radius) of just under 8m/s. However, Haan et al. (2008) reported a core radius of 0.43 m and tangential velocity (at the core radius) of around 9.8 m/s. This shows around 20% underestimation of both core radius and maximum tangential velocity. Vortex wandering was suspected to be the source of this discrepancy.

Vortex wandering is the random motion of vortex core with respect to a fixed observer. Jacquin (2001) suggested perturbation of the vortex core by wind tunnel unsteadiness, perturbation of the core by turbulence, co-operative instabilities as some of the causes of vortex wandering. While real tornadoes (tornadoes in nature) also wander, measurements of mean profiles made with fixed probes can be misleading because of wandering observed

in simulated tornado-like vortices. Further, vortex wandering can make it harder to make reliable conclusions from temporally averaged measurements, which reduces their value for CFD validation unless its effects are dealt with (Hayes et al. (2004)). Yang et al. (2011), based on their PIV measurements reported random movement of vortex core in ISU tornado simulator around its time averaged centre. They attributed this movement to the turbulent nature of such flows. Refan (2014) also reported vortex wandering during experiments conducted in mini WindEEE (1:11 scale prototype of WindEEE). Zhang and Sarkar (2012) conducted experiments in a 1:3 scaled model version of the tornado simulator at ISU and quantified the extent of underestimation of tangential velocity and core radius due to wandering effects. Baker (1974) developed an equation relating the "true mean" and "apparent mean" using the probability density function of the vortex centre location. Following Baker (1974), Devenport et al. (1997) proposed that fluctuations in the mean profile are due to turbulence and wandering effects. A spectral decomposition technique was developed to filter out the wandering effects to create a "corrected mean profile". Reductions in core radius and tangential velocity measurements were observed after correction. Errors of up to 15% and 20%, due to vortex wandering, were reported in core radius and tangential velocity measurements. (Devenport et al. (1997) and Heyes et al. (2004)).

It should be noted that wandering seems to cause an apparent enlargement of the core and the error in core radius observed in the present study falls well within the error range reported in Devenport et al. (1997) and Heyes et al (2004). Large Eddy Simulations were carried out to demonstrate the existence of wandering and its extent for so called "stationary vortices" simulated during the present study, without attempting to rigorously quantify or correct its effects. The details of Large Eddy Simulation set-up and the findings from these simulations have been presented in the following section.

2.3.3 Large eddy simulations (LES)

The solutions obtained from RSM (steady RANS) were used to initialize Large Eddy Simulations. Care was taken to satisfy Courant–Friedrichs–Lewy (CFL) condition. For this, the time step was chosen to maintain Courant number value below 1, at least in the region of interest.

$$C = \frac{U\Delta t}{\Delta x} < 1$$

Here, C is the courant number, U is the local velocity, Δx is the mesh size and Δt is the time step. A series of simulations, each equivalent to 9 seconds of physical time were then conducted. The boundary conditions and other details of the CFD models were the same as previously described, ie, the fans were treated like interfaces, guide vanes were physically modeled, etc.

To demonstrate the existence of wandering, ground static pressure was monitored at various strategically chosen locations (on the ground) as shown in Figure 2-15. The maximum ground suction occurs at the centre of the vortex, so the idea was to monitor the ground static pressure to observe how far the centre of the vortex wanders from the geometric centre of the simulator. It can be seen from the pressure time series located 10 cm north of centre that at several instants the suction is higher at that location as compared to the geometric centre, indicating that the vortex must have wandered up to that distance. It is interesting to note that the point located 10 cm east of the geometric centre consistently records suction higher than the geometric centre indicating that the vortex was not only wandering but was also off centered towards east. From this discussion, it is evident that wandering of vortex is the most probable cause of mismatch of core radius and maximum tangential velocity obtained from steady simulations as compared to experimentally reported values (measured by fixed point intrusive techniques).

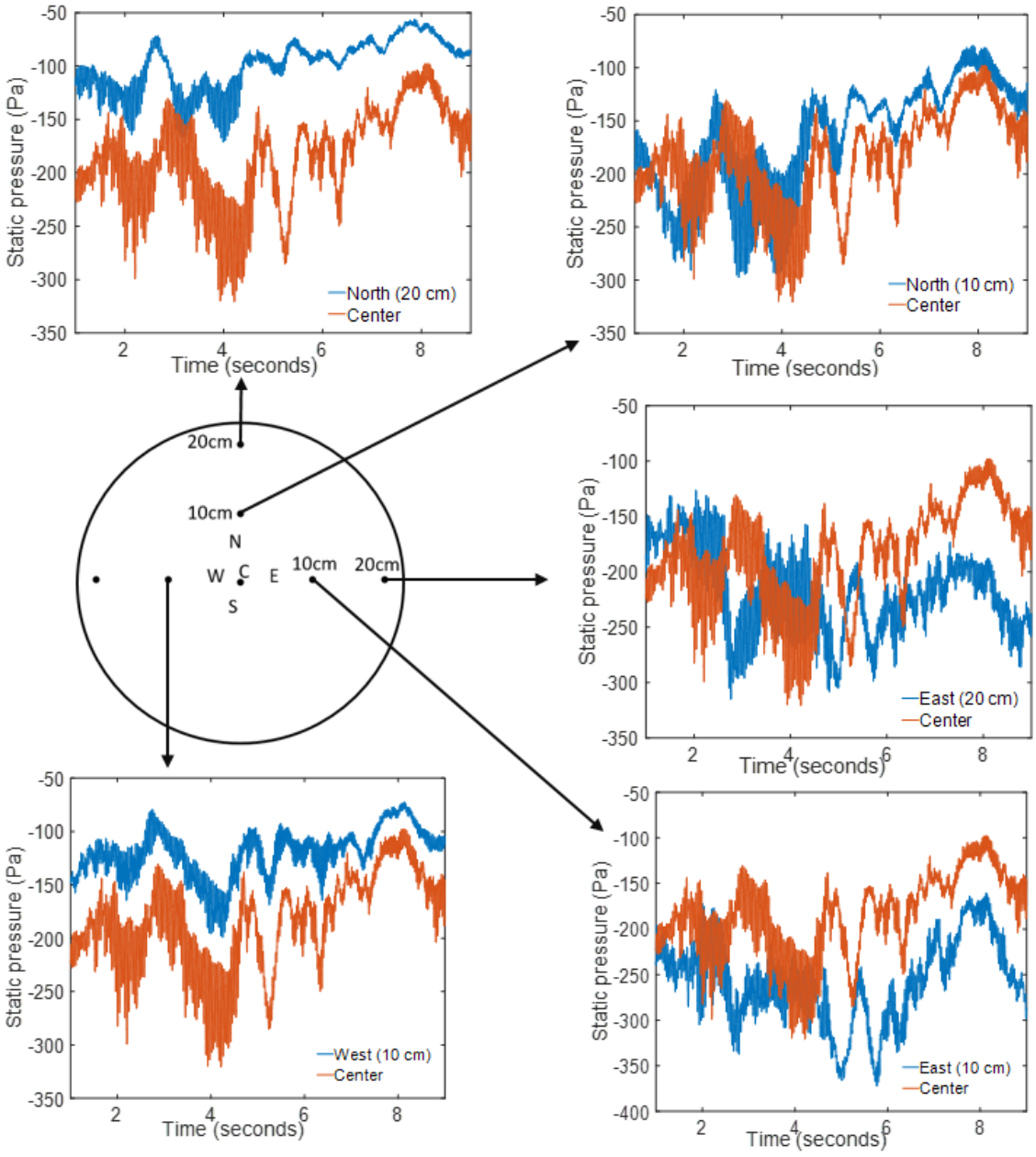

Figure 2-15 Demonstration of vortex wandering by monitoring the ground static pressure obtained using Large Eddy Simulations.

2.4 Results and discussion

After establishing that the mismatch of near core flow features was due to vortex wandering, the simplification process was carried out as initially proposed since the conditions away from the core (near the radius of updraft) were found to be steady. The following sections present the procedure adopted for the development of the generic numerical tornado model.

2.4.1 VorTECH (TTU)

Wind fields obtained from the numerical simulations of various configurations of VorTECH were examined and the parameters for a simplified numerical model were identified, while keeping the original flow in consideration. To show a typical tornado-like vortex produced in laborary, Figure 2-16 is provided for visual aid.

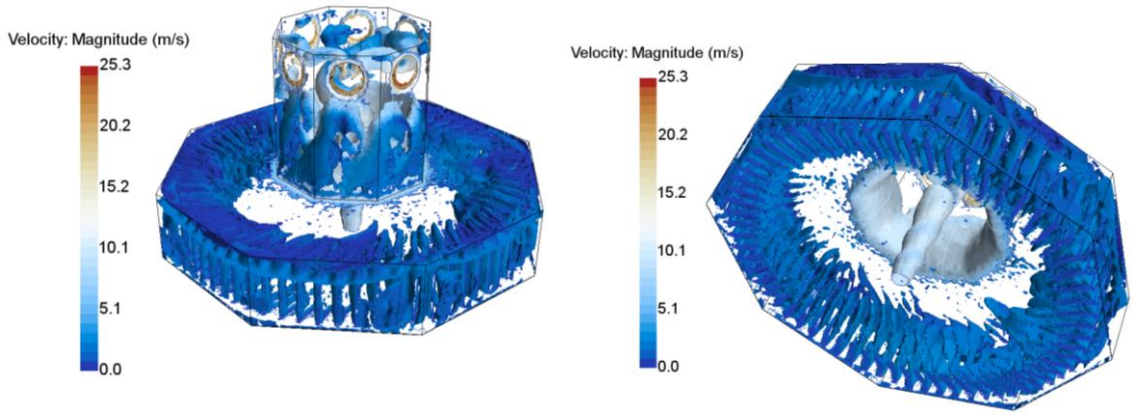

Figure 2-16 Velocity magnitude color map shown on Q criterion isosurface for a typical TTU VorTECH configuration.

The simplification process for 20-degree configuration is presented below to illustrate the typical procedure adopted during this study. First, the radial profiles of axial velocity at various heights are inspected to identify the radius of updraft (r_0). As mentioned previously, at the radius of updraft $v_z \approx 0$ must hold good (to allow only v_t and v_r as inlet velocity). It is evident from Figure 2-17 that even though the radius of updraft hole in the physical simulator is 2m, the actual radius of updraft is around 3m for this configuration

and a significant updraft develops by 2m distance from the centre, which shows the inadequateness of using physical dimenions of the simulator to determine the characterizing parameters.

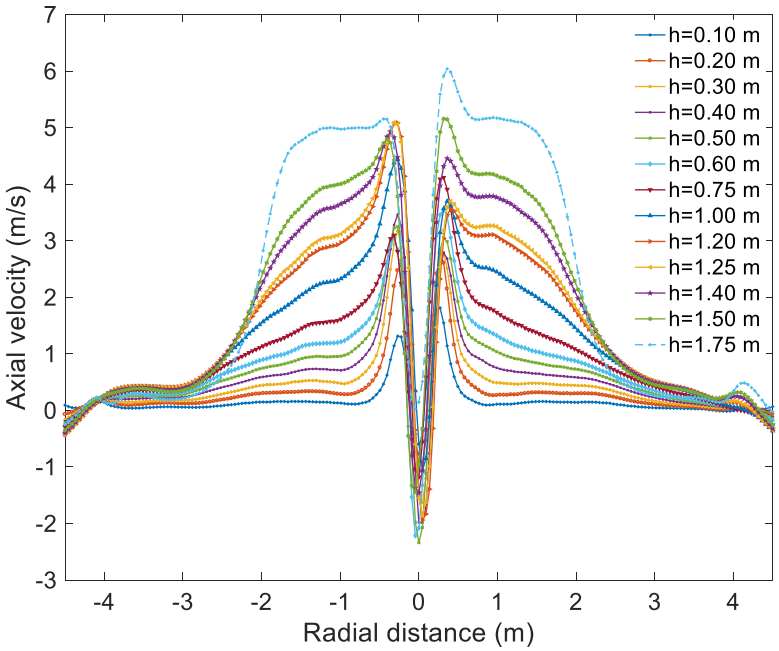

Figure 2-17 Radial variation of axial velocity for TTU 20-degree configuration.

Next, around the radius of updraft (3 m in this case), vertical profiles of radial and tangential velocity are plotted at various radial distances, as shown in Figure 2-18. The vertical profiles around the radius of updraft region were observed to be uniform for both, radial and tangential velocity.

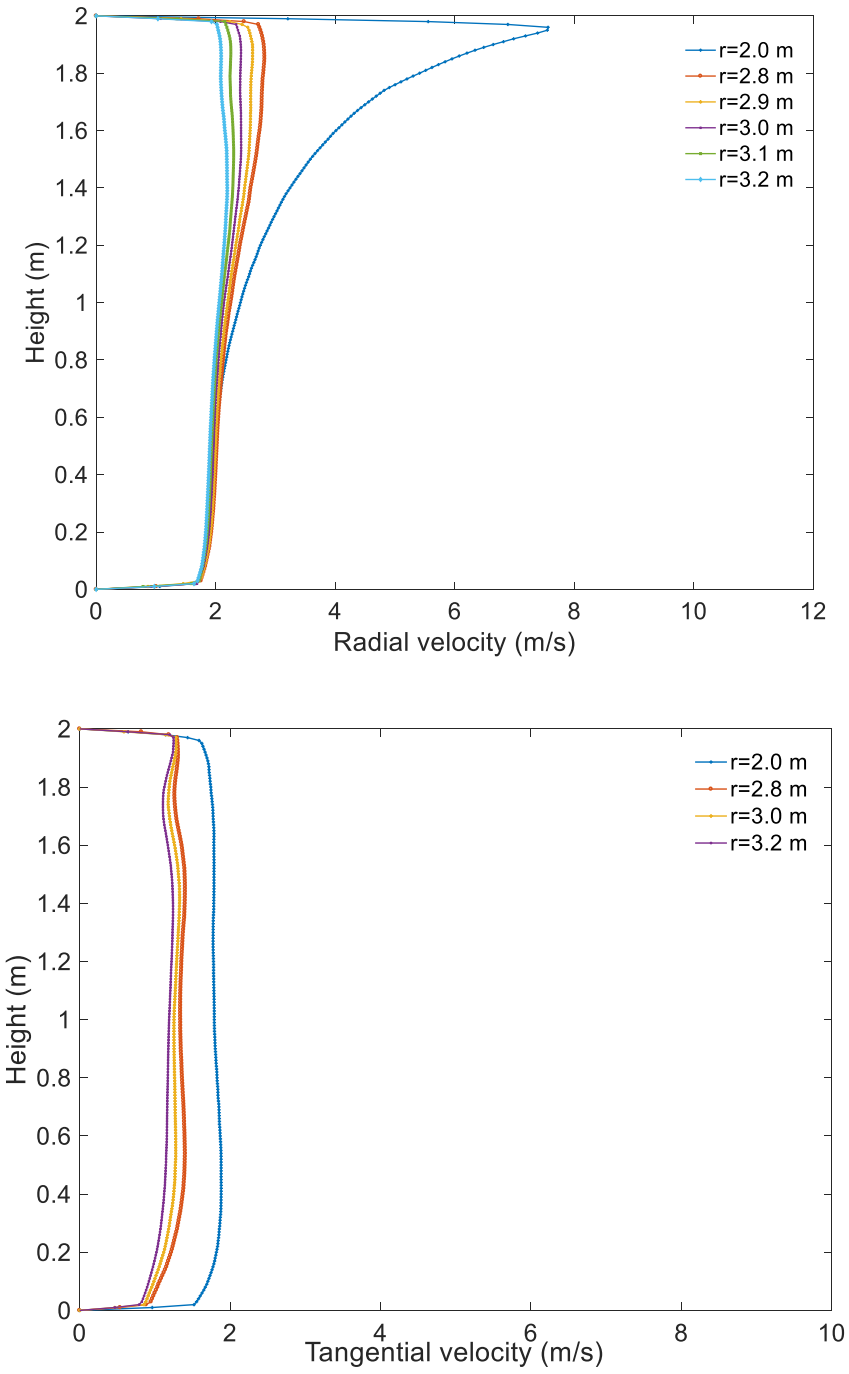

Figure 2-18 Vertical profiles of radial and tangential velocities at the inlet for TTU 20-degree configuration.

The mean values of radial and tangential velocities at r=r_0, were used to represent the uniform inlet velocity for the simplified model. In this case, $v_r = 2.12\, m/s$ and $v_t =$

$1.23\ m/s$. The three requirements at the radius of updraft, for this simplification are, (i)$v_z = 0$ approximation should hold good, (ii) the vertical profile for v_r should be uniform and (iii) the vertical profile for v_t should be uniform.

Since the flow is bounded by a wall, $h_0 = 2\ m$ is fixed (the inflow is protected by physical walls, so inflow depth is easily identifiable) . Therefore, for this configuration, $S = \frac{v_t}{v_r.2a} = \frac{1.2}{(2.1)(2)(^2/_3)} = 0.43$. On qualitatively examining the flow structure obtained from this configuration (Figure 2-19), a swirl ratio value of 0.43 looks reasonable.

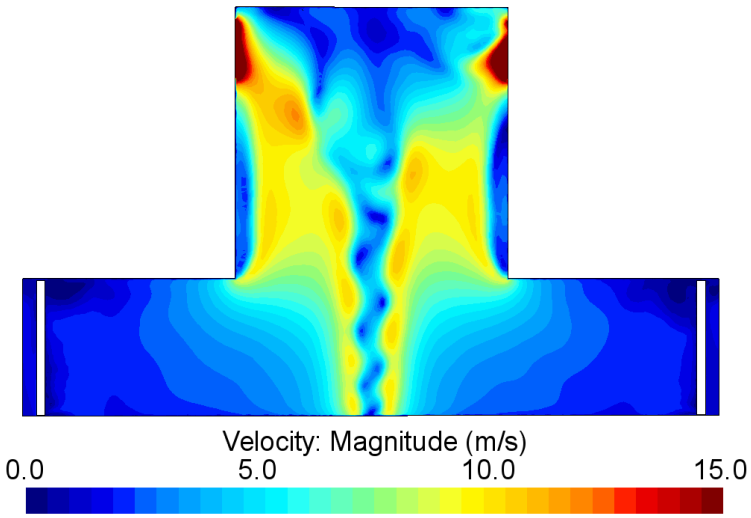

Figure 2-19 TTU VorTECH 20-degree configuration CFD model.

Next, a simplified model with dimensions based on the geometric parameter (aspect ratio) and the inflow boundary condition based on the kinematic parameter (swirl ratio, v_t and v_r) was prepared. For comparison of near ground flow features, the ground static pressure profiles obtained from the original and simplified models were compared.

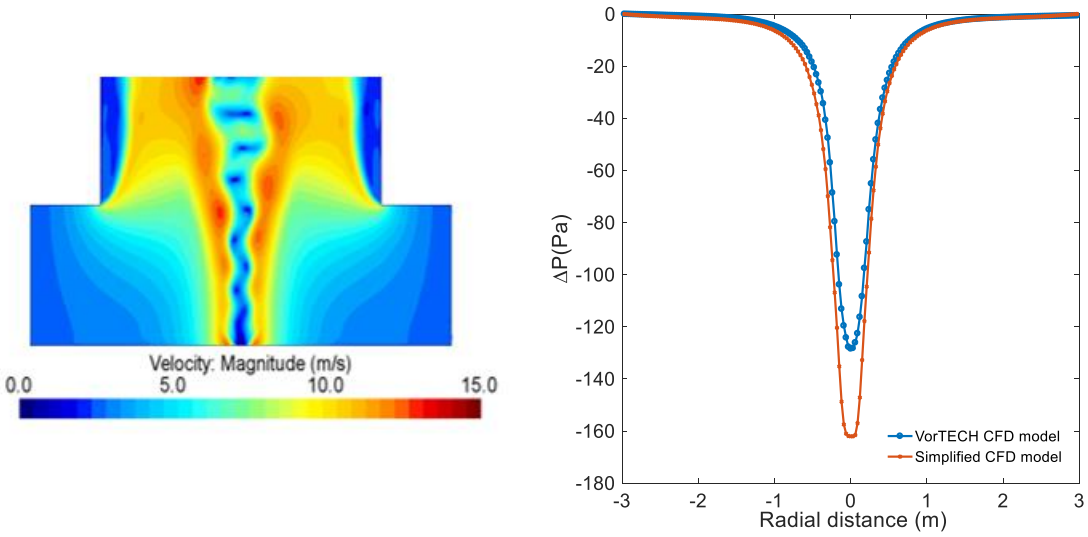

(a) Simplified model (b) Ground static pressure profile

Figure 2-20 20-degree simplified numerical model.

A qualitative (appearance-wise) similarity in flow structures obtained from the simplified model and TTU CFD model can be instantly noticed from Figure 2-20. However, from the ground static pressure profile, it is can be seen that even though they have the same shape, the simplified model produces a higher suction. It is suspected the size of guide vanes as compared to the experimental facility plays a key role in this mistmach, due to large blockage, causing the flow to accelerate. It was found that this mismatch (suspected due to flow acceleration) was most pronounced in TTU VorTECH and absent in WindEEE (as will be seen later). From Figure 2-21, it can be seen that velocity near the guide vanes sees a sudden increase. Further this this increment was seen to be more drastic as the guide vane angle was increased, as shown in Figure 2-21. It is speculated that this amplification of velocity near the guide vanes could be potentially due to reduction in effective inflow area. The inflow velocity (obtained at the radius of updraft in TTU VorTECH CFD model) for the simplified model is therefore amplified and creates higher static pressure drop.

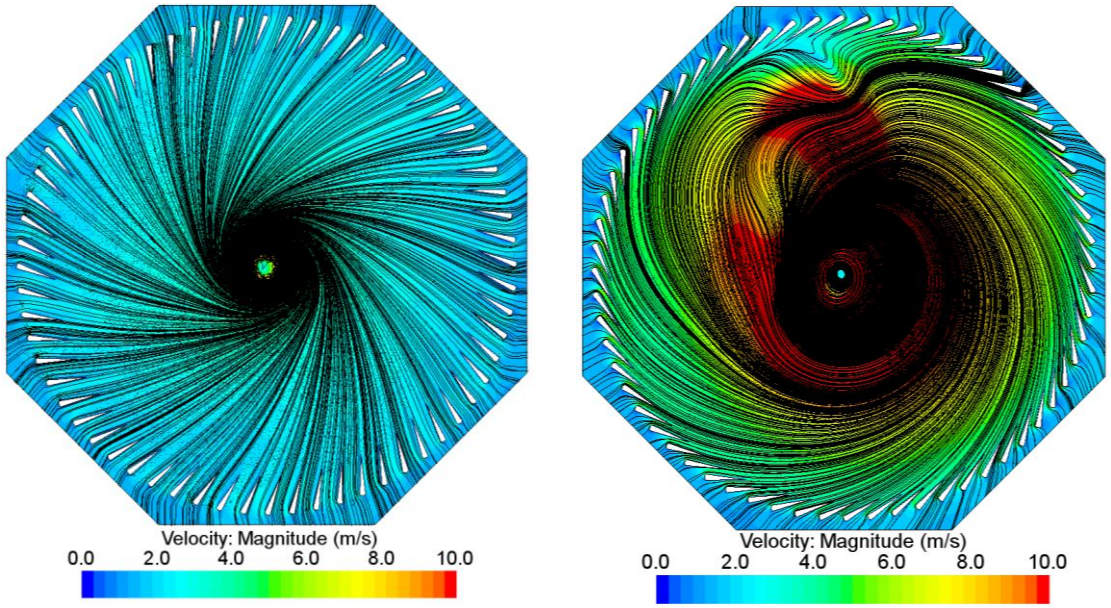

(a) Vane angle 20° Vane angle 60°

Figure 2-21 VorTECH plan view.

To account for this, a calibration of velocity magnitude to achieve the target pressure drop was done by calculating a correction factor (α) using cyclostrophic momentum balance as shown below. Cyclostrophic momentum balance has been previously used in tornado research for predicting tangential velocity based on pressure deficit in the core, for example Lilly (1969) [analytical study], Lee et al. (2004) [study of field data], Mishra et al. (2008) [experimental study], etc.

$$\frac{\partial p}{\partial r} = \frac{\rho v_t^2}{r}$$

$$\int_{P_{r=0}}^{P_{r=r_i}} \partial p = \int_0^{r_i} \frac{\rho v_t^2}{r} \partial r$$

$$P_{r=r_i} - P_{r=0} = \Delta P = \int_0^{r_i} v_t^2 \rho \frac{\partial r}{r}$$

$$\Delta P \propto v_t^2$$

$$\frac{\Delta P_{target}}{\Delta P_{observed}} = \frac{v_{t,target}^2}{v_{t,osberved}^2}$$

$$v_{t,target} = v_{t,observed}\sqrt{\frac{\Delta P_{target}}{\Delta P_{observed}}}$$

$$v_{t,target} = \alpha . v_{t,observed}$$

$$\alpha = \sqrt{\frac{\Delta P_{target}}{\Delta P_{observed}}}$$

To achieve the target static pressure-drop while preserving the original flow structure, both tangential and radial velocities at the inlet of the simplified domain were corrected by α (to maintain the same swirl).

$$v_t = \alpha . v_{t,old} = 1.11\ m/s$$

$$v_r = \alpha . v_{r,old} = 1.91\ m/s$$

With the corrected velocity magnitude, the flow structure and magnitude of static pressure drop were seen to match well with the original model as shown in Figure 2-22. The average difference between the static pressure drops obtained from TTU VorTECH CFD model and the generic numerical model was found to be around 0.9 Pa. It should also be noted that changing the inflow tangential and radial velocities in the same proportion for the simplified domain (before and after correction) doesn't seem to change the flow structure (qualitatively or appearance wise), reflecting the independence of flow structure and Re, which is also consistent with Church (1979).

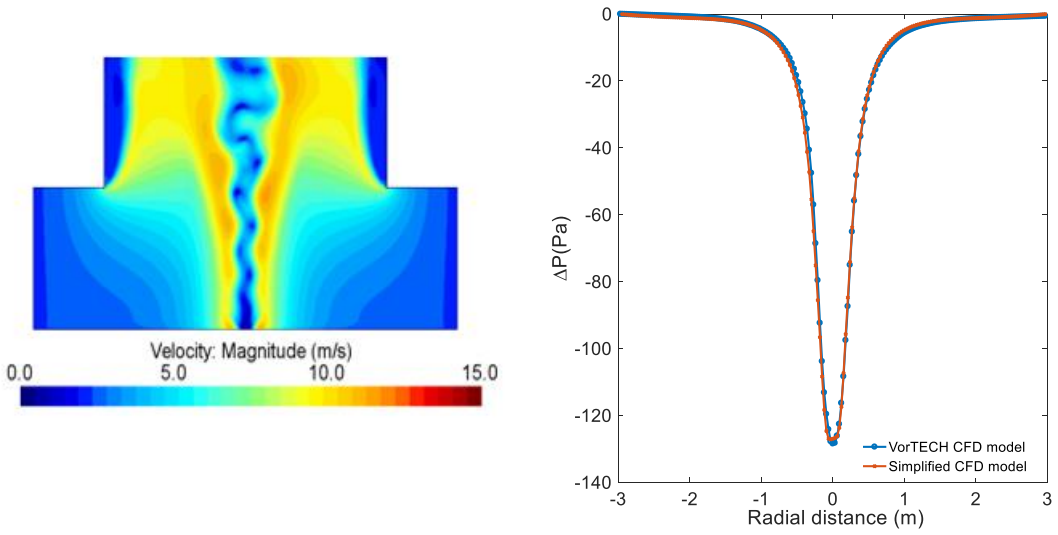

(a) Simplified model (b) Ground static pressure profile

Figure 2-22 Calibrated simplified numerical model.

Figure 2-24 is presented for a visual aid in recognizing the similarity in flow structures obtained from TTU CFD model and simplified CFD model for the same configuration (20-degree guide vane). The appearance looks quite similar, the turbulent nature of vortex breakdown is manifested as a disturbance inside the core which can be seen from the vector field presented.

A concern while calibrating the simplified model for VorTECH using cyclostrophic momentum balance was that it might affect the radial profiles and cause them to mismatch. However, as shown in Figure 2-23, the radial profiles (of tangential velocity) were observed to have a good match, along with the ground static pressure profiles (as previously shown).

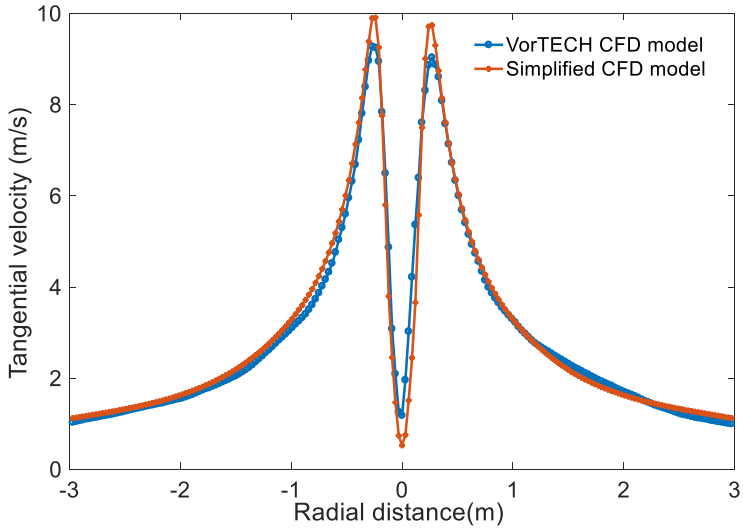

(a)

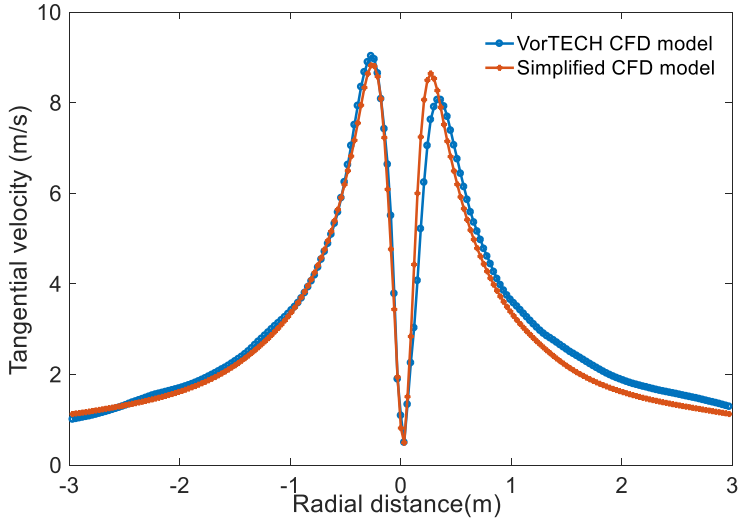

(b)

Figure 2-23 Radial profile of tangential velocity (20-degree guide vane configuration) for TTU VorTECH CFD model and simplified CFD model at (a) 0.2 m height, (b) 0.5 m height.

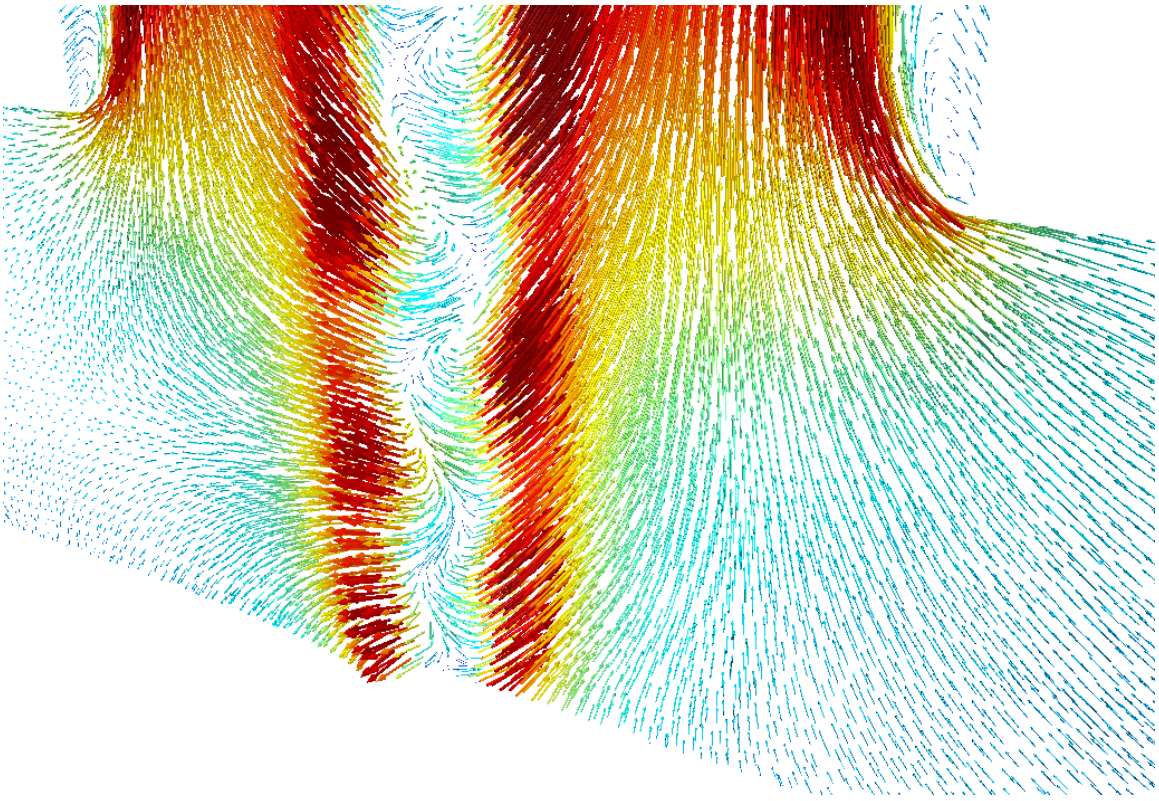

(a) TTU CFD model

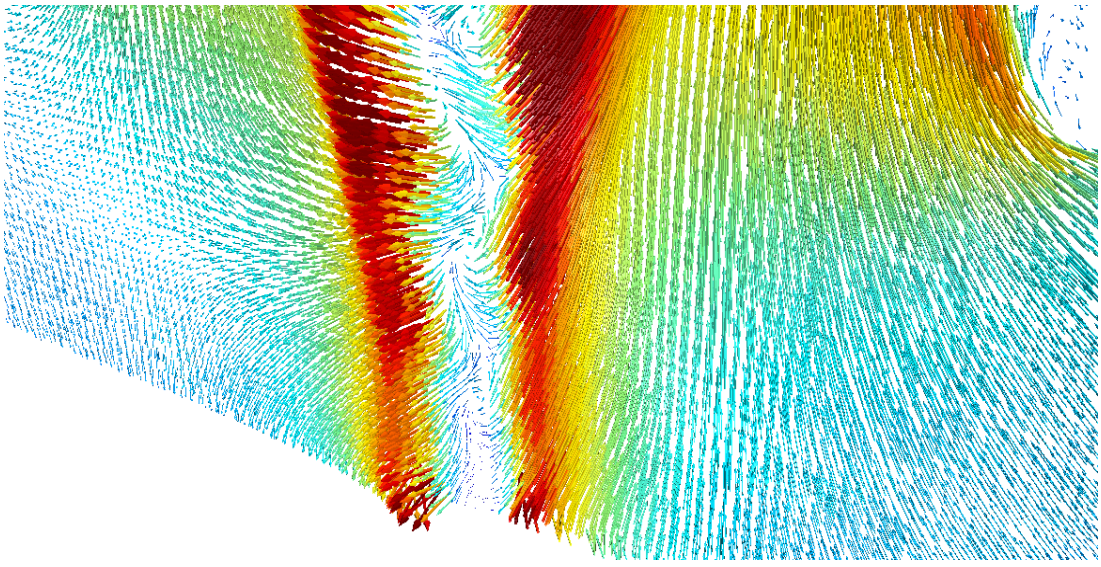

(b) Simplified CFD model

Figure 2-24 A visual comparison of flow fields from full TTU CFD model and simplified TTU model for 20-degree guide vane configuration.

A similar procedure was adopted for other configurations as well. Give below (Figure 2-25) is the simplification obtained from 10-degree guide vane configuration. Although the flow structure matches well, the vortex centre coincides with the geometric centre for the simplified domain but for the full system it does not. They were observed to be off-set by around 10 cm, in this case. It was observed that, in general, the simplified generic numerical model yielded centered vortices, due to axis-symmetry imposed by a cylindrical domain.

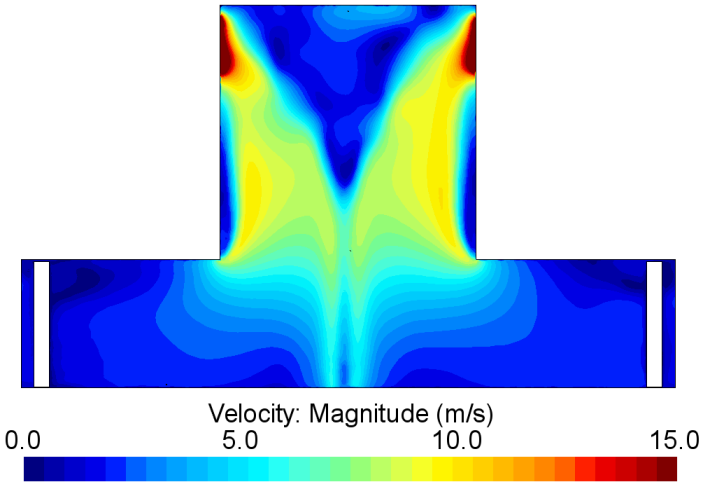

(a) TTU VorTECH CFD model

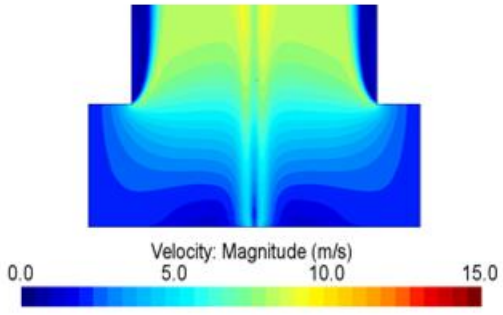

(b) Simplified model

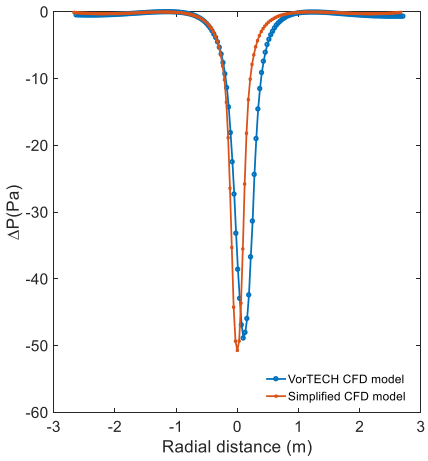

(c) Ground static pressure profile

Figure 2-25 TTU 10-degree guide vane configuration velocity scene for full TTU and simplified CFD models.

Following this procedure, the various geometric and inflow parameters for TTU numerical were identified for the remaining configurations and the summary of results obtained has been tabulated below.

Vane angle	r_0 (m)	h_0 (m)	$a = \frac{h_o}{r_0}$	r_u (m)	v_t (m/s)	v_r (m/s)	v_t/v_r (at h_i, r_i)	$S = \frac{v_t/v_r}{2a}$
10°	2.7	2.0	0.75	2.0	0.39	1.34	0.29	0.19
20°	3.0	2.0	0.67	2.0	1.11	1.91	0.58	0.44
30°	3.1	2.0	0.65	2.0	1.80	2.30	0.78	0.60
40°	3.1	2.0	0.65	2.0	3.19	2.78	1.15	0.88
50°	3.4	2.0	0.59	2.0	~3.26	~1.98	~1.65	~1.40
60°	~3.5	2.0	~0.57	2.0	-	-	≥2	≥2

Table 2-3 Parameters for simplified numerical model (TTU VorTECH).

It should be noted from Table 2-3 that while up to 40-degree configuration, the values of various parameters are reported with confidence, for 50-degree or higher, the conditions gradually became slightly unsteady even at the radius of updraft and therefore the values are an approximation. Further for higher swirl ratios (50 and 60-degree guide vane configuration), the conditions are highly unsteady and aerodynamically unstable, so comparison of mean ground static pressure profiles may not be the best choice. Moreover, while 70-degree guide vane configuration was simulated, the results obtained where discarded because the various characteristic features like ground static pressure profile shape, Rankine vortex tangential velocity profile, etc. were found absent for this configuration.

2.4.2 Tornado Simulator (ISU)

Although the overall strategy for simplification of tornado simulator at ISU was the same as previously discussed for VorTECH, there were some differences that primarily arose because the system is unbounded, which means identifying the inflow depth is not as straightforward as in the case of VorTECH. To show a typical tornado-like vortex produced in ISU Tornado Simulator, Figure 2-26 is provided for visual aid.

Result after the simplification process for vane 2 configuration of ISU tornado simulator is presented in Figure 2-27. The average difference between the static pressure drops obtained from ISU Tornado Simulator CFD model and the generic numerical model was found to be around 0.5 Pa, indicating a good agreement between the two.

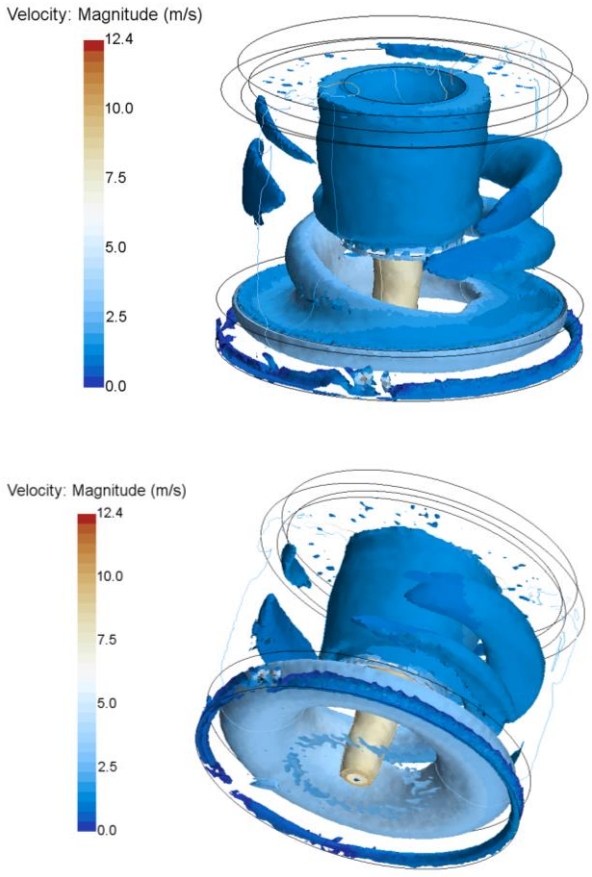

Figure 2-26 Velocity magnitude color map shown on Q criterion isosurface for a typical ISU Tornado Simulator configuration.

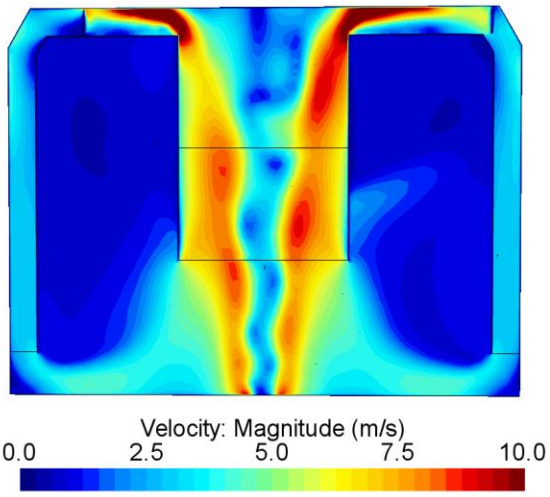

(a) ISU CFD model

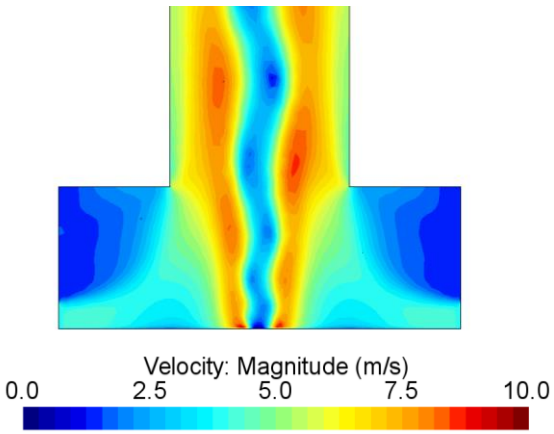

(b) Simplified model

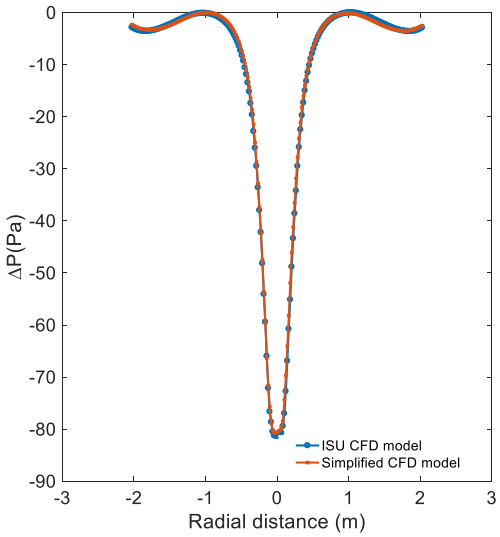

(c) Ground static pressure profile

Figure 2-27 Vane 2 configuration (a) ISU Tornado Simulator (b) simplified numerical model (c) comparison of ground static pressure

To identify the inflow depth for such a system (unbounded), visual methods like inspecting the vector and streamline fields (shown in Figure 2-28 and Figure 2-29) were also used along with the velocity profiles. This because a recirculation zone was found right above the inflow region in case of unbounded systems like ISU tornado simulator (and WindEEE)

as shown in Figure 2-28. This makes the vertical profiles misleading and the flow field needs to be visually examined as well. The recirculation zone was found to have non- zero radial and tangential velocity, but a close inspection revealed that part of the flow does not contribute to the flow in the vortex (and can be treated as secondary flow inside the system). This has been visually shown in Figure 2-28. Secondary flows are also observed in real tornadoes.

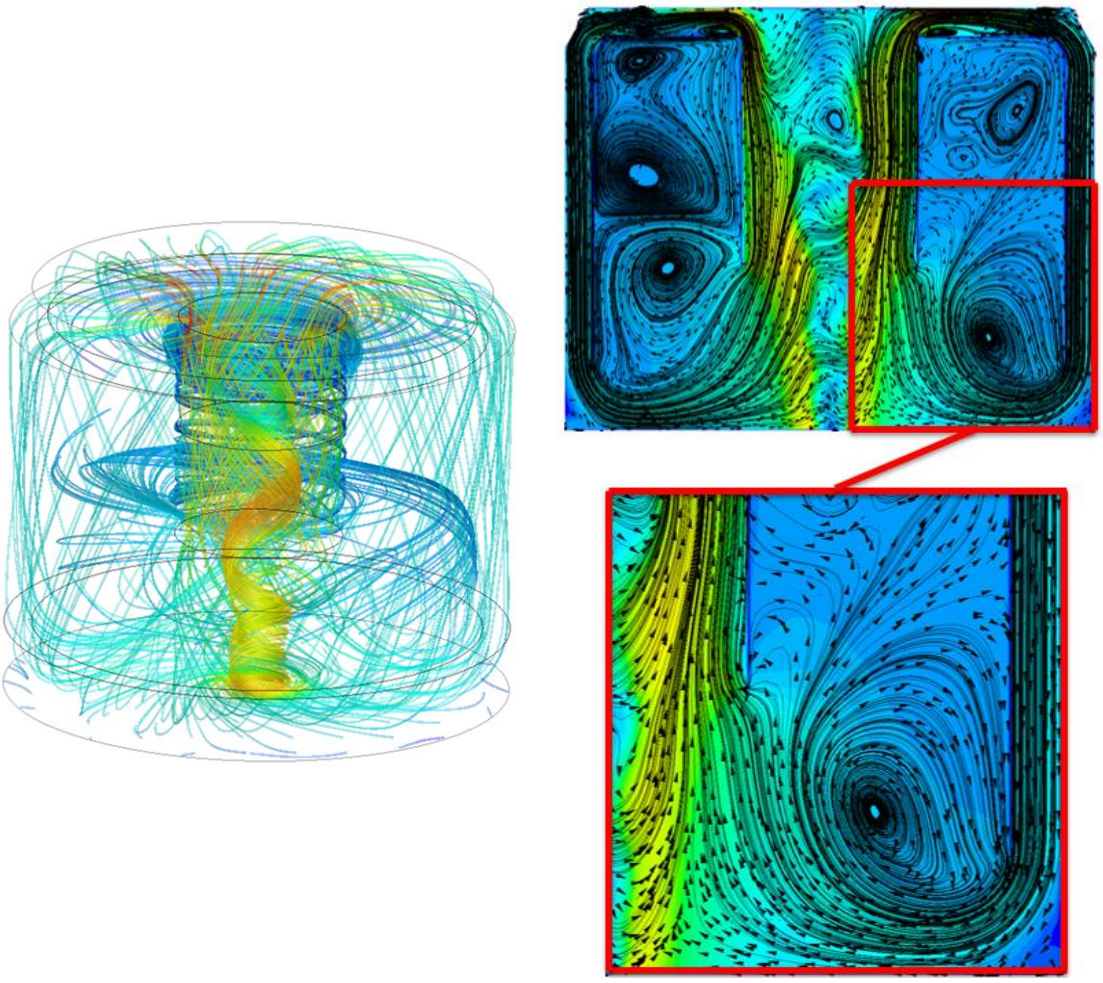

Figure 2-28 A typical configuration from ISU tornado simulator showing recirculation zone above the inflow (secondary).

Another interesting feature in certain configurations like floor 3, as shown in Figure 2-29 is that the flow from the recirculation zone finds its way into the exhaust system without

being a part of the main vortex flow, essentially reducing the effective radius of the updraft hole.

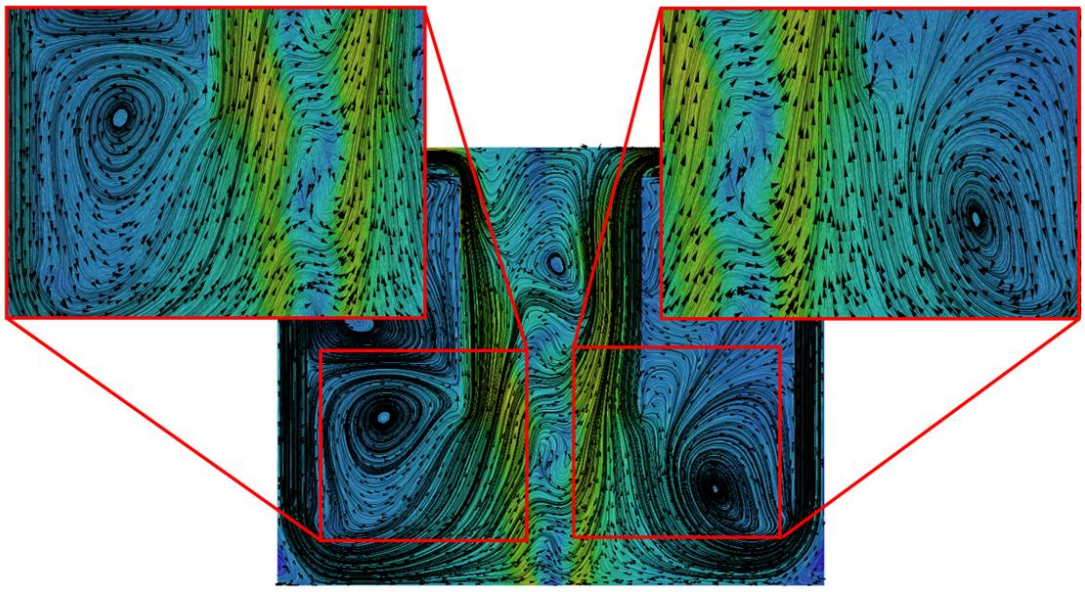

Figure 2-29 Demonstration of reduction in effective bell mouth size.

The results obtained after accounting for this reduction and following the procedure described earlier have been presented in Figure 2-30 and Figure 2-31 The flow structure (qualitatively) and the ground static pressure profile show a decent match (Figure 2-31). The average difference between the static pressure drop obtained from TTU VorTECH CFD model and the generic numerical model was found to be around 1.1 Pa, showing a good agreement between the two.

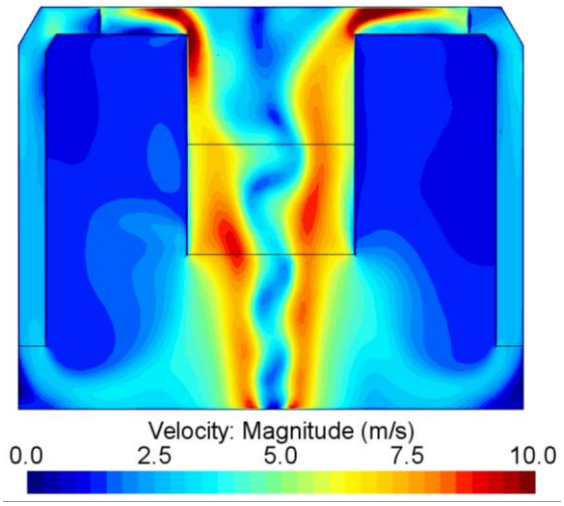

Figure 2-30 Floor 3 configuration ISU Tornado Simulator CFD model.

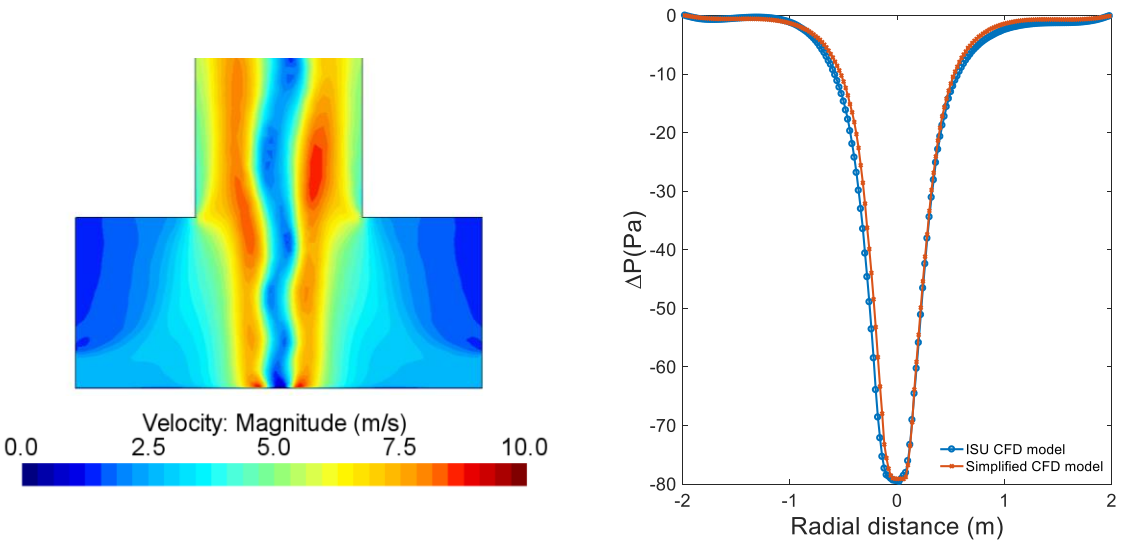

(a) Simplified model (b) Ground static pressure profile

Figure 2-31 ISU Tornado Simulator floor 3 configuration (a) simplified numerical model (b) comparison of ground static pressure.

Following this procedure, various geometric and inflow parameters for ISU numerical were identified for the remaining configurations and the summary of results obtained has been tabulated below.

Configuration	r_0 (m)	h_0 (m)	h_u (m)	r_u (m)	v_t (m/s)	v_r (m/s)	v_t/v_r (at h_o, r_o)
Vane 1	2.05	0.27	1.45	0.915	0.83	3.74	0.22
Vane 2	2.05	0.27	1.45	0.915	1.16	3.81	0.31
Vane 3	2.05	0.27	1.45	0.82	1.25	2.76	0.45
Vane 4	2.1	0.27	1.45	0.915	-	-	~0.6
Vane 5	2.1	0.27	1.45	0.915	-	-	~1
Fan 1	2.05	0.27	1.45	0.82	1.25	2.76	0.45
Fan 2	2.05	0.27	1.45	0.82	1.88	4.14	0.45
Fan 3	2.05	0.27	1.45	0.82	2.5	5.54	0.45
Floor 1	2.2	0.16	1.22	0.93	1.38	4.37	0.32
Floor 2	2.05	0.27	1.45	0.82	1.25	2.76	0.45
Floor 3	2	0.35	1.68	0.79	1.25	2.21	0.57

Table 2-4 Parameters for simplified numerical model (ISU Tornado Simulator).

2.4.3 WindEEE

The simplification strategy for WindEEE was the same as ISU tornado simulator since both systems are unbounded. To show a typical tornado-like vortex produced in WindEE, Figure 2-32 is provided for visual aid. As previously discussed, visual aid was used while examining the profiles to identify the recirculation zone above the convergent layer.

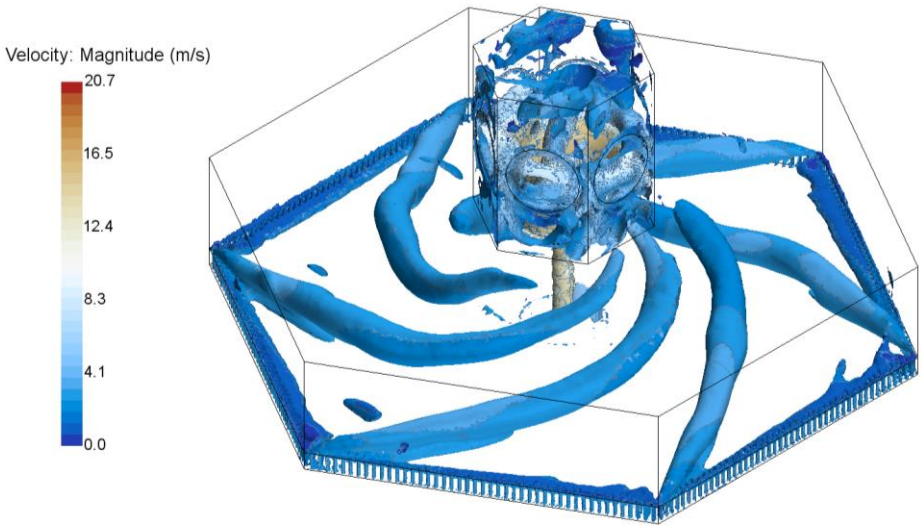

Figure 2-32 Velocity magnitude color map shown on Q criterion isosurface for a typical WindEEE configuration.

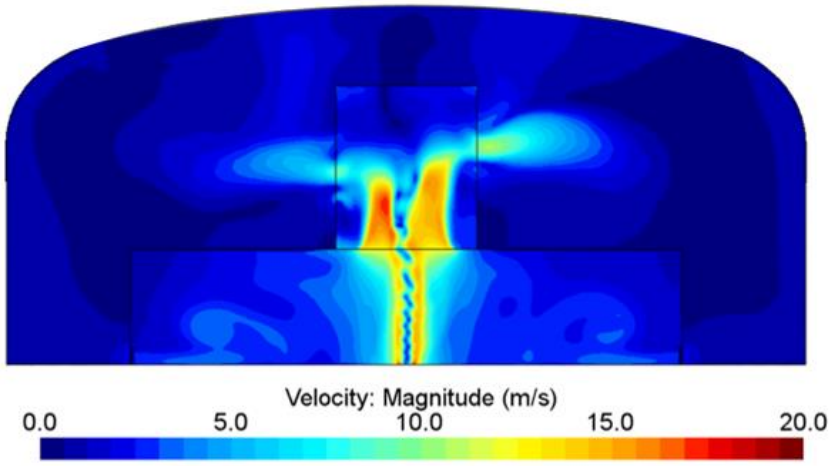

(a)

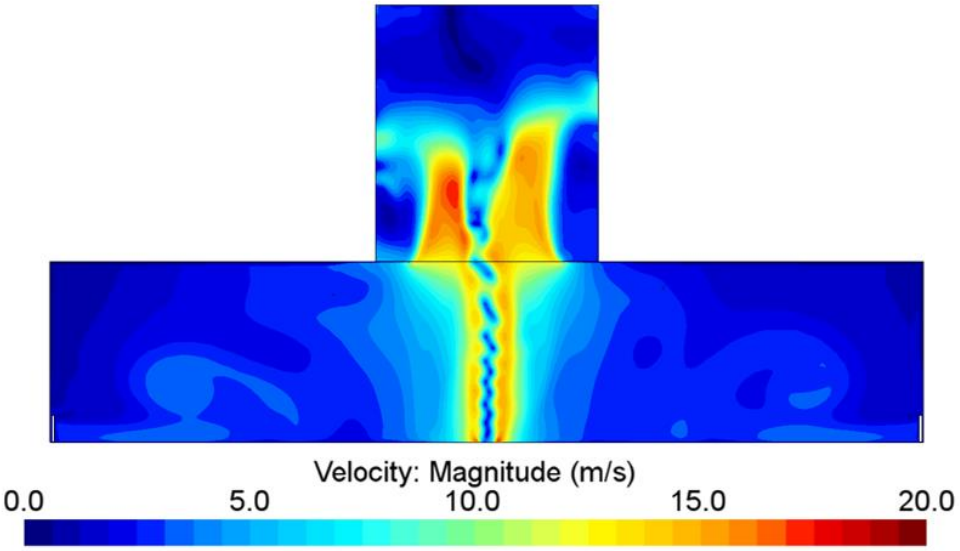

(b)

Figure 2-33 WindEEE CFD model (a) shown with dome (b) shown without dome.

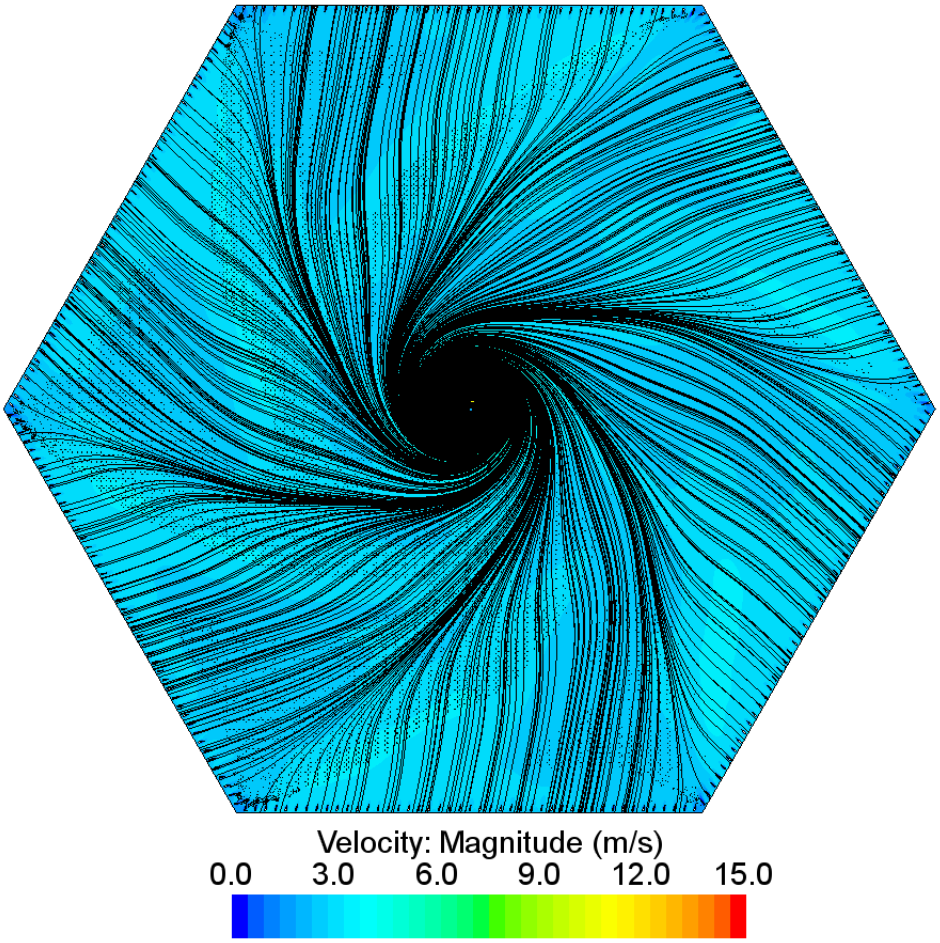

Figure 2-34 WindEEE plan view.

In an experiment conducted at WindEEE during this study, it was found that the core radius of 0.5 m and maximum mean tangential velocity of around 15 m/s were recorded at 0.17 m (17 cm) height from the ground for 15-deg guide vane configuration. Figure 2-35 presents the tangential velocity profile at 17 cm obtained from numerical simulations and shows reasonable agreement not only between WindEEE CFD model and simplified numerical model but also with experimentally reported values, given the presence of vortex wandering. Numerical simulations predicted a core radius of around 0.46 m and maximum mean tangential velocity of around 14.5 m/s.

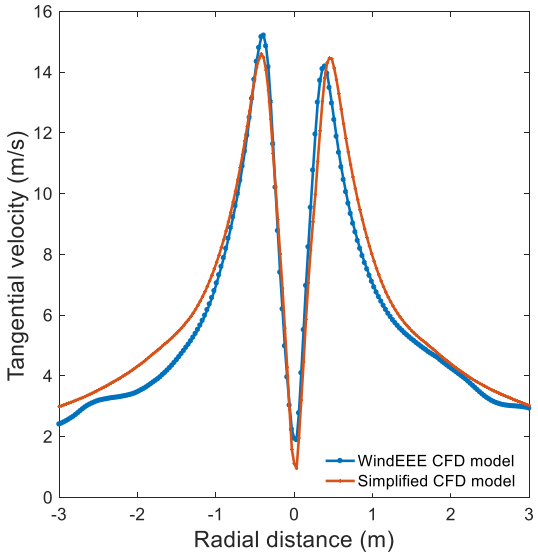

Figure 2-35 Radial profile of tangential velocity at 0.17 m height for WindEEE CFD model and simplified numerical model.

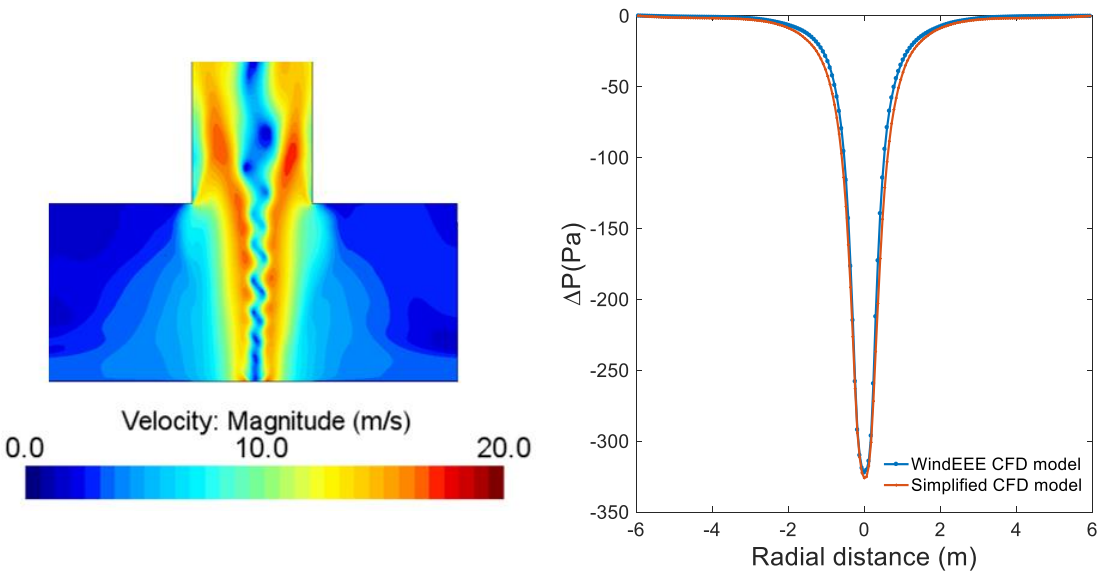

(a) Simplified model (b) Ground static pressure profile

Figure 2-36 (a) WindEEE simplified numerical model, (b) ground static pressure comparison.

From Figure 2-36, a good match of overall flow structure and ground static pressure profile between WindEEE CFD and simplified numerical model is evident.

Vane angle	r_0 (m)	h_0 (m)	h_u (m)	r_u (m)	v_t (m/s)	v_r (m/s)	v_t/v_r (at h_o, r_o)
15°	6	0.8	4	1.8	1.52	2.85	0.53

Table 2-5 Parameters for simplified WindEEE numerical model.

2.5 Comparison of flow structures

To demonstrate unification, flow structures of from each simulator are qualitatively compared to show that vortices with similar swirl ratios have similar flow structures.

Figure 2-37 shows the flow structures of 20-degree guide vane configuration from TTU VorTECH (S=0.43), floor 3 configuration from ISU Tornado Simulator (S=0.5) and 15-degree guide vane configuration at WindEEE (S=0.5). All three vortices are observed to have very similar appearance ("alternating bubbles" in the core). This is due to the turbulent nature of vortex break down that becomes prominent around a swirl ratio of 0.4 and manifests itself as "alternating bubbles" in the mean velocity field (in the r-z plane).

From calculations presented in section 2.4.1, it was shown that 20-degree guide vane configuration from VortTECH corresponds to S=0.44. Also, Haan et al. (2008) reported a swirl ratio value of 0.5 for floor 3 configuration and the swirl ratio for 15-degree guide vane configuration for WindEEE was reported to be around 0.5 as well. While the swirl ratios for the three configurations are very comparable, it can also be seen from Figure 2-37 that the flow structures for these three configurations also look very similar. This indicates that they could each possibly represent the same tornado but at different length (and velocity) scales due to geometric differences in the facilities as described in the following discussion.

Refan et al. (2014) proposed a scaling technique based on the axial (z_{max}) and radial (r_{max}) location of maximum tangential velocity. It was shown that to replicate a real tornado in

lab, the axial $\left(\frac{z_{max,full\ scale}}{z_{max,lab\ scale}}\right)$ and radial $\left(\frac{r_{max,full\ scale}}{r_{max,lab\ scale}}\right)$ length scales must converge to around the same value at some swirl ratio. This means if two vortices have similar swirl ratio values (same flow structure), then regardless of which experimental facility they are produced in, they should be able to replicate the same real tornado, but just at different length scales. This difference in length scales is expected to arise from the difference in physical size of simulators. This is further demonstrated as following.

It was observed from the numerical simulations conducted in this study that for 15-degree guide vane angle configuration for WindEEE (corresponding to S=0.5), $z_{max,WindEE} = 0.1\,m$ and $r_{max,WindEE} = 0.4\,m$. Further, for floor 3 configuration of ISU Tornado Simulator (also corresponding to S=0.5), it was observed that $z_{max,ISU} = 0.05m$ and $r_{max,ISU} = 0.21m$. Therefore,

$$\frac{z_{max,ISU}}{z_{max,WindEE}} \approx \frac{r_{max,ISU}}{r_{max,WindEE}} \approx 0.5$$

This implies that floor 3 configuration in ISU tornado simulator produces the same vortex as 15-degree guide vane configuration at WindEEE at half the geometric scale (ISU vortex is half as a small as WindEEE with same flow structure). This means that if 0.5 swirl ratio vortex produced at WindEEE, for example, represents a real tornado at a length scale of 1:500, the same real tornado can be represented by 0.5 swirl ratio vortex produced in ISU Tornado Simulator at a length scale of 1:1000.

Similarly, it was found that for 20-degree guide vane configuration in TTU VorTECH (corresponding to S=0.43). $z_{max,TTU} = 1.25m$ and $r_{max,TTU} = 0.3m$.

$$\frac{z_{max,TTU}}{z_{max,WindEE}} > \frac{r_{max,TTU}}{r_{max,WindEE}}$$

$$1.25 > 0.75$$

This is expected because 20-degree guide vane configuration in VorTECH corresponds to S=0.43 and15-degree guide vane configuration in WindEEE corresponds to S=0.5. While the swirl ratio magnitudes are very close and therefore the flow structures look comparable,

they do not represent the same scenario. Hangan and Kim (2008) reported that increasing swirl ratio increases r_{max} and lowers z_{max}. This implies that if swirl ratio for VorTECH is increased from 0.43, $\frac{z_{max,TTU}}{z_{max,WindEE}}$ would reduce and $\frac{r_{max,TTU}}{r_{max,WindEE}}$ would increase and at certain swirl ratio value close to 0.5 , we could expect $\frac{z_{max,TTU}}{z_{max,WindEE}} = \frac{r_{max,TTU}}{r_{max,WindEE}}$. Since for TTU VorTECH, 20-degree configuration corresponds to S=0.43 and 30-degree configuration corresponds to S= 0.6 (refer to Table 2-3), it anticipated that the guide vane should be set to an angle between $20°$ and $30°$ to achieve geometric similarity, as described above.

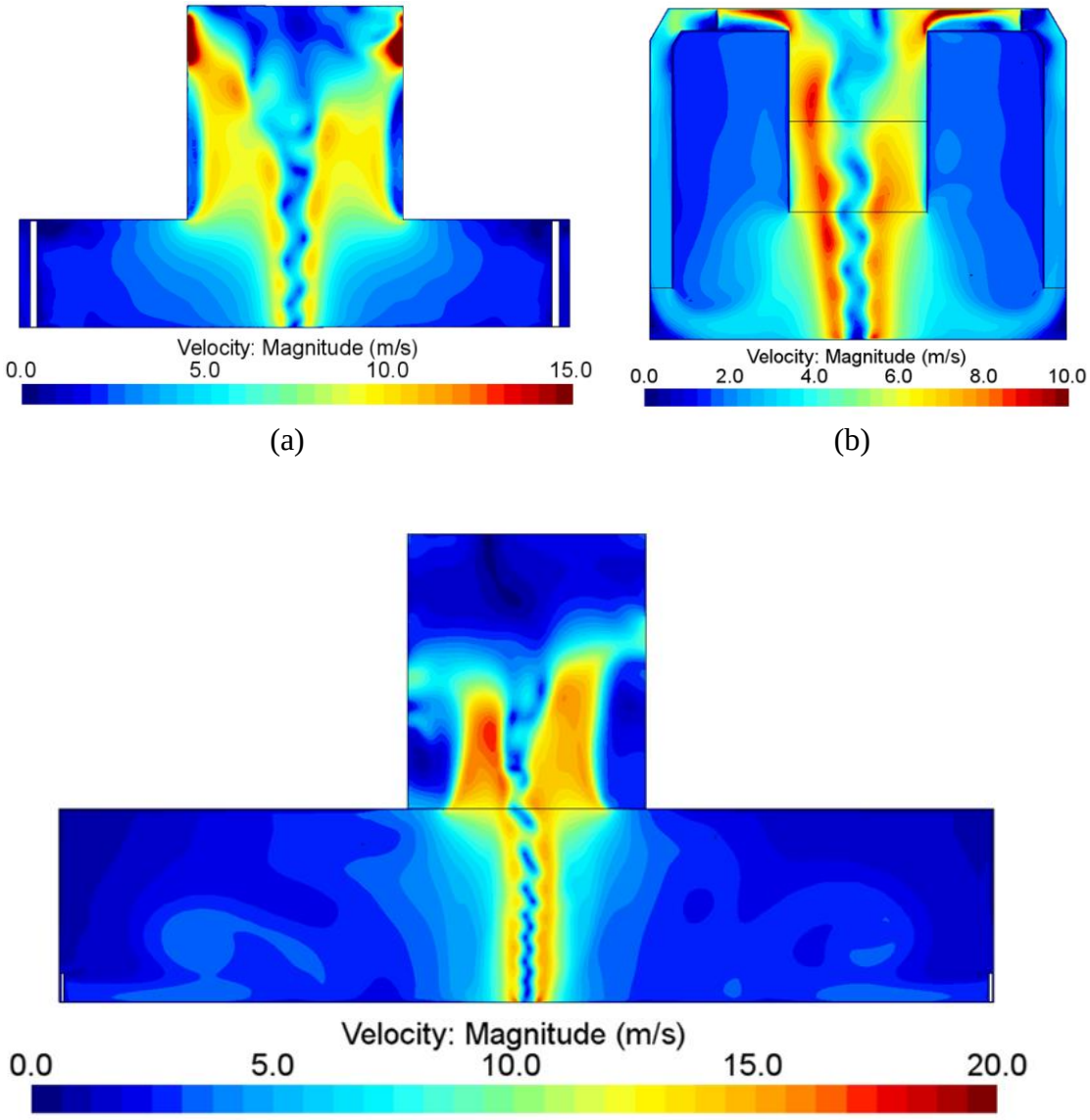

Figure 2-37 (a) TTU VorTECH S=0.43, (b) ISU Tornado Simulator S=0.5, (c) WindEEE S=0.5.

2.6 Conclusions

The following conclusions can be made from this study.

- It was demonstrated that by identifying the parameters used to characterize a vortex strictly from the flow-field, as opposed to directly using the geometric dimenions and confugrations of physical elements of an experimental simulator, it is possible to simplify the experimental tornado simulators into one generic numerical model, where the flow structures of the vortices with comparable swirl ratios were found to be very similar.

- A major difference between bounded systems like VorTECH at Texas Tech University (based on Ward type design) and unbounded systems like Iowa State University Tornado Simulator and WindEEE Dome at Western University is the presence of a recirculating zone above the inflow/convergent layer observed in unbounded systems. This recirculating zone can not only affect the vortex flow structure but also make inflow velocity profiles somewhat misleading unless visual aid is utilized

- The size of the updraft hole (or bell mouth/exhaust opening) was observed to have a significant impact on the flow structure of laboratory produced vortices. In certain cases, it was also observed that this updraft hole size was effectively reduced and this reduction had to be accounted for, in the simplified generic numerical model.

- It was also shown that vortices with similar swirl ratio produced in different experimental facilities can represent the same real tornado, but at different length scales.

- Vortex wandering was found to be a common feature of simulated tornadoes (experimentally and numerically produced vortices). While wandering is commonly observed in real tornadoes (tornadoes in nature) as well, care must be taken when measurements are made using fixed probes for simulated tornadoes, particularly when validating numerical results with experimental data.

References

[1] Baker, G. R., Barker S.J., Bofah K.K., and Saffman P.G. "Laser anemometer measurements of trailing vortices in water." *Journal of Fluid Mechanics* 65.2 (1974): 325-336.

[2] Church C. R., Snow J. T, and Agee E.M. "Characteristics of tornado-like vortices as a function of swirl ratio: A laboratory investigation." *Journal of the Atmospheric Sciences* 36.9 (1979): 1755-1776.

[3] Davies-Jones, R.P. "The dependence of core radius on swirl ratio in a tornado simulator." *Journal of the Atmospheric Sciences* 30.7 (1973): 1427-1430.

[4] Davies-Jones, R. P. "Tornado dynamics, Thunderstorm Morphology and Dynamics." 2d ed., *E. Kessler, Ed.*, University of Oklahoma Press, 197–236 (1981): 197-236.

[5] Devenport, W. J., Zsoldos J.S. and Vogel C.M. "The structure and development of a counter-rotating wing-tip vortex pair." *Journal of Fluid Mechanics* 332 (1997): 71-104.

[6] Haan Jr F.L., Sarkar P., and Gallus W.A. "Design, construction and performance of a large tornado simulator for wind engineering applications." *Engineering Structures* 30.4 (2008): 1146-1159.

[7] Hangan H., and Kim J.D. "Swirl ratio effects on tornado vortices in relation to the Fujita scale." *Wind and Structures* 11.4 (2008): 291-302.

[8] Hangan H., "The Wind Engineering Energy and Environment (WindEEE) Dome at Western University, Canada", *Wind Engineers, JAWE*, Vol. 39, No.4 (2014)

[9] Heyes, A. L., Jones R. F., and Smith D. A. R. "Wandering of wing-tip vortices." *Proceedings of 12th International Symposium on the Applications of Laser techniques to fluid mechanics. Lisbon, Portugal*. 2004.

[10] Lee J.J., Samaras T., and Young C.R. "Pressure measurements at the ground in an F-4 tornado." *Preprints, 22nd Conf. on Severe Local Storms, Hyannis, MA, Amer. Meteor. Soc., CD-ROM*. Vol. 15. 2004.

[11] Lilly K. "Tornado dynamics." (1969). *National Center for Atmospheric Research Manuscript* 69-117.

[12] Mayer L.J. “Development of a large-scale simulator.” *M.S. Thesis. Texas Tech. University* (2009).

[13] Mishra A.R., James D.L., and Letchford C.W. "Physical simulation of a single-celled tornado-like vortex, part A: flow field characterization." *Journal of Wind Engineering and Industrial Aerodynamics* 96.8 (2008): 1243-1257.

[14] Natarajan D., and Hangan H. "Large eddy simulations of translation and surface roughness effects on tornado-like vortices." *Journal of Wind Engineering and Industrial Aerodynamics* 104 (2012): 577-584.

[15] Nasir Z., "Numerical modeling of tornado-like vortex and its interaction with bluff-bodies." *PhD Thesis. Western University, Canada* (2017).

[16] Orf L., Wilhelmson R.B., Wicker L., and Lee B.D. "Genesis and maintenance of a long-track EF5 tornado embedded within a simulated supercell." *27th Conference on Severe Local Storms. American Meteorological Society*. 2014.

[17] Orf L., Wilhelmson R.B., and Wicker L. "Visualization of a simulated long-track EF5 tornado embedded within a supercell thunderstorm." *Parallel Computing* 55 (2016): 28-34.

[18] Refan M., Hangan H., and Wurman J. "Reproducing tornadoes in laboratory using proper scaling." *Journal of Wind Engineering and Industrial Aerodynamics* 135 (2014): 136-148.

[19] Tang Z., Feng C., Wu L., Zuo D., and James D.L. "Simulations of Tornado-Like Vortices in A Large-Scale Ward-Type Tornado Simulator." (2016). *8th International Colloquium on Bluff Body Aerodynamics and Applications Northeastern University, Boston, Massachusetts, USA*

[20] Ward, N.B. "The exploration of certain features of tornado dynamics using a laboratory model." *Journal of the Atmospheric Sciences* 29.6 (1972): 1194-1204.

[21] Yang Z., Sarkar P., and Hu H. "An experimental study of a high-rise building model in tornado-like winds." *Journal of Fluids and Structures*27.4 (2011): 471-486

[22] Zhang W., and Sarkar P. "Near-ground tornado-like vortex structure resolved by particle image velocimetry (PIV)." *Experiments in Fluids* 52.2 (2012): 479-493.

Chapter 3

3 Application of the generic numerical tornado model to bluff-body aerodynamics and wind load evaluation

Tornadoes are violently rotating columns of air with high speed winds that often leave behind a destruction trail. Based on damage total and number of fatalities due to natural hazards, tornadoes are ranked third, after floods and hurricanes, in the Unite States (Cutter 2002). With an estimation of around 1200 tornadoes per year, the United States ranks first in terms of annual tornado occurrences. Further, from a statistical perspective, the year 2011 stands out in terms of maximum annual tornado damage in the United States since the 1950s. According US National Oceanic and Atmospheric Administration (NOAA), tornadoes caused 550 deaths and 28 billion dollars in damage that year alone. While most tornadoes in United States occur in the south-central region (termed as 'tornado alley), significant tornadoes have also been witnessed in other areas outside of that region. In fact, it has been commonly observed that tornadoes outside of tornado alley cause more damage than anticipated merely because they are relatively less expected to occur outside of the tornado alley.

Alerted by the damage potential of tornadoes and to enhance the resiliency of our community towards this extreme weather phenomenon, numerous studies have been conducted to understand wind loads on structures arising from tornadoes. While experimental studies like Mishra et al. (2008), Haan et al. (2010), Thampi et al. (2011), Sabareesh et al. (2013) and Case et al. (2014) studied the effect of tornadic wind loads on low-rise buildings, studies like Wen (1973) and Yang et. al (2011) studied the effects of tornadic wind on tall buildings. Similarly, Selvam and Millet (2003), Selvam and Millet (2004), Savory et al. (2001), Gorecki and Selvam (2015), Sengupta et al. (2008), Nasir and Bitsuamlak (2016), Hamada et al. (2010) and Natarajan and Hanagn (2012) are some examples of studies which used numerical techniques to understand the interaction tornado with ground and civil structures.

The present study is carried out to demonstrate the application of previously developed generic numerical tornado model towards bluff-body aerodynamics and wind load

evaluation by numerically replicating prior conducted experiments on tornado-building interaction and then comparing the results. First, the interaction of a typical mid-rise building model is carried out numerically (using the previously developed model) and the results are compared with experimentally obtained data from WindEEE Dome at Western University. Next, wind load evaluation of a typical high-rise building model is conducted numerically and compared with the experimentally obtained results reported in Yang et al. (2011), where a similar test was previously carried out using Iowa State University Tornado Simulator.

3.1 Mid-rise building (validation of WindEEE model)

To validate the previously developed numerical tornado model for WindEEE, an experiment was conducted at WindEEE Dome at Western University, the details of which have been presented in the following section.

3.1.1 Experimental set-up (I)

A typical mid-rise building model was subject to tornado-like flow field generated at WindEEE dome and a High Frequency Pressure Integration (HFPI) test was conducted. To achieve this, WindEEE was operated in the second mode (non-functional peripheral fans) and the 15-degree guide vane configuration was used. The generated vortex was reported to have a swirl ratio of around 0.5 with a core radius and maximum mean tangential velocity at 0.17 m (building height) to be around 0.5 m and 15m/s, respectively.

Height (H)	0.17 m
Length	0.21 m
Width	0.15 m

Table 3-1 Building model dimensions.

The building was placed at two locations with respect to vortex centre i.e. core centre and core radius, as shown in Figure 3-1.

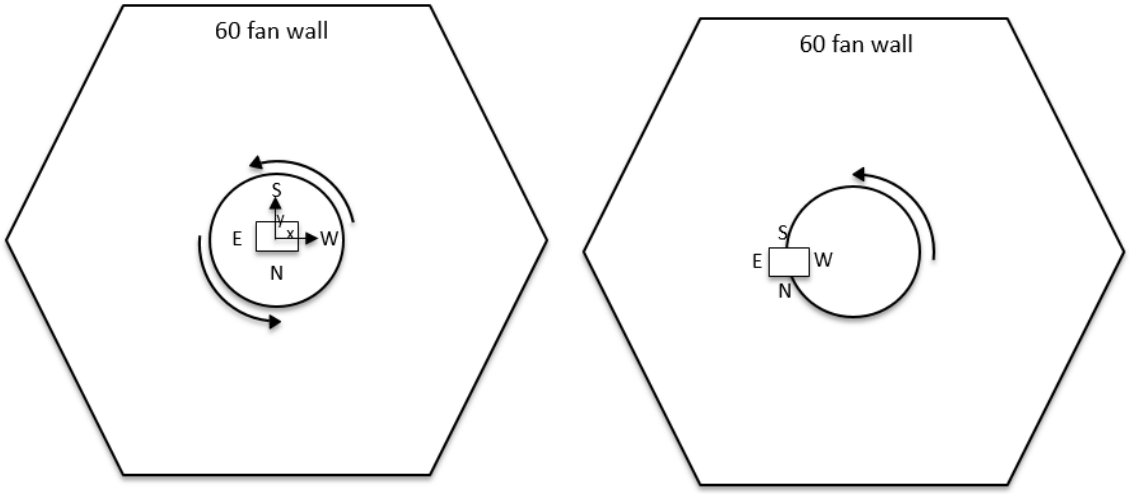

(a) Core centre location (b) Core radius location

Figure 3-1 Building model locations.

Surface pressure and force coefficients acting on the building model were then computed as shown below.

$$Cp = \frac{P - P_0}{\frac{1}{2}\rho\, U_{ref}^2}$$

Here, P_0 is the reference static pressure (atmospheric pressure in this case, measured outside the test chamber) and U_{ref} is the reference velocity (mean maximum tangential velocity measured at building height, in the absence of building).

Further, the experimentally obtained surface pressures were integrated to obtain forces acting on the model. The pressure data obtained from the wind tunnel test (at WindEEE) was integrated to evaluate wind loads using MATLAB. An outline of the process along with a brief description of the sign convention for forces and torsion have been presented in this section.

$$F = \iint (\frac{1}{2}\rho v^2\, Cp) dA$$

$$M = r \times \iint (\frac{1}{2}\rho v^2 \, Cp) dA$$

Here, F is the force, M is the moment (torsion), Cp is the pressure coefficient and its values for the above equation were calculated as shown in the previously, v is the reference velocity (at building height in this case), dA represents the tributary area of each tap and r is the length of lever arm. These forces and moments were then converted to respective coefficients as shown below.

$$CF_x = \frac{F_x}{\frac{1}{2}\rho U_{ref}^2 A}$$

$$CF_y = \frac{F_y}{\frac{1}{2}\rho U_{ref}^2 A}$$

$$CM_z = \frac{M_z}{\frac{1}{2}\rho U_{ref}^2 AH}$$

F_x is the component of force in the x direction, F_y is the component of force in y direction and M_z is the component of moment of force (torsion) in z direction (shown in Figure 3-2), A is the projected area, H is the building height, ρ is air density and U_{ref} is the reference velocity.

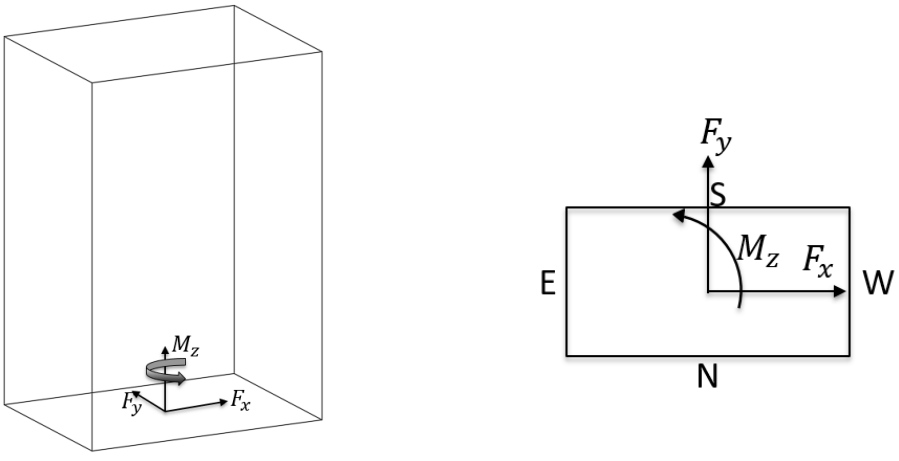

Figure 3-2 Sign convention for forces and moments.

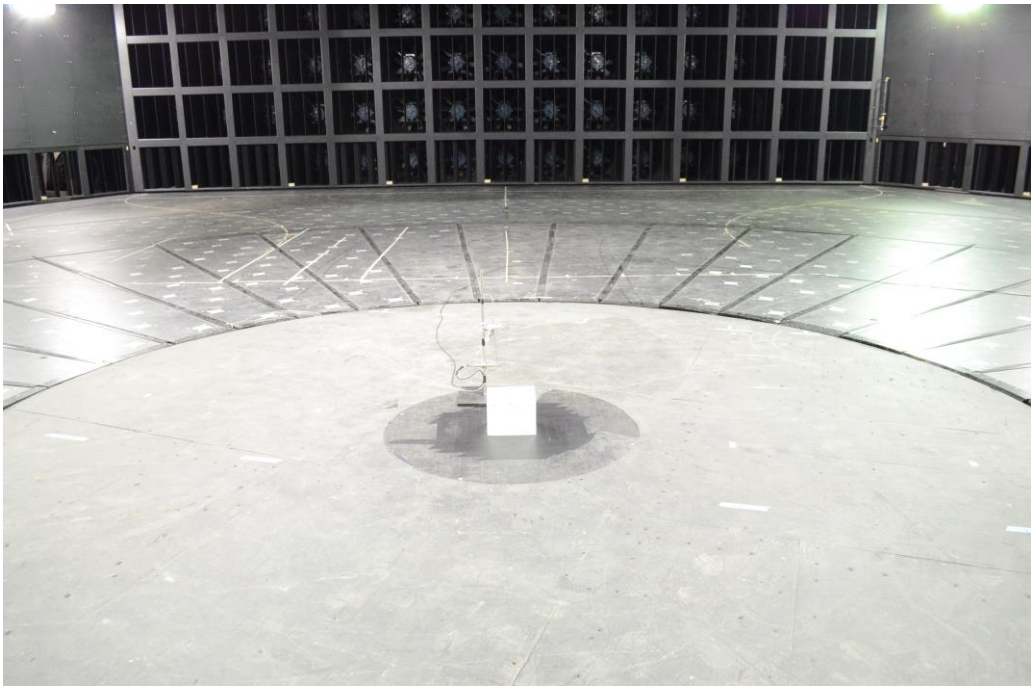

(a)

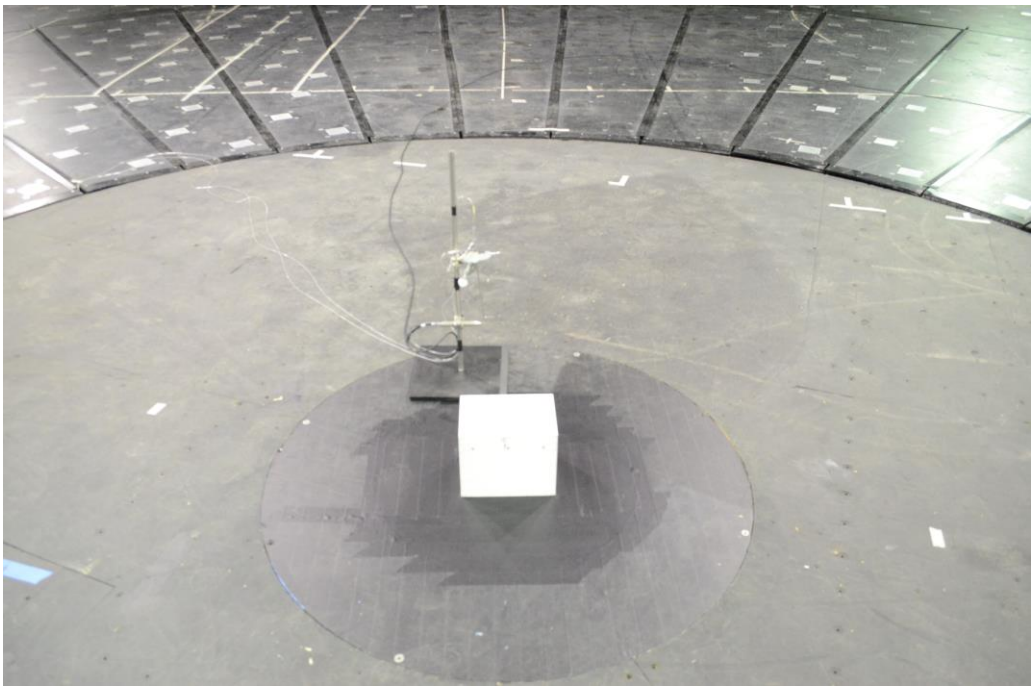

(b)

Figure 3-3 Building model placed at core centre location with a pitot tube to measure the mean maximum tangential velocity at building height (a) far view (b) close-up view

3.1.2 Numerical simulation set-up (I)

To replicate the flow field generated in WindEEE during the experiment described above, the generic numerical model developed in Chapter 2 was utilized. The details of numerical set-up to achieve the required flow field have been tabulated below. The paramters shown in Table 3-2 will be utilized in the generic numerical model as illustrated in Figure 3-4.

Vane angle	r_0 (m)	h_0 (m)	h_u (m)	r_u (m)	v_t (m/s)	v_r (m/s)	v_t/v_r (at h_o, r_o)
15°	6	0.8	5.2	1.75	1.52	2.85	0.53

Table 3-2 Parameter for simplified WindEEE numerical model.

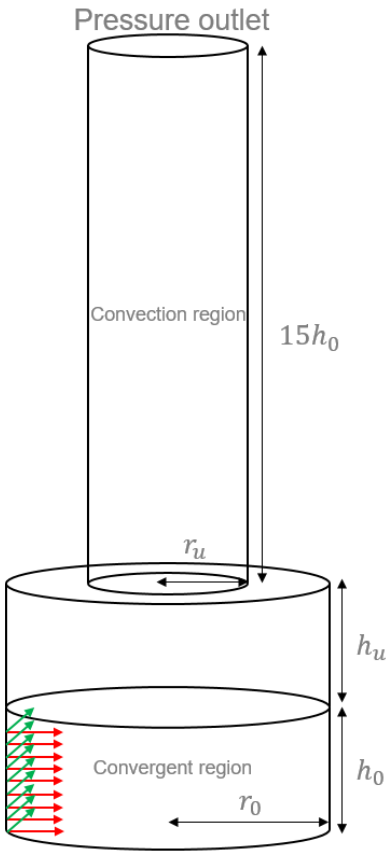

Figure 3-4 Generic numerical model schematic.

The core size and maximum mean tangential velocity at 0.17 m height for this configuration were validated with the numerical results in the previous chapter.

Large Eddy Simulations carried out during this study were initialized with the solution obtained through RANS (RSM) simulations. It was ensured that Courant–Friedrichs–Lewy (CFL) condition was satisfied. For this, the time step was chosen to maintain Courant number value below 1, at least in the region of interest. As a result, the time step for the transient simulations (Large Eddy Simulations) was of the order of 0.0001 seconds.

$$C = \frac{U\Delta t}{\Delta x} < 1$$

To capture flow details around the building, further refinement was made around the model region, as shown in the Figure 3-5.

The resulting pressure, force and moment coefficients were computed as described before and then compared with experimentally obtained results.

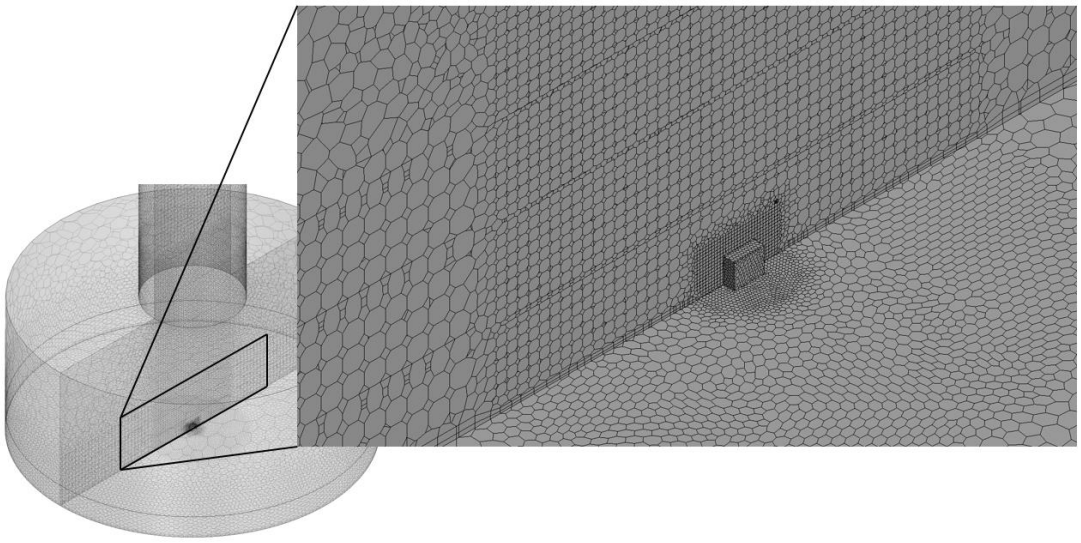

Figure 3-5 Mesh strategy.

3.1.3 Results and discussion (I)

From Figure 3-6 and Figure 3-7, a reasonable match (qualitatively) in the surface pressure distribution can be observed between numerical and experimental results. However, an

interesting difference is the symmetry displayed for core centre case by numerical simulation, which is absent in experimental results. Although it is not entirely clear at this point as to what could have caused it, one possible explanation is based on the phenomenon of vortex wandering. It was previously observed that while wandering is an inherent property of these vortices, it can be augmented due to unsteadiness arsing from the mechanical system of the wind tunnel. It was seen that the extent of wandering is reduced for the simplified generic model as compared to the full CFD models of the entire system. Further for simplified models, the extent of wandering was higher for lower swirl ratios while it was somewhat mitigated for swirl ratios around 0.5. It is speculated that this is the reason for symmetry in pressure distribution for the simplified numerical results since the vortex simulated for this test had a swirl ratio of around 0.5 and therefore the simplified model showed mitigation in wandering. This has been illustrated in Figure 3-8.

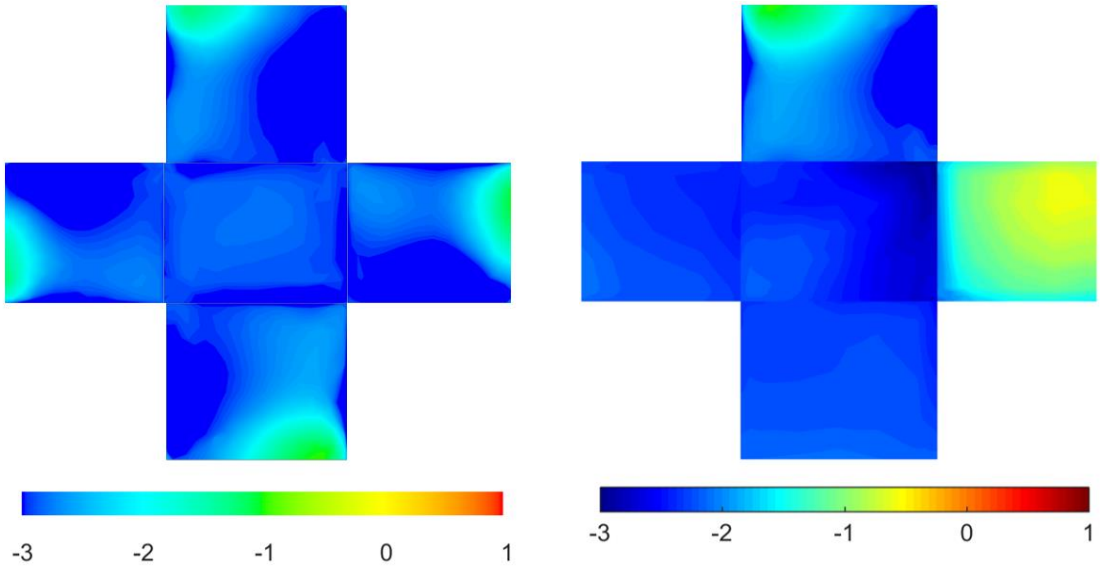

(a) (b)

Figure 3-6 Surface pressure coefficient distribution for core centre location obtained from (a) generic numerical model (b) WindEEE experiment.

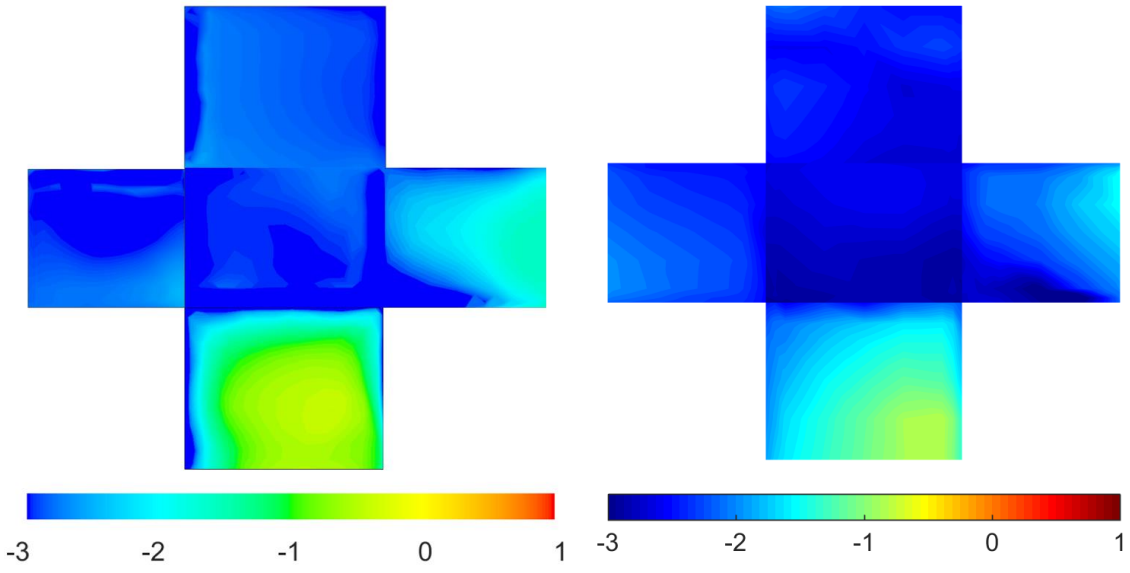

(a) (b)

Figure 3-7 Surface pressure coefficient distribution for core radius location obtained from (a) generic numerical model (b) WindEEE experiment.

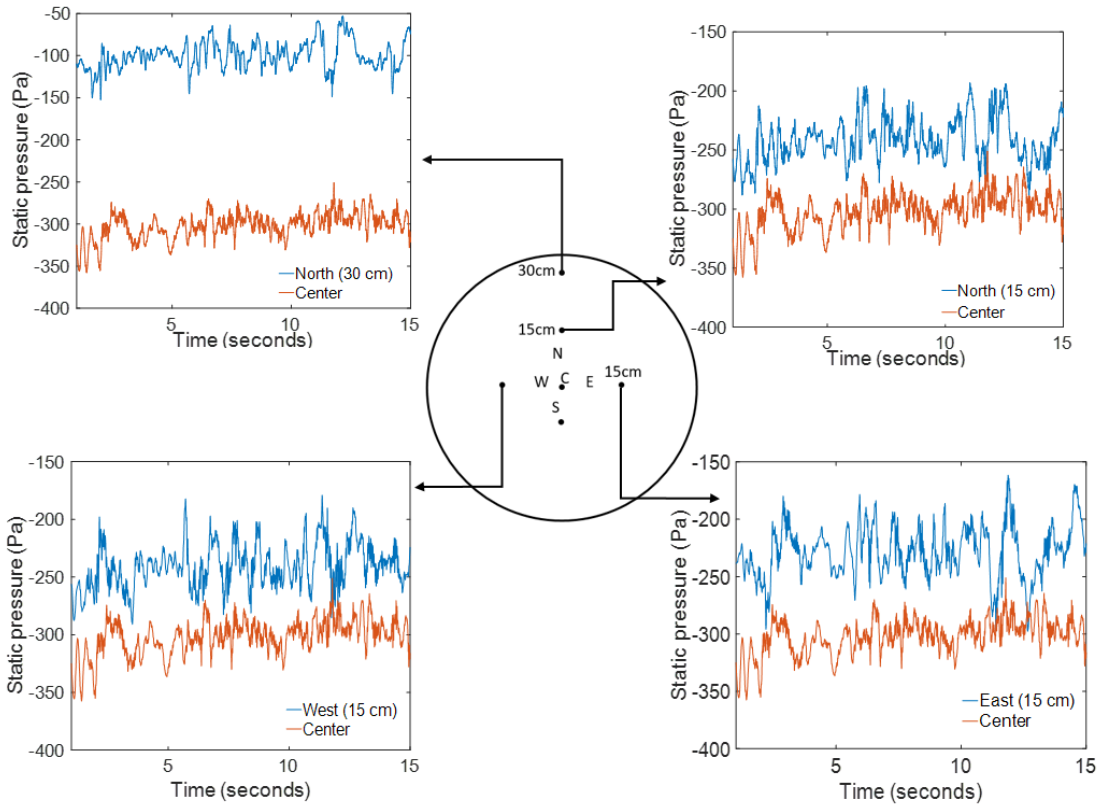

Figure 3-8 Mitigation of wandering in simplified numerical simulations.

The number of up-crossings between ground static pressure time series at the centre and other locations away from the centre has been used to estimate the extent of wandering throughout the study. From Figure 3-8, it can be observed that wandering for simplified numerical simulations is mitigated (no upcrossing) around 0.5 swirl ratio, however for full WindEEE CFD model, wandering was found to persist. Further, it is anticipated that the extent of wandering in actual WindEEE experimental set up would be even higher than what is predicted by WindEEE CFD model. This is because of the coasting of peripheral fans in WindEEE experimental set-up (that could introduce unwanted turbulence and asymmetry in the flow) that were not modelled in WindEEE CFD simulations (peripheral fans were not modelled in this study that mimics first mode of WindEEE operation). From Figure 3-7, a reasonable agreement of building surface pressure coefficients between numerical and experimental results for core radius location. Minor differences are attributed to vortex wandering in experimental set-up as previously described.

Further, the base load (force and moment) coefficients were also computed as described previously, for both numerical and experimental simulations, and compared.

		CFx	CFy	Mz
Experimental	CC	0	1.3	0
	CR	-0.4	1.6	0.2
Numerical	CC	0	0	0
	CR	-0.8	2.1	0.1

Table 3-3 Comparison of base loads obtained from numerical and experimental simulation.

From Table 3-3, experimental and numerical simulations indicate very small values of torsional moment coefficient for both locations, which also consistent with what was reported in Yang et al. (2011) as will be seen in the upcoming sections. The force coefficients obtained experimentally and numerically showed some minor discrepancies. This can also be explained based on vortex wandering. As presented before, simplified numerical simulations yield a symmetric pressure distribution on the building surface (since wandering is mitigated), this cancels out the forces on the structure. However, due to wandering, the net forces did not seem to have cancelled out even for the core centre location which is believed to be the reason for discrepancy seen from Table 3-3. Similar argument holds for core radius location as well.

The discussion on wandering presented in this study is not fully conclusive and would require detailed experimentation (simulation) to fully quantify its effect during future studies.

3.2 High-rise building (validation of ISU Tornado Simulator model)

3.2.1 Experimental set up (II)

Yang et al. (2011) tested the effect of tornado-like winds on a typical high-rise building model of plan area 34.4 mm x 34.4 mm and height 140 mm. The building was subject to tornado-like wind field achieved by vane 1 setting of the ISU Tornado Simulator. The building position was altered with respect to the centre of a stationary vortex and the

resulting force and moments coefficients were computed. The force and moment coefficients were computed as following.

$$CF_x = \frac{F_x}{\frac{1}{2}\rho V_{ref}^2 A}$$

$$CF_y = \frac{F_y}{\frac{1}{2}\rho V_{ref}^2 A}$$

$$CM_z = \frac{M_z}{\frac{1}{2}\rho V_{ref}^2 AH}$$

Here F_x is the component of force in the x direction, F_y is the component of force in y direction and M_z is the component of moment of force in z direction (torsion) (shown in Figure 3-9), A is the projected area, H is the building height, ρ is air density and V_{ref} =7m/s (maximum mean tangential velocity at 70 mm height).

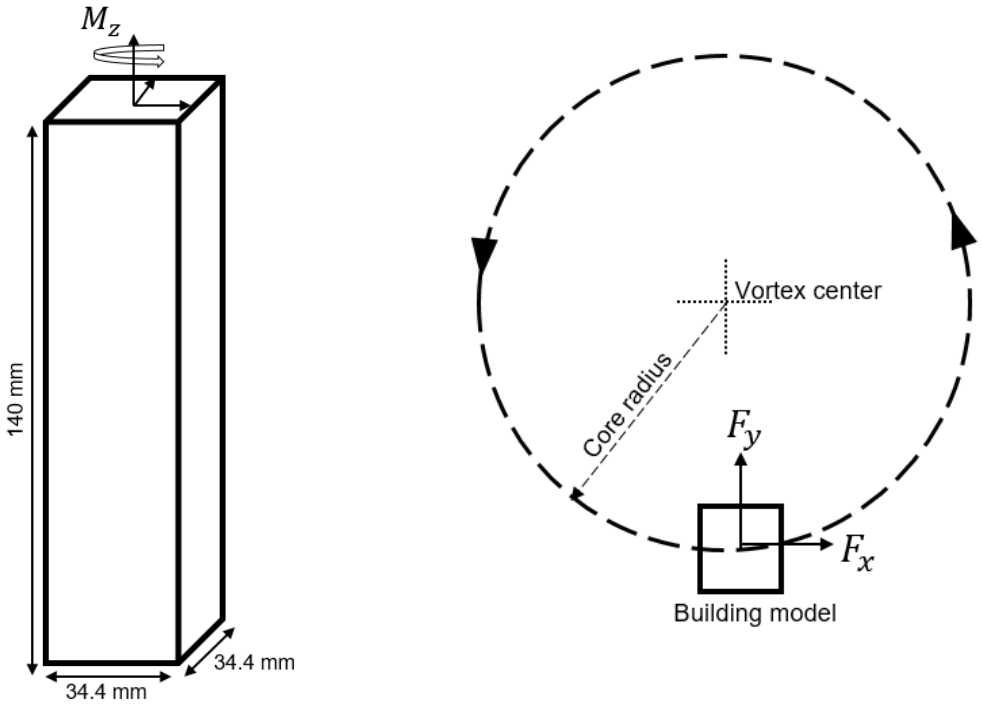

Figure 3-9 Illustration of sign convention for forces and moments.

Based on Yang et al. (2011), the building was positioned at 6 locations as summarized in Table 3-4.

Position	Distance
r1	0
r2	$0.5r_c$
r3	$2.3r_c$
r4	$3r_c$
r5	$4.5r_c$
r6	$6r_c$

Table 3-4 Building locations with respect to the vortex-centre (r_c is the core radius).

Wind load evaluation of a building model of same dimensions under similar tornadic flow was conducted numerically to asses the performance of the numerical model developed in the previous chapter.

3.2.2 Numerical simulation set-up (II)

The numerical model used to replicate the flow field was based on the geometric and inflow parameters identified during the development of generic numerical tornado model for vane 1 setting of ISU tornado simulator (presented in Chapter 2). The details of the parameters have been tabulated below. Large Eddy Simulations were then conducted to numerically obtain wind load coefficients and flow field around the building model.

r_0 (m)	h_0 (m)	h_u (m)	r_u (m)	v_t (m/s)	v_r (m/s)	v_t/v_r
2.05	0.27	1.45	0.915	0.83	3.74	0.22

Table 3-5 Simplified ISU tornado simulator numerical model parameters.

Yang et al. (2011) reported a core radius of 0.165 m at 70 mm height (from the ground) and a mean tangential velocity of 7 m/s (at the core radius) and described the vortex as thin and laminar with low swirl for vane 1 configuration. The numerical model using Large Eddy Simulations predicted very comparable values of core radius and mean tangential velocity at that location as shown in Figure 3-10. The appearance of numerically produced vortex for this study was also found to be thin and laminar. This indicates at least some basic agreement between experimentally and numerically generated flow fields, to begin with.

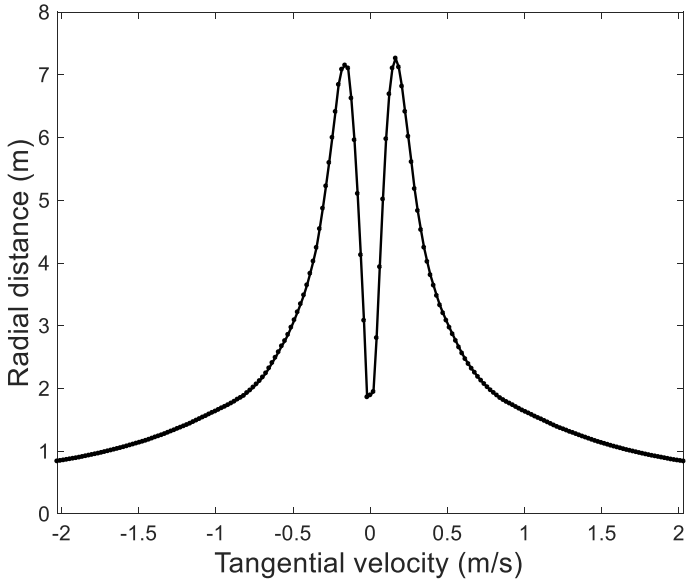

Figure 3-10 Radial profile of tangential velocity at 70 mm height obtained through numerical model using LES (time averaged values presented here).

The core radius obtained numerically at 70 mm height was about 0.165m and tangential velocity at that location was around 7 m/s (Figure 3-10).

3.2.3 Results and discussion (II)

In this section, the results obtained from numerical analysis are discussed and compared with experimentally reported results in Yang et al. (2011). Figure 3-11 shows the velocity field plotted at 70 mm height (half height) for the core radius location of the building at five time instances as well as the time averaged streamlines. It can be seen from Figure 3-11(a) through (e) that the system is very dynamic due to wandering of the vortex and vortex moves significantly, completely altering the wake around the building model as it does so. This observation is also consistent with Yang et al. (2011), who reported movement in the vortex centre, based on PIV measurements. At time instant t1, the vortex is close to the geometric centre of the simulator. The flow hits the building and separates; however, it can be seen from Figure 3-11 (a) that on the side of the building away from the vortex centre, the separation is not very prominent. In fact, even the wake behind building is asymmetric and is skewed towards the vortex centre. This indicates that while aerodynamic phenomenon associated with bluff-bodies, like flow separation and formation

of wake, do occur locally, the overall structure of wake is influenced (and dominated by suction inside the vortex). Time instant t2 is right before the vortex centre overlaps with the building and time instant t3 is right after it crosses the building. It can be observed that the wake around the building significantly changes between these two instances. At time instant t4, the vortex is at a location such that the flow strikes the building model near the corner edge and this results in a large wake behind the model. The wandering was observed to have a periodic cycle, i.e. the vortex would return to original position after about every 4-5 seconds. This can also be seen from Figure 3-11 (e), at time t5, the vortex is almost back to where it was at t1. The discussion above also arises questions about associating mean values with a fixed location of building model with respect to vortex centre of a "stationary" tornado. For example, in this case the location of the building model was intended to be at the core radius of the vortex but from Figure 3-11 and discussion presented here, it can be concluded that there were several instances when the vortex was over the building (like core centre location) and when the building was at a distance less than the core radius from the vortex centre etc., making mean values relatively less informative and possibly even misleading. Overall, it can be seen from Figure 3-11 that the wake structure around the building model, even for a stationary vortex case, is highly unsteady which is consistent with what was reported in Yang et al. (2011).

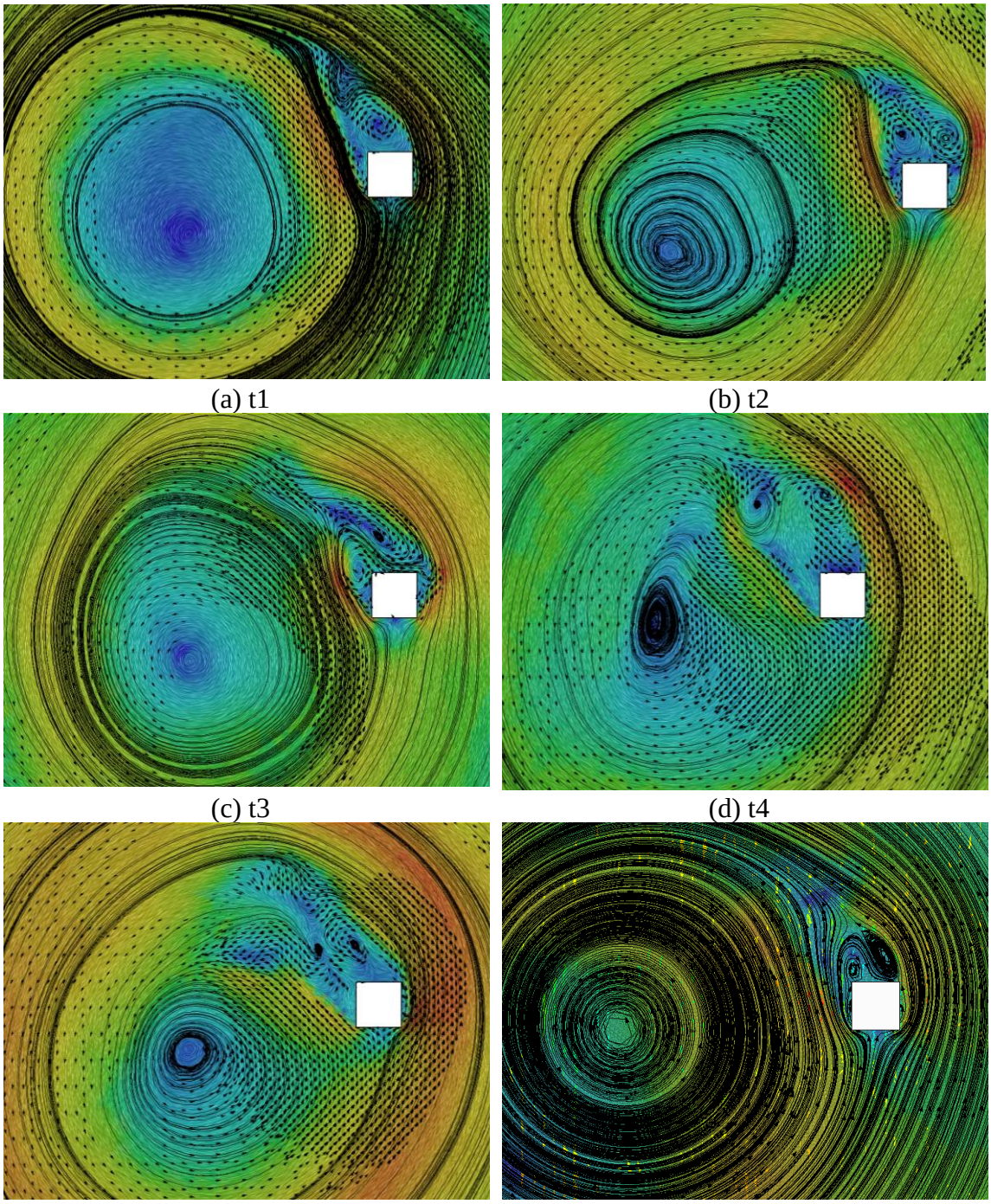

(a) t1 (b) t2

(c) t3 (d) t4

(e) t5 (f) Time-averaged LES

Figure 3-11 (a) Velocity field at time instant t1, (b) Velocity field at time instant t2, (c) Velocity field at time instant t3, (d) Velocity field at time instant t4, (e) Velocity field at time instant t5, (f) Time-averaged LES.

Figure 3-12 shows a comparison of time averaged velocity field obtained from the numerical model and Yang et al. (2011). A reasonably good agreement between the two can be instantly observed. Slight difference between the average velocity field obtained from steady RANS and time-averaged LES, and the similarity between time-averaged PIV and time-averaged LES can be seen from Figure 3-12.

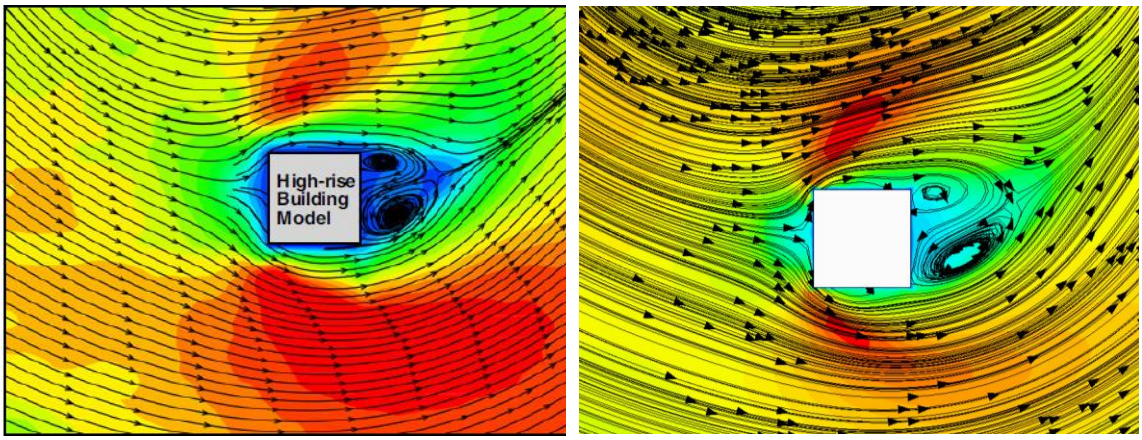

(a)Yang et al. (2011) (b) Time-averaged LES

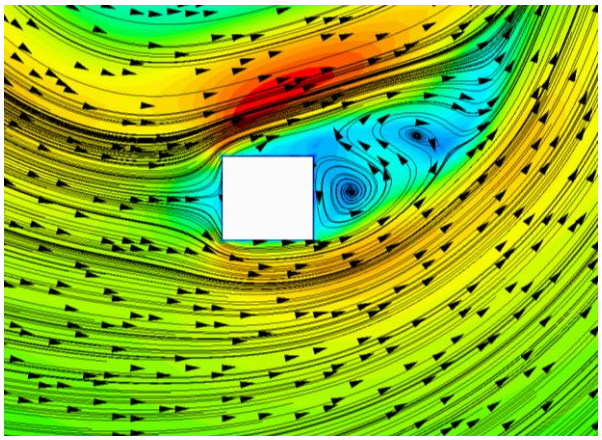

Steady RANS

Figure 3-12 (a) Time averaged velocity field from PIV (Yang et al. 2011)) (b) Time averaged velocity field from LES, (c) velocity field from steady RANS.

Figure 3-13 through Figure 3-15 present a comparison of numerically and experimentally obtained force and moment coefficients. The force coefficients (x and y) obtained from numerical simulations (Figure 3-13 and Figure 3-14) show the same trend as experimentally obtained values. However, the numerically obtained force coefficients are

seen to be slightly lower in magnitude. The experimentally obtained measurements were recorded using a JR3, model 30E12A-I40 (force balance), which has a precision of ± 0.25% of the full range (40N), i.e. 0.1 N, as reported in Yang et al. (2011). The building model used for this experiment had dimensions of 34.4 mm x 34.4 mm x 140 mm and experienced very small forces. With this argument, while the numerically obtained forces were slightly lower but the difference was close to the ± 0.1 uncertainty of the experimentally obtained values. Further, this mismatch might also be an indication of inappropriate choice of reference pressure to evaluate pressure and load coefficients. During the development of the generic numerical model (in Chapter 2), all pressures were referenced to the ground static pressure at the updraft radius (commonly observed practice in numerical studies). However, to be consistent with experimentally obtained data, during pressure and load coefficient evaluation in Chapter 3, atmospheric pressure was used as reference. It is possible that atmospheric pressure might not be the best choice for reference pressures when comparing results between different facilities and between experimental and numerical studies. This would, however, require more detailed research in the future.

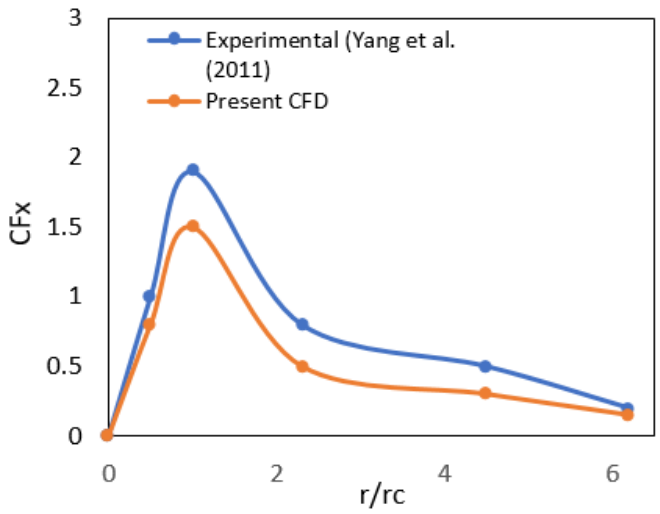

Figure 3-13 Comparison of force (Fx) coefficient obtained from numerical and experimental simulations.

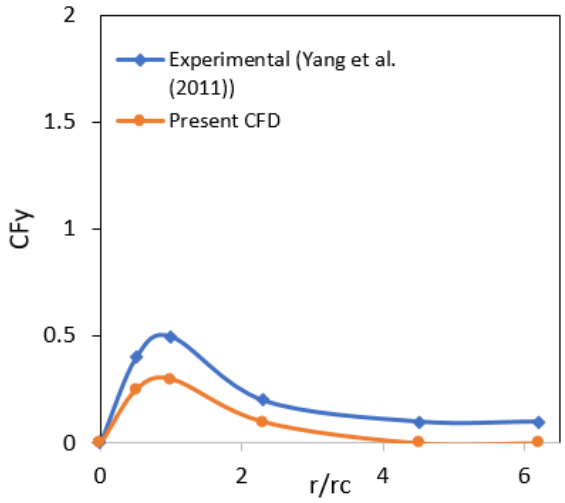

Figure 3-14 Comparison of force (Fy) coefficient obtained from numerical and experimental simulations.

From Figure 3-15, it can be observed that both numerical and experimental simulations show negligible torsional moment at every location and are therefore in good agreement.

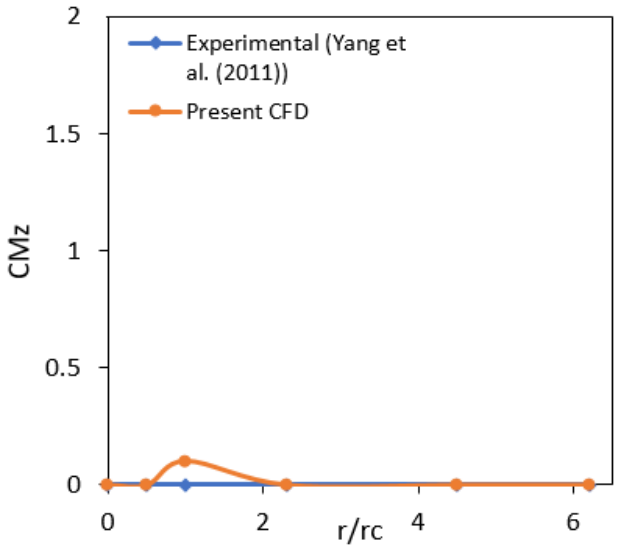

Figure 3-15 Comparison of moment (torsion) coefficient obtained from numerical and experimental simulations.

3.3 Conclusions

The following conclusion can be made from this study.

- The generic numerical tornado model developed in Chapter 2 displayed good promise for its application to bluff-body aerodynamics and wind load evaluation.

- On comparing experimental and numerical results, similar surface pressure distribution, flow structures around bluff bodies and trend in force coeffects were observed. The discrepancies between numerical and experimental results are suspected to arise due to vortex wandering.

- It was also seen that while wandering is an inherent property of tornado-like vortices at low swirl ratios, it is somewhat mitigated around mid-range swirl ratios (S~0.5) in the simplified generic numerical model (cylindrical in shape).

- Further, turbulent flow structures (wake) around a bluff body were found to be highly unsteady, even for a so called “stationary vortex”.

References

[1] Case J., Sarkar P., and Sritharan S. "Effect of low-rise building geometry on tornado-induced loads." *Journal of Wind Engineering and Industrial Aerodynamics* 133 (2014): 124-134.

[2] Cutter S. L., ed. *American hazardscapes: The regionalization of hazards and disasters*. Joseph Henry Press, 2002.

[3] Gorecki P.M., and Selvam R.P. “Visualization of tornado-like vortex interacting with wide tornado-break wall”. *Journal of Visualization* (2015): 393-406.

[4] Mishra A. R., James D.L., and Letchford C.W. "Physical simulation of a single-celled tornado-like vortex, Part B: Wind loading on a cubical model." *Journal of Wind Engineering and Industrial Aerodynamics* 96.8 (2008): 1258-1273.

[5] Nasir Z. "Numerical modeling of tornado-like vortex and its interaction with bluff-bodies." (2017).

[6] Natarajan D., and Hangan H. "Large eddy simulations of translation and surface roughness effects on tornado-like vortices." *Journal of Wind Engineering and Industrial Aerodynamics* 104 (2012): 577-584.

[7] Haan Jr, F. L., Balaramudu V., and Sarkar P. "Tornado-induced wind loads on a low-rise building." *Journal of structural engineering* 136.1 (2009): 106-116.

[8] Hamada A., El Damatty A. and Hangan H., Shehata A.Y., "Finite element modelling of transmission line structures under tornado wind loading" *Wind and Structures,* Vol. 13, No. 5 (2010) 451-469

[9] Sabareesh G.R., Matsui M., and Tamura Y. "Characteristics of internal pressures and net local roof wind forces on a building exposed to a tornado-like vortex." *Journal of Wind Engineering and Industrial Aerodynamics* 112 (2013): 52-57.

[10] Savory E., Parke G.A.R., Zeinoddini M., Toy N., and Disney P. “Modelling of tornado and microburst-induced wind loading and failure of a lattice transmission tower”. *Engineering Structures* 23.4 (2001): 365-375.

[11] Selvam, R. P., and Millett P.C. "Computer modeling of tornado forces on a cubic building using large eddy simulation." *Journal of the Arkansas Academy of Science* 57.1 (2003): 140-146.

[12] Selvam R.P., and Millett P.C. "Large eddy simulation of the tornado-structure interaction to determine structural loadings." *Wind and Structures* 8.1 (2005): 49-60.

[13] Sengupta A., Haan Jr F.L., Sarkar P., and Balaramudu V. "Transient loads on buildings in microburst and tornado winds." *Journal of Wind Engineering and Industrial Aerodynamics* 96.10 (2008): 2173-2187.

[14] Thampi H., Dayal V., and Sarkar P. "Finite element analysis of interaction of tornados with a low-rise timber building." *Journal of Wind Engineering and Industrial Aerodynamics* 99.4 (2011): 369-377.

[15] Wen Y.K. "Dynamic tornadic wind loads on tall buildings." *Journal of the Structural Division* 101.1 (1975): 169-185.

[16] Yang Z., Sarkar P., and Hu H. "An experimental study of a high-rise building model in tornado-like winds." *Journal of Fluids and Structures* 27.4 (2011): 471-486.

Chapter 4

4 Conclusions and future research direction

This chapter presents some concluding remarks based on current work and lays out future research in this direction.

4.1 Conclusion

The following conclusions can be drawn from this study.

- It was demonstrated that by identifying the parameters used to characterize a vortex strictly from the flow-field, as opposed to directly using the geometric dimenions and confugrations of physical elements of an experimental simulator, it is possible to simplify the experimental tornado simulators into one generic numerical model, that can generate similar flow structures for vortices with comparable swirl ratios.

- A major difference between bounded systems like VorTECH at Texas Tech University (based on Ward type design) and unbounded systems like Iowa State University Tornado Simulator and WindEEE Dome at Western University is the presence of a recirculating zone above the inflow/convergent layer observed in unbounded systems. This recirculating zone can not only affect the vortex flow structure but also make direct use of inflow velocity profiles as a boundary condition in the generic numerical model somewhat difficult, unless visual aid is utilized

- The size of the updraft hole (or bell mouth/exhaust opening) was observed to have a significant impact on the flow structure of laboratory produced vortices. In certain cases, it was also observed that the effective updraft hole size was reduced and this reduction had to be accounted for, in the simplified generic numerical model.

- It was also shown that vortices with similar swirl ratio produced in different experimental facilities can represent the same real tornado, but at different length scales.

- Vortex wandering was found to be a common feature of simulated tornadoes (experimentally and numerically produced vortices). While wandering is commonly observed in real tornadoes (tornadoes in nature) as well, care must be taken when measurements are made using fixed probes for simulated tornadoes, particularly when validating numerical results with experimental data.

- Further, the potential application of this generic numerical tornado simulator to bluff-body aerodynamics and wind load evaluation was demonstrated and, while the results obtained from numerical simulations showed some minor but explainable discrepancies with experimental observations, the proposed numerical simulator displayed promising results for its utility in the future.

4.2 Future research direction

The following recommendations for future research can be made to compliment and extend the current study.

- To fully demonstrate the robustness of the generic numerical model developed in this study, a more rigorous validation with xperimentally obtained data is desirable. Further, along with mean quantities that have already been compared in this study, peak values should also be computed and compared.

- Real tornadoes are also reported to wander, so quantifying the effects of vortex wandering would aid in making future studies more conclusive, at least from a Wind Engineering perspective.

- It would also be interesting to conduct a parametric study to identify the role of geometric and physical parameters of an experimental tornado simulator, particularly the size of updraft hole and location of honeycomb section (which are less discussed in past studies).

- Exploring the effect of translation and ground roughness on tornadic flow and resulting wind loads and the appropriate choice of reference velocity and pressure for tornadic flow would help in simulating more realistic scenarios.

- Further, it would be the ultimate goal to be able to link metereological tornado models with engineering models to simulate more realistic scenarios at a city level. Computational Fluid Dynamics could play an instrumental role in achieving this and moving towards mechanics based loss modelling approach for tornado hazard.

Curriculum Vitae

Name: Anant Gairola

Post-secondary Education and Degrees:

State University of New York at Stony Brook
Stony Brook, New York, USA
2011-2015, B.E. (Honors), Mechanical Engineering

Western University
London, Ontario, Canada
2015-2017 M.E.Sc., Civil Engineering

Related Work Experience

Research Assistant
Western University
Department of Civil & Environmental Engineering
Fall 2015-present

Teaching Assistant
Western University
Department of Civil & Environmental Engineering
Winter 2016-present

Research Intern
Iowa State University
Department of Aerospace Engineering
Summer 2014

Publications:

Journal publications

Ahmed Elshaer, Anant Gairola, Kimberley Adamek, Girma Bitsuamlak, 2017," Variation in Wind Load on Tall Buildings due to Urban Development", Sustainable Cities and Society.

Conference presentations/ publications

Anant Gairola, Zoheb Nasir, Girma Bitsuamlak, 2017," A Numerical Tornado Model Unifying the Existing Experimental Tornado Simulators", 14th US National Congress on Computational Mechanics, Montreal, Canada.